Pictogram for the Graphical Abstract

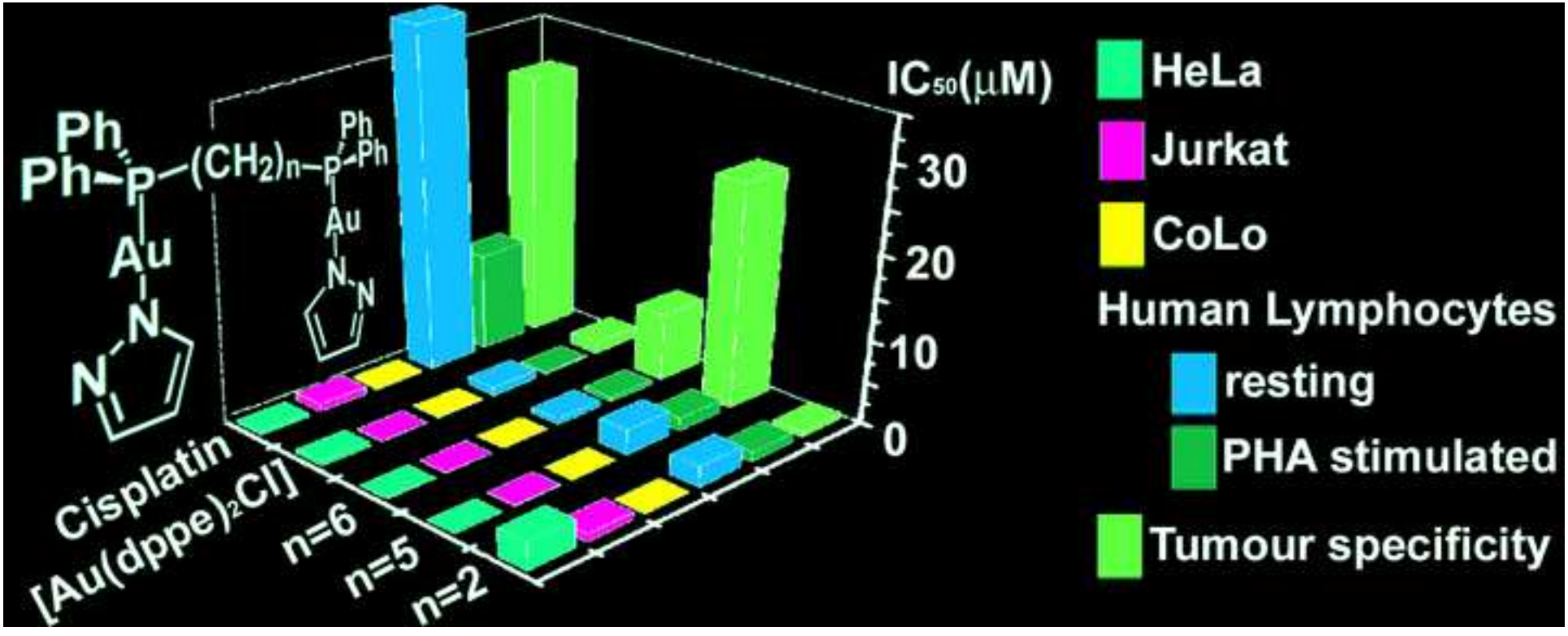

***Synopsis for the Graphical abstract**

Synopsis

Among a new series of gold(I) complexes that contain diphosphine and deprotonated N-heterocyclic ring systems as ligands, the compounds containing diphenyl(phosphino)pentane and pyrazolate (lypophilic) or 1,2,4,-triazolate (hydrophilic) have high anti-tumour specificities. They induce an apoptic cell death pathway and have the maximum tolerated dose of 1.5 μmol/kg when administered to Balb/C mice.

***Highlights**

- In 25 new complexes diphosphines and azolate-type ligands coordinate to gold
- Solvent molecules and counterions appear within channels of a crystalline complex
- Cytotoxicity is dependent upon aliphatic C chain length in the ligands
- An apoptosis cell death with certain mitochondrial involvement is indicated
- Tolerated doses compared to $[Au(dppe)_2]Cl$, tumour specificity is much better

Amides of gold(I) diphosphines prepared from N-heterocyclic sources and their *in vitro* and *in vivo* screening for anticancer activity

Ulrike E. I. Horvath[a], Liliana Dobrzańska[a,b], Christoph E. Strasser[a], Wilna Bouwer (neé Potgieter)[c], Gisela Joone[c], Constance E. Jansen van Rensburg[c], Stephanie Cronje[a,d] and Helgard G. Raubenheimer[a,*]

[a] *Department of Chemistry and Polymer Science, University of Stellenbosch, Private Bag X1, Matieland, 7602, Stellenbosch, South Africa*

[b] *Department of Chemistry, Katholieke Universiteit Leuven,Celestijnenlaan 200F - bus 2404, B-3001 Heverlee, Belgium*

[c] *Department of Pharmacology, University of Pretoria, P.O. Box 2034, Pretoria 0001, South Africa*

[d] *Institut für Anorganische und Analytische Chemie, Goethe-Universität Frankfurt, Max-von-Laue-Strasse 7, D-60348 Frankfurt am Main, Germany*

*Corresponding author.

E-mail address: hgr@sun.ac.za (H. G. Raubenheimer)

A B S T R A C T

A series of new neutral mononuclear or dinuclear gold(I) complexes and a cyclic cationic tetranuclear amidogold(I) complex comprising of the phosphines 1,2-bis(dimethylphosphino)ethane (dmpe), μ-1,2–bis(diphenylphosphino)ethane (dppe), μ-1,3-bis(diphenylphosphino)propane (dppp), μ-1,5-bis(diphenylphosphino)pentane (dpppe), μ-1,6-bis(diphenylphosphino)hexane (dpph) or trimethylphosphine, and several N-heterocyclic ring systems (imidazolate, pyrazolate, 1,2,3-triazolate, 1,2,4-triazolate, pyrrolate, 9*H*-purine-9-ate or 9*H*-purine-6-amine-9-ate) as ligands, reveal intermolecular aurophilic interactions and 2D channels available for solvent molecules in some of their crystal structures. The antitumour

activity of the acyclic gold(I) compounds is highly dependent on the substituents on the phosphorus atoms being highest for phenyl groups and lower for methyl groups. The activity of these compounds against selected cell lines is linked to the length of the carbon bridge between the two phosphorus atoms being highest with a bridge consisting of 5 or 6 carbons. Two compounds with the highest tumour specifities that contain dpppe and pyrazolate (a lipophilic compound) or 1,2,4-triazolate (a hydrophilic compound) induce the apoptic cell death pathway and tolerate a maximum dose of 1.5 μmol/kg when administered to Balb/C mice.

Keywords:

Azolate; Purine-ate; Gold(I) diphosphines; Cytotoxicity; Pyrazolate; Anti-tumour

1. Introduction

The pharmacological application of gold(I) compounds in the treatment of rheumatoid arthritis and their potential activity as anticancer, antiviral and antimicrobial agents has provided a powerful incentive for the continued interest in the bonding of biologically active molecules to gold(I) [1–5].

Chemotherapy remains the most effective cancer treatment. Platinum compounds such as cisplatin, carboplatin and oxaliplatin are widely used in clinical settings [6] and a variety of gold compounds are potential anticancer drugs [3]. Of the many gold complexes that have been investigated, the gold(I) phosphine derivatives show the highest activity as anticancer agents [7]. A study carried out by Mirabelli *et al*. [8] in 1987 on the antitumour activity of di(phosphino)alkanes and their chlorogold(I) coordination complexes against a variety of tumour models provides evidence that bis(diphenylphosphino)ethane (dppe), a lipophilic compound, is active against Murine B16 melanoma cells *in vitro*. Replacement of phenyl groups with ethyl or benzyl groups in free phosphines results in a loss of activity. On the other hand, such an exchange with cyclohexyl or heterocyclic ring systems affords better antitumour activity. The length of the carbon bridge between the two phosphorus atoms also influences the activity: the longer the

carbon chain the lower the activity of the diphosphine compounds against Murine B16 melanoma cells. Similar results with respect to the exchange of phenyl groups apply to chloro(phosphine)gold(I) compounds. In contrast to the free diphosphines, their gold chloride adducts show better activity with increasing length of the carbon chain between the two phosphorus atoms.

The central metal, gold, apparently protects diphosphine ligands from oxidation, and subsequently they are transported into tumour cells where they can unfold their activity. The diphosphine gold chloride complexes tested on mice bearing P388 leukemia show good results for [(dppe)$(AuCl)_2$] at much lower dose levels, compared to dppe, and an increase in life span of the mice.

The exact mechanism according to which the gold(I) phosphines induce antitumour activity is unclear but it is known that they are directly cytotoxic and many appear to have antimitochondrial activity and cause the formation of DNA strand breaks and DNA protein crosslinks [9–12]. Mitochondria are the primary target of both neutral, linear gold(I) phosphine compounds [11, 13] as well as tetrahedral gold(I) phosphine cations [10, 12]. The non-selectivity of cancer drugs in differentiating between tumour cells and normal tissue leads to severe host toxicity. Lipophilic cations, $[(dppe)_2Au]Cl$, are a relatively new class of anticancer drugs displaying selective targeting of mitochondria with hyperpolarised membranes in cancer cells [14]. Strong anticancer activity has been detected for such compounds; however, *in vivo* toxicity remains too high for their clinical use [7, 13]. In these cationic gold(I) disphosphines a decrease in lipophilicity correlates with enhanced selectivity while an increase in potency has been reported with increased lipophilicity [14]. Very hydrophobic and very hydrophilic compound, however, exhibit high cytotoxic activity with low tumour specificity. An optimal lipophilicity seems to be an important factor in the successful design of compounds with high anticancer activity. Reducing lipophilicity compared to that of well-tested $[(dppe)_2Au]Cl$ should eventually form part of the synthetic strategy for anticancer studies. More hydrophilic compounds are more selective, less cytotoxic and show fewer side effects.

It has been suggested that the combination of nucleoside analogues with gold(I) might be beneficial in eliminating resistance and delayed toxicity [15, 16]. An azole-platinum compound

displaying *in vitro* anticancer activity comparable to that of cisplatin is only slightly more active against cisplatin-resistant cancer cells [17]. In another approach, and by using Lin's method, Raubenheimer and co-workers [18] have reported a heterobimetallic N-heterocyclic carbene (NHC) complex of gold conjugatively attached to a ferrocenyl moiety. This phosphine-free 'complex of a complex' is tumour specific against the HeLa and Jurkat cancer cell lines. Exocyclic imine complexation of azol-2-ylideneamine ligands with $[(Ph_3P)Au]^+$ increases their antitumour as well as antimalarial activity [19].

Preparative investigations into phosphine gold complexes bonded to N-deprotonated azoles were carried out in the mid-1970s by Jonassen [20] and the early 1980s by Bonati and co-workers [21, 22] as well as Usón [23]. The number of known complexes and their structural data have been significantly expanded by Nomiya and co-workers [4]. Their investigations revealed the monomeric character of the complexes in solution and, significantly, the antimicrobial activity of $[(Ph_3P)AuL]$ (HL = pyrazole and imidazole) against two gram-positive bacteria (*B. subtilis*, *S. aureus*), and modest activity against a yeast (*C. albicans*) [24]. Recently, more complex deprotonated N-heterocycles based on 9*H*-purine and the DNA base adenine (9*H*-purine-6-amine) were successfully coordinated to mono- and bisphosphines.[25]

Here, we describe a series of neutral mononuclear and dinuclear gold(I) complexes formed when simple N-donor molecules like imidazole, pyrazole, pyrrole, 1,2,3-triazole, 1,2,4-triazole, and the more complex molecules 9*H*-purine and adenine were deprotonated and then coordinated to (phosphino)gold(I) cations. In contrast to the diphosphine bis(chlorogold(I)) compounds with their obvious disadvantages described above, the newly prepared neutral heterocyclic gold(I) complexes could potentially fulfil the lipophilicity requirements for antitumour activity towards a variety of tumour cells, while eliminating resistance and delayed toxicity. Screening tests were performed with a number of cancer cell lines.

Biological assays of the new compounds, as well as $[(dppe)_2Au]Cl$ and cisplatin used as benchmarks with positive well-documented cytotoxicity, toxicity and mechanisms of action, were carried out i) to

establish whether there is a correlation between drug lipophilicity and cytotoxicity, ii) to identify the two most promising compounds based on cytotoxicity assays and, using these compounds, iii) to investigate a possible mechanism by which toxicity is induced (i.e., a preliminary investigation to determine the induced cell death pathway, apoptosis or necrosis, and then to establish whether an extrinsic/receptor-linked or intrinsic/mitochondrial-mediated apoptosis pathway is involved), and iv) to explore the effect of the compounds on the cell cycle. Finally, the two most promising compounds were then further investigated in an *in vivo* toxicity study.

2. Results and discussion

2.1 Synthesis

One monophosphine (PMe_3) complex and a wide range of gold chloride complexes were prepared from the appropriate amount of [(tht)AuCl] (tht = tetrahydrothiophene) [26] by ligand substitution. Subsequent treatment with deprotonated imidazole, pyrazole, 1,2,3-triazole, 1,2,4-triazole, pyrrole and adenine or purine in methanol or dimethoxyethane, according to a procedure we have described previously (Chart 1) [25], afforded the series of neutral products shown in Schemes 1 and 2. Three complexes **20**, **22**, and **23** from the already mentioned investigation are included here. Surprisingly, an unusual cyclic tetranuclear complex **26** (Scheme 3) was isolated from the reaction of [(μ-dppe)$(AuCl)_2$] with two mole quantities of deprotonated imidazole.

All the new products are soluble in more polar and protic organic solvents, show good stability at room temperature, are stable in air and in the presence of deoxygenated water, and decompose only gradually over time. Their stability and good solubility makes them even more appealing candidates for biological screening, since the stability of such compounds in solution is a vital consideration for biological evaluation. A low melting point is a prominent feature of most of these new products. Compounds **3**, **5**, **6**, **9–11** and **18** melt between 60 °C and 100 °C, whereas **8**, **12**, **14** and **17** even melt below 60 °C. All the other compounds except **26** (that melts above 100 °C) decompose upon heating.

2.2 Characterisation

2.2.1 NMR spectroscopy

The absence of any NH protons in the ^{1}H NMR spectra of the new complexes recorded under the same conditions as the free azoles indicates successful deprotonation of the N-bases. Due to H/D exchange in the N-deprotonated adenine-containing compound **24**, in a 1:1 mixture of CD_2Cl_2/CD_3OD, no signal for the NH_2 group was observed.

The phenyl carbon atoms display well-resolved signals in their ^{13}C NMR spectra. The phenyl rings of the phosphine ligands in **6**, **11, 15** and **26** contain magnetically inequivalent carbon atoms, resulting in pseudo-triplets ("t") for the *meta* and *ortho* carbons (doublet of doublets, with J_{PC} = $J_{PC'}$ = 7 or 6 Hz). The magnetic inequivalence, which is observed in the bridging segments of the ligands, is not unexpected, owing to the symmetry of the molecule [27]. The methyl groups on the phosphine ligands in compounds **1** and **10** also display magnetic inequivalence, resulting in signals for an AA'XX' spin system.

The mostly downfield shifts obtained for the resonances of the heterocyclic ring carbons upon complexation are very small because the rings are deprotonated when coordinated to gold.

The ^{31}P NMR spectra of all compounds (**1–26**) measured at room temperature exhibit only one resonance. Except when n = 2, this signal moves downfield as the number of connecting carbons (n) in the phosphine ligand backbone increases. Such a trend, also observed previously [25], has been ascribed to small variations in the dihedral or bond angles at the phosphorus atom with increasing alkyl chain length [28, 29].

2.2.2 Infrared spectroscopy

The absence of typical ν(NH) vibrations (3432–3401 cm^{-1}) in all the IR spectra (KBr pellets) indicate substitution of the most ionisable protons of the heterocyclic bases. For deprotonated adenine, coordination to its original amine group is excluded by the $\nu_s(NH_2)$ and very intense

$\nu_{as}(NH_2)$ vibrations that are still present and remain essentially unchanged.

2.2.3 Mass spectrometry

Due to the relatively high molecular masses of these new compounds, fast atom bombardment mass spectrometry (FAB-MS) or electrospray ionization mass spectrometry (ESI-MS) was used to determine the fragmentation of the compounds. Molecular ions were only observed for compounds **2** and **25** as well as for the cation of complex **26**. A signal corresponding to the cation of complex **26** (z = 2) is present in both types of mass spectra. All the other compounds have a typical fragmentation pattern. The most characteristic signals observed at high m/z values represent fragments formed by the loss of one heterocyclic ring radical unit: $[M]^+$, $[M\text{-pyrazol-N-yl}]^+$, $[M\text{-triazol-N-yl}]^+$, $[M\text{-pyrrol-N-yl}]^+$, $[M\text{-purine-N-yl}]^+$ or $[M\text{-purine-6-amine-N-yl}]^+$.

*2.2.4 Molecular structures of **1**, **18** and **26***

Crystal and molecular structures of three new compounds were determined. These are shown in Figs 1–4, SI 1-2. Typical selected bond lengths and angles that involve the central gold atom are shown in Table 1.

The dinuclear neutral gold(I) complex **1** crystallises in the monoclinic space group *C*2/*c* as a methanol solvate (Fig. 1). The two gold atoms are almost linearly coordinated to the phosphorous atoms of the bridging dmpe ligand and to one of the nitrogen atoms in each of the two distinct imidazolate ions. The Au–P and Au–N bond lengths do not differ significantly from reported values [25]. The angles P1–Au1–N1 and P2–Au2–N21 are 177.19(9)° and 176.56(10)°, respectively. The methanol molecule interacts *via* hydrogen bonding with one imidazolate ring of the complex. Intermolecular aurophilic interactions, $Au1\cdots Au2^{i}$ with bond length 3.2913(4) Å (symmetry operation: (i) 1/2-x, 1/2-y, 1-z) occur between pairs of molecules, thus forming dimers. These are further supported by weak C-H$\cdots\pi$ interactions C8-H8C$\cdots$Cg1 (where Cg1 is the centroid of N21-C25) and C28-H28C$\cdots$Cg2 (where Cg2 is the centroid of N1-C5) between corresponding methyl groups of dmpe and imidazolate rings with C$\cdots$Cg distances of 3.626(5) Å and 3.726(5) Å, respectively. Longer intermolecular $Au1\cdots Au1^{ii}$ contacts of 3.3879(5) Å (symmetry operation (ii):

1-x, y, 3/2-z) between the adjacent dimers, together with weak C7-H7A···Cg2 interactions (with a C···Cg distance of 3.605(5) Å), lead to the formation of supramolecular 1D chains (Fig. 2).

Compound **18** (Fig. 3) crystallises in the triclinic space group P-1 with half a molecule in the asymmetric unit. The dinuclear structure of the neutral complex **18** has a crystallographically imposed centre of symmetry located at the midpoint of the dpph ligand, bridging two gold centres. Therefore, the 1,2,4-triazolate ligands, participating in the slightly distorted linear coordination around the gold(I) atoms (Table 1), are pointed in opposite directions with regard to the plane passing through the bridging diposphine segment. No aurophilic interactions are present in the crystal structure of **18**. However, there are weak hydrogen bonds between the dpph ligand and the triazolate rings C6-H6A···N4^{i} (symmetry operation (i): x, y, -1+z) with a C···N distance of 3.472(4) Å which extend the molecules to a 1D railroad-like motif, expanding along the c axis (Supplementary Information I, Fig. SI 1). The packing is further stabilised by a net of C-H···π interactions, namely: C5-H5···Cg1 (where Cg1 is the centroid of C10-C15), C8-H8A···Cg2 (where Cg2 is the centroid of C16-C21), C12-H12···Cg2, C19-H19···Cg3 (where Cg3 is the centroid of N1-C5), with C···Cg distances in the range 3.6–3.7 Å. Additional stabilisation is provided by offset π–π stacking between neighbouring triazolate rings, with a distance of 3.751(2) Å between their centroids.

Upon using a bis(diphenylphosphine) bridging ligand with a short bridge (n = 2) and deprotonated imidazole as the second ligand it was possible to isolate the tetranuclear 18-membered heterometallocyclic gold complex **26** (Fig. 4). The light-yellow product crystallised in the monoclinic space group C2/*m* with half a dppe ligand (the second half is related by a two-fold rotation), half of the imidazolate ligand (as C15 is located in a special position on a proper mirror plane) and one gold(I) ion, in the asymmetric unit. The counterion (1/2 Cl per asymmetric unit) could not be assigned because of the very diffuse electron density (for more details see the crystal structure determination section). The X-ray structure analysis revealed comparably short intramolecular Au···Au interactions with a distance of about 3.05 Å [30]. Coordination at the Au(I) centre is almost linear, as expected, with a P–Au–N angle of 176.7(3)°, which is in accordance

with literature data [31]. The Au1–N1 bond lengths are also in good agreement with previously reported values. See for example Au(I) trinuclear complexes with pyrazolato ligands [32, 33].

The packing of these discrete molecules is worth mentioning (Supplementary Information, Fig. SI 2). The position of the dppe phenyl rings in the cationic gold(I) complex enables interactions of C1-C6 rings with the corresponding symmetry related ones from neighbouring metallocycles *via* offset π-π stacking with a centroid to centroid distance of 3.71(1) Å (slippage = 1.184 Å) and facilitates C-H···π weak hydrogen bonding such as: C4-H4···Cg1 (where Cg1 is the centroid of C7-C12 with a C···Cg1 = 3.51(2) Å) and C10-H10···Cg2 (where Cg2 is the centroid of C1-C6 with a C···Cg2 distance of 3.57(2) Å). This facilitates the formation of 2D channels along the a and c axes with internal van der Waals dimensions of *ca*. 3.6 by 3.2 Å and 9.3 by 4.9 Å, respectively. These channels are occupied by disordered counterions and solvent molecules (PLATON estimates the accessible space at 43% of the total cell volume) [34].

2.3 Lipophilicity assays

The mean values for log {octanol/water partition coefficient (PC)} of new and known [25] phosphine-bridged amido gold(I) compounds and control compounds were determined. Results are shown in Table 2. The complex $[(dppe)_2Au]Cl$, for example, has a value of 1.62±0.06 as its mean log (octanol/water PC), indicating its lipophilicity [mean log (PC) > 1: lipophilic and mean log (PC) < 1: hydrophilic]. This result is in agreement with previous studies [14], which includes HPLC analysis [35].

Using a Kruskal-Wallis nonparametric test, a statistically significant decrease (p value ≤ 0.05) in lipophilicity is observed when the number of heteroatoms in the 5-membered heterocyclic ring increas from two to three: the imidazole and pyrazole derivatives (**3** and **8**) are the most lipophilic while the triazolate (**17**) is more hydrophilic. In a series of different diphosphines [dppp (3C bridge), dpppe (5C bridge) and dpph (6C bridge)] with purine-9-ate as the second ligand attached to each gold atom, the

dpppe complex (**23**) is the most hydrophilic. The low mean value of log (octanol/water PC) for cisplatin determined in this study, correlates with previous results [36].

2.4 Cytotoxicity assays

The cytotoxic potencies and *in vitro* tumour specificity of the new and known [25] phosphine-bridged amido gold(I) compounds and the control compounds at concentrations < 0.5μM were determined using HeLa, CoLo and Jurkat cancer cell lines and normal resting and PHA (phytohaemagglutinin) stimulated human lymphocytes (Table 3).

More than half of the new compounds display significant cytotoxicity, similar to that previously reported for bis{1-[(*E*)-2-butenyl]-3-(4-ferrocenylphenyl)-2*H*-imidazol-2-ylidene}gold(I) tetrafluoroborate (**27)** [18] against all cancer cells, as well as better *in vitro* selectivity than $[(dppe)_2Au]Cl$. Compounds containing dpppe (5C bridge between phosphorus atoms) and dpph (6C bridge) exhibit the highest cytotoxic potencies, even higher than cisplatin, as well as the highest tumour specificities, although lower than cisplatin against HeLa, Jurkat and CoLo cells. Compounds with phenyl groups on the phosphine ligand instead of methyl groups (compounds **1** and **5**) have higher tumour specificities, in accordance with observations by Mirabelli *et al*. [8]. The tumour specificities of **8** and **17** are are much higher than those of $[(dppe)_2Au]Cl$. The fact that the latter (as well as cisplatin) contains only one gold atom per formula against the two of most of the other new compounds should, however, be taken into account. Considering only the dpppe complexes, those containing pyrazolate (**8**) and 1,2,4-triazolate (**17**) ligands exhibit the highest tumour specificities and those with imidazolate, purine-9-ate and purine-6-amine-9-ate ligands still have higher tumour specificities than $[(dppe)_2Au]Cl$ but, again, carry more gold per mole of test substance. In the series of dpph complexes, the 1,2,4-triazolate compound (**18**) performs best, and the pyrazolate compound (**9**) has a tumour specificity similar to those of imidazolate (**4**), 1,2,3-triazolate (**14**) and purine-9-ate (**24**) compounds.

Four of the compounds that displayed some of the best cytotoxicity/selectivity profiles, **3**, **8**, **17** and **23**, were subsequently screened against additional cell cultures (MCF-7 cells, A2780 cells, A2780cis

cells and chicken embryo fibroblasts) (Table 4). With the increased data set, compounds **8** and **17**, both of which contain a five-carbon diphosphine bridge and pyrazolate or 1,2,4-triazolate ligands, respectively, are the most promising of the new compounds displaying the highest tumour specificity. Both though, are still less specific than cisplatin.

Evaluation of the resistance factors (RFs) (Table 4) indicate that the A2780cis (cisplatin-resistant ovarian cancer) cells are more resistant to the new compounds and to $[Au(dppe)_2Cl]$ than to cisplatin. Thus cross-resistance exists between cisplatin and **3**, **8**, **17** and **23**.

As mentioned earlier, a correlation between octanol/water PCs (lipophilicity) and cytotoxicity has been indicated for lipophilic cations of the type $[Au(P\text{^}P)_2]^+$ [14]. According to the Spearman procedure, no correlation exists between the octanol/water PCs (refer to Section 2.3) of the newly prepared neutral, linear digold complexes and the IC_{50} values obtained with HeLa, CoLo, Jurkat, human lymphocytes (resting) and human lymphocytes (PHA stimulated). The *in vitro* assay indicated that the most lipophilic compound with a five-carbon phosphine bridge and with pyrazolate as additional ligand (**8**), and the hydrophilic compound **17**, also with a five-carbon phosphine bridge but with a 1,2,4-triazolate ligand in the second coordination position, both display large antitumour selectivities.

2.5 Apoptosis

The induction of apoptosis *via* anticancer compounds is a desirable result in cancer chemotherapy [37]. It has been documented that $[Au(dppe)_2]Cl$ induces intrinsic/mitochondria-mediated apoptosis [38, 12]. In contrast, it is known that cisplatin causes extrinsic/receptor-linked apoptosis, not involving mitochondria [39]. The results of the present study indicate that the two selected new compounds **8**, and **17**, as well as the control compounds generate an apoptic cell death pathway within 24 h when exerting their cytotoxic effects in Jurkat cells (Table 5; Table SI contains results obtained after 48 h exposure and appear in the Supplementary Information). The observed presence of necrotic cells after 48h is explained by the binding of PI (propidium iodide) to the DNA of these cells upon prolonged

exposure to the test compounds. The next step was to investigate whether the apoptotic pathway induced by the new compounds involves the mitochondria or not.

2.6 Mitochondrial membrane potential

The mitochondrial function parameter, MMP (mitochondrial membrane potential), allows discrimination between the extrinsic/receptor-linked or the intrinsic/mitochondria-mediated apoptic pathways. A collapse/depolarisation of MMP indicates mitochondrial toxicity [40]. Results are reported in Supplementary Information, Table SI 2.

Cisplatin induces cytotoxicity by DNA intrastrand cross-linking without involvement of mitochondria [39, 41], thus it does not induce the depolarisation of the MMPs of either cells. The lack of selectivity of $[(dppe)_2Au]Cl$ is evident from the dose-dependent collapsed MMP observed for the cancer cells (Jurkat) as well as for the normal (PHA stimulated lymphocytes) cells.

Although the MMP remains almost unaltered by **8** and **17** at low concentrations, some involvement of the mitochondria is indicated at higher concentrations in both Jurkat cells (at a very high concentration of **8**) and PHA stimulated lymphocytes (at high concentrations of **8** and **17**), as evidenced by MMP depolarisation. It is thus not likely that the mitochondria are targeted by **8** and **17** at low concentrations. However, their involvement can not be excluded at higher concentrations.

2.7 Effects on cell division

The cell cycle can be divided into two phases, namely interphase and mitosis. Interphase cell growth occurs in the first gap (G1) phase, DNA replication takes place during the synthesis (S) phase and cells continue to grow in the second gap (G2) phase before mitosis (M) occurs, which consists of orderly cell division into two daughter cells. By quantifying the amount of DNA present in the cell it can be determined in which phase the cell has been arrested (Tables SI 3 and SI 4). All four selected

compounds inhibited/arrested further cell replication. Since DNA synthesis occurs during the S phase, the accumulation of the cells in this phase upon exposure to cisplatin is consistent with the well-known mode of action of the drug involving the formation of platinum-bonded purine intrastrand cross-links [6]. [$(dppe)_2AuCl$] causes cell accumulation in the G1 phase, with a concurrent decrease in the percentage of cells assigned to the S and G2/M phases. These results corroborate previous findings in which certain gold(I) phosphines have been shown to induce cell growth inhibition by means of the elongation of the G1 phase [42]. The present data show that **8** and **17** also cause cell accumulation in the G1 phase, with a resultant decrease in the percentage of cells continuing to the S and G2/M phases.

2.8 Assessment of in vivo acute toxicity

Complexes **8** and **17** were tested in a mouse model according to procedure of Berners-Price *et al*. [14]. It is known that elevated plasma levels of AST (aspartate amino transferase), ALT (alanine amino transferase) and GGT (γ-glutamyl transpeptidase) are indicative of liver damage [43]. Parameters indicative of nephrotoxicity include elevated plasma urea and creatinine levels [44, 45]. Plasma concentrations of these liver and kidney markers, together with organ and body weights, whole blood analysis and observation of the mice were used as indicators of induced toxicity in the experimental animals.

The *in vivo* acute toxicity of complexes **8** and **17** was determined in female Balb/C mice by assessing the following markers after five days of drug exposure: (i) observed adverse effects and weight loss, (ii) liver markers (AST, ALT, GGT), (iii) kidney markers (urea and creatinine) and (iv) organ weight. The gold complexes were injected intraperitoneally once daily for five consecutive days (day 1 to 5) at concentrations of 1.5, 3 and 6 μmol/kg, respectively. The results are collected in Tables SI 5 – SI 11 in the Supplementary Information.

Toxicity is indicated by severe piloerection, diarrhoea and significant body weight loss (Tables SI 5 – SI 8) in the mice that received 3 and 6 μmol/kg of both compounds **8** and **17**. No significant elevation of AST or ALT levels for the mice in the test groups, compared to the untreated control group, occurs (Table SI 9). This result is consistent with the apparent absence of hepatotoxicity. However,

considering the severe dose-dependent increase of GGT plasma levels an argument for hepatotoxicity can be made. Some increased (liver weight)/(body weight) ratios (Table SI 10) might also be indicative thereof and might be substantiated clinically in a prolonged study. The absence of plasma creatinine elevation in this study cannot exclude nephrotoxicity [46]. A significant increase in plasma urea levels is detected in the groups that received **8** (1.5 and 6 μmol/kg) and **17** (3 μmol/kg), compared to the untreated control group. Haematology results show signs that are sometimes associated with kidney damage [47]. A significant increase in the heart weight/body weight ratio is also seen in the mice that received 3 and 6 μmol/kg of **17** (Table SI10), indicating cardiotoxicity at these dosages. Cardiotoxicity might perpetuate further kidney damage in animals by virtue of decreased cardiac output [48]. No significant conclusions can be drawn from the full blood count analysis of mice after being subjected to the gold complexes **8** and **17** (Table SI 11)**.**

Altogether, our results reveal minimal observable adverse effects in the groups that received 1.5 μmol/kg of **8** or **17**. However, increased (kidney weight)/(body weight) ratios and (liver weight)/(body weight) ratios compared to the untreated control, are indicative of some toxicity being induced by both compounds. Our study suggests that the maximum tolerated dose (MTD) for **8** and **17** in Balb/C mice is 1.5 μmol/kg, which is half that for $[Au(dppe)_2]Cl$ or equal to the value for the latter compound per mole gold used. This result needs to be confirmed in a chronic study.

3. Conclusions

Neutral dinuclear diphosphine gold(I) complexes that also contain deprotonated biologically active N-heterocycles as ligands are active against selected tumour cells. The activity is modulated by the length of the aliphatic carbon chain between the two phosphorus donor atoms, with an optimum length of five or six carbons. Replacement of the phenyl groups on the phosphine ligand with methyl groups (compounds **1** and **5**) reduces tumour specificity. The new compounds, lipophilic **8** (tumour specificity, 26) and hydrophilic **17** (tumour specificity, 24), have much higher *in vitro* tumour specificities than $[(dppe)_2Au]Cl$ (tumour specificity, 1.4). The former compounds cause apoptosis with involvement of the mitochondria only a possibility at higher doses. At lower concentrations it is not likely that the mitochondria are the primary target for cytotoxic induction, and further investigations should be conducted to elaborate on their mode of action. The MTD of both new compounds was determined as 1.5 μmol/kg compared to the 3 μmol/kg observed previously for $[(dppe)_2Au]Cl$, which, however, contains only one gold atom per formula compared to the two in the synthesized test compounds.

Further work, including efficacy studies, are warranted given the higher selectivity exhibited by **8** and **17** when compared to $[(dppe)_2Au]Cl$. Future investigations should preferably concentrate on phosphine-free compounds, and exo-bidentate NHC complexes present themselves as viable alternatives if a similar relationship between spacer chain length and anti-tumour activity can be established. Once, more active but less toxic compounds are identified, further testing in animal models of cancer to assess their clinical potential might follow.

4. Experimental

4.1 Synthesis and characterization

All reactions were carried out under argon using standard vacuum-line and Schlenk techniques.

Pentane was dried and deoxygenated by distillation over sodium, diethyl ether over sodium benzophenone ketyl radical, dichloromethane from CaH_2 and methanol from magnesium methoxide, under an atmosphere of dry nitrogen.

Gold(I) starting materials (μ-1,2–bis(diphenylphosphino)ethane)bis(chlorogold) [49], (μ-1,3-bis(diphenylphosphino)propane)bis(chlorogold) [50], (μ-1,5-bis(diphenylphosphino)pentane)bis(chlorogold) [51], (μ-1,6-bis(diphenylphosphino)hexane)bis(chlorogold) [52] and chloro(trimethylphosphine)gold [53] were prepared by substitution of tetrahydrothiophene (tht) in [(tht)AuCl] [54, 55] with the appropriate phosphine. The synthesis of (μ-1,2-bis(dimethylphosphino)ethane)bis(chlorogold) followed the same method. Complex $[(dppe)_2Au]Cl$ was prepared according to the method of Berners-Price et al. [9]. Comparison with the characterisation data in the literature confirmed the purity of the starting materials. All the other reagents were purchased from commercial suppliers and used without further purification.

Melting points were determined on a Stuart Scientific SMP3 melting point apparatus and are uncorrected. Mass spectra were recorded on an AMD 604 (EI, 70 eV), an Waters API Quattro Micro (ESI, 70 eV, solvent MeOH) or VG 70SEQ (FAB, 70 eV, nitrobenzyl alcohol matrices) instrument, the infrared spectra on a Nicolet Avatar 330 FT-IR with ZnSe ATR (attenuated total reflection) accessory (Smart Performer) and NMR spectra on a Varian 300 FT, a Varian Unity INOVA 400 MHz or an INOVA 600 MHz spectrometer (δ reported relative to the solvent resonance or external reference 85% H_3PO_4). Elemental analyses were carried out in the Department of Chemistry, University of Witwatersrand or by the Department of Chemistry, University of Cape Town, South Africa.

4.1.1 Preparation of dichloro{μ-[1,2-ethanediylbis(dimethylphosphine-κP)]}digold(I)

A mixture of 1,2-bis(dimethylphosphino)ethane (1.0 g, 5.7 mmol) and [(tht)AuCl] (3.65 g, 11.4 mmol) in CH_2Cl_2 (50 mL) was stirred for 2 h at room temperature. The formed precipitate was filtered off, washed with CH_2Cl_2 (2 x 15 mL) and dried *in vacuo*, to afford colourless,

microcrystalline material. Yield: 3.45 g, 98%. Mp: 124 °C (dec). IR (KBr, cm^{-1}): ν(aromatic C-H) 3053w; ν(aliphatic C-H) 2983w, 2974w, 2968m. EI MS: m/z (%) 580 [M^+-Cl, 14%], 383 [M^+-AuCl, 36], 150 [$dmpe^+$, 14]. Anal. calcd. for $C_6H_{16}Au_2Cl_2P_2$: C, 11.72; H, 2.62, found: C, 12.03; H, 2.24 %.

4.1.2 Preparation of {μ-[1,2-ethanediylbis(dimethylphosphine-κP)]}bis(1H-imidazolato-κN^1)digold(I), ***1***

A mixture of NaOH (0.082 g, 2.1 mmol), imidazole (0.14 g, 2.1 mmol) and (μ-1,2-bis(dimethylphosphino)ethane)bis(chlorogold) (0.62 g, 1.0 mmol) in MeOH (20 mL) was stirred for 1 h at room temperature. After solvent removal, the residue was washed with ether (2 × 20 mL) and then water (2 × 20 mL). It was then dissolved in 20 mL CH_2Cl_2, washed again with 2 portions of 10 mL H_2O, filtered twice slowly over anhydrous Na_2SO_4, concentrated and layered with ether to effect precipitation at -20 °C. After filtration and drying *in vacuo*, **1** was obtained as a colourless, microcrystalline material. Yield: 0.43 g, 69%. Mp: 180 °C (dec). IR (KBr, cm^{-1}): ν(aromatic C-H) 3111s, 3051s; ν(aliphatic C-H) 2989s, 2962s, 2897s; ν(C=N) 1635w. ^{1}H NMR (300 MHz, MeOH-d_4): δ = 7.43 (2 H, bs, H2), 7.01 (4 H, s, H4, H5), 2.32 (4 H, d, ^2J = 7.4 Hz, P-$(CH_2)_2$-P), 1.69 (12 H, d, ^2J = 10.5 Hz, CH_3). ^{13}C NMR (75 MHz, MeOH-d_4): δ = 145.1 (bs, C2), 126.9 (bs, C4, C5), 24.9 (m, P-$(CH_2)_2$-P), 13.4 (m, CH_3). ^{31}P NMR (121 MHz, MeOH-d_4): δ = -1.3 (s). ESI MS: m/z (%): 611 [M^+-imidazol-N-yl, 100%]. FAB MS: m/z (%) 1221 [M^++dmpeAu_2, 1%], 611 [M^+- imidazol-N-yl, 12]. Anal. calc. for $C_{12}H_{22}Au_2N_4P_2$: C, 21.25; H, 3.27; N, 8.26, found: C, 20.89; H, 2.99; N, 7.99 %.

Since essentially the same procedures were used for the preparation of complexes **2**-**26**, these methods as well as characterization data for the complexes are deposited as Supplementary Information: SI 4.1.3 – SI 4.1.24.

4.2 Crystal structure determinations

The crystal data collection and refinement details for complexes **1**, **18** and **26** are summarised in Table 6. Single crystals suitable for X-ray analysis were obtained by slow crystallisation from MeOH at room temperature by slow evaporation (**1**) or from CH_2Cl_2 layered with ether at -20 °C (**18, 26**). A Bruker SMART Apex CCD diffractometer [56] with graphite-monochromated Mo-K_α radiation (λ = 0.71073 Å) was used for data collection. Intensities were measured using the ω-scan mode and corrected for Lorentz and polarisation effects. Cell refinement and data reduction were performed using the program SAINT [57] and all empirical absorption corrections were performed using SADABS [58, 59]. All structures were solved by direct methods and refined by full matrix least squares on F^2 using the SHELXL-97 program package [60].The program X-SEED was used to prepare molecular graphics images [61].

All non-hydrogen atoms were refined with anisotropic displacement parameters. All hydrogen atoms were placed in calculated positions. In the case of **26**, the data were limited and their quality was very poor. However, as all our efforts to collect a better data set failed, we decided to present the obtained structure as we found the structural aspects of the tetranuclear cationic Au(I) complex that formed rather unique. The counterions (1/2 chloride ion in the asymmetric unit) and solvent molecules could not be assigned. We could not find a suitable referent model for the extremely diffuse electron density in the crystal channels. Therefore, the electron density was subtracted and the SQUEEZE instruction of PLATON was applied [62]. Since the crystals have been grown from a mixture of solvents, it is difficult to make any assumptions regarding the exact location of these molecules. Consequently, the tabulated molecular formula and weight, F(0 0 0), and absorption coefficient (Table 6) are not fully correct since solvent molecules were not taken into account in these calculations. Restraints were placed on bond lengths of the ring C1-C6 as well as on the displacement parameters of some of the C atoms in the phenyl rings and N1.

4.3 Biological assays

4.3.1 Formulation of drugs

The complexes $[(dppe)_2Au]Cl$ [9] and cisplatin were included as controls for comparison. Stock solutions (10 mM) of the experimental compounds in DMSO were prepared and then, just before use, diluted in the appropriate tissue culture medium supplemented with 10% heat-inactivated foetal calf serum (FCS).

4.3.2 Cell lines and culture conditions

The following cancer cell lines were used:

(i) human cervical carcinoma (HeLa, ATCC no CCL2) – adherent epithelial cells maintained in Eagles minimum essential medium (EMEM) containing 2 mM L-glutamine, 0.1 mM non-essential amino acids, 1.0 mM sodium pyruvate and 5% bovine FCS.

(ii) colon cancer cell line (CoLo 320 DM, ATCC no CCL-220) and Jurkat cells (human T-cell line) (NRBM no 0062, ATCC no.TIB-152) that grow loosely attached in suspension and are rounded and refractile. They are maintained in RPMI 1640 medium with 10% bovine FCS.

(iii) breast carcinoma (MCF 7, ATCC no HTB 22) - adherent epithelial cells maintained in Dulbecco's minimum essential medium (DMED) containing 2 mM L-glutamine, 0.1 mM non-essential amino acids, 1.0 mM sodium pyruvate and 5% bovine FCS.

(iv) human ovarian carcinoma, (A2780, ECACC no 93112519), and a variant thereof, resistant to cisplatin (A2780 Cis, ECACC no 93112517)-adherent epithelial cells maintained in RPMI 1640 medium with 10% bovine fetal calf serum. In the case of A2780cis, 0.3 mg/mL cisplatin was added to the growth medium to maintain cisplatin resistance. Cisplatin in growth media was removed 24 hours prior to experiments.

To determine the tumour specificity for each experimental compound the following non-cancerous and primary cell cultures were used:

(i) primary chicken embryo fibroblasts adherent cells that are isolated from chicken embryos [63], maintained in RPMI 1640 medium with 10% bovine fetal calf serum

(ii) primary human lymphocytes were isolated as described by Anderson *et al*. [64], from heparinised peripheral blood and maintained in RPMI 1640 medium with 10% bovine FCS.

The bovine FCS that was used to supplement the growth media was heat inactivated at 56 °C for 30 minutes. All the cultures were cultivated in the presence of 1% penicillin and streptomycin and were maintained at 37 °C with 5% CO_2. Cultures were sub-cultured as needed.

4.3.3 Lipophilicity assays

Partition coefficients (PC) between water and octanol were determined using standard methods (Shake-flask method). Concentrations in each phase were calculated from UV–vis absorption data using extinction coefficients determined in water-saturated octanol and in octanol-saturated water [65]. Results are expressed as the mean log values of the final octanol/water partition coefficient value. Statistical evaluation was performed with a Kruskal-Wallis non-parametric test with BMDP Statistical Software©.

4.3.4 Cytotoxicity assays

Cytotoxicity assays are performed to establish the sensitivity of cancer cell lines and normal cell cultures to the experimental compounds. A known concentration of cells was exposed to different concentrations (0.05-50 μM) of the experimental drug in a 96 well tissue culture plate and incubated for a period of time. Drug free solvent controls were included. Cancer cells were seeded at 4–5× 10^2/well and were incubated for 7 days. Fibroblasts were seeded at 2×10^4/well and also incubated for 7 days. Lymphocytes were seeded at 2×10^5/well and incubated for 3 days. The viability of cells was determined with the MTT method [66]. A volume of 20 μl MTT [3-(4,5-dimethylthiazol-2-yl)-2,5-diphenyltetrazolium bromide] (Sigma Diagnostics Inc.) was added to each well. MTT is a pale yellow substance that is metabolized to dark blue formazan crystals by unaffected metabolically active cells, which is then quantified by means of spectrometry. The same method was used for both cancer cells and normal cell lines. A minimum of three independent experiments were performed. Data were processed using a Wilcoxon signed-rank test at a confidence interval of 95% and with GRAPHAD Prism 4 software©.

4.3.5 Apoptosis

A standard flow cytometer method with propidium iodide (PI) and Annexin V-FITC staining was used as described by Michie *et al*. [67]. This method measures the decline of viable cells and the appearance of early apoptotic and late apoptotic/necrotic cells in one assay. The method is based up on Annexin V-FITC binding to early apoptotic cells and PI staining that identified late apoptotic/necrotic cells [67, 68]. Cisplatin, $[(dppe)_2Au]Cl$, **8** and **17** were tested to determine whether they induce apoptosis in Jurkat cells. Concentrations equal to the IC_{50} value (concentration of compound that causes 50% of cell death), double and five times the IC_{50} value were used. Statistical evaluation was done by a Mann-Whitney non-parametric test with GRAPHAD Statistical software©.

4.3.6 Determination of the mitochondrial membrane potential

A standard flow cytometric method with the cationic mitochondrial membrane stain, JC-1, was used for this study as described by Cossarizza *et al*. [69]. By using JC-1 it is possible to detect single cell variations in mitochondrial membrane potential. JC-1 is able to enter selectively into mitochondria and this is dependant on the mitochondrial membrane potential. The colour of the dye changes reversibly from green to orange as the mitochondrial membrane becomes more polarized. The selected complexes (**8** and **17**) were tested on Jurkat cells and normal PHA stimulated lymphocytes for effects on mitochondrial membrane potential together with $[Au(dppe)_2]Cl$ and cisplatin. Concentrations equal to the IC_{50} value, double and five times the IC_{50} value of the experimental compounds were used. An untreated control and a positive control were included. Valinomycin was used as the positive control at a concentration of 10 μM [69, 70].

4.3.7 Cell cycle division

A standard flow cytometric method was used in which DNA concentration profiles were produced through PI staining of nucleic acid within ethanol-induced membrane-permeabilised cells. The PI staining was quantified and cells were classified into three different phases of the cell cycle: G1 phase, S phase, or G2/M phase. Results are expressed as the mean percentage of cells in each phase ± SEM.

4.3.8 Assessment of in vivo acute toxicity

All studies were performed after approval by the Ethics Committee of the University of Pretoria, according to the guidelines of the National Code for Animal Use in Research, Education, Diagnosis and Testing of Drugs and Related Substances in South Africa. A total of 45 female syngeneic Balb/C

mice of 6-8 weeks from the same breeding batch were used [9]. Animals were housed in groups of six in individually ventilated (IVC) mouse cages in rooms with controlled environmental conditions (temperature: 22±2 °C, humidity 40–60%). Environmental enrichments were allowed. The animals were fed irradiated Purina 5LG4 and water *ad libitum* at the UBPRC (University of Pretoria Biomedical Research Centre). In this acute toxicity study, **8** and **17** were injected intraperitoneally (ip) in three phases. The starting dosages of the experimental compounds were selected based on the maximum tolerated dose of $[(dppe)_2AuCl]$, documented as 3 μmol/kg in the literature [9], and on the *in vitro* cytotoxic findings in this study. Although the starting doses for the experimental compounds are higher than the maximum tolerated dose of $[(dppe)_2AuCl]$, the tumour specificities of both the **8** and **17** are *about* nine times higher than that of $[(dppe)_2AuCl]$. Should any adverse events occur, lower dosages would be administered during the following phase. The weight of each mouse was determined to adapt the dosages accordingly. Due to the water insoluble nature of the test compounds the chosen solvent for this study was a DMSO (0.5%) – olive oil solution. Olive oil, as a drug-carrying vehicle, has successfully been used in previous studies [71, 72]. A final dose of 0.5 mL per mouse was administered ip. The DMSO-olive oil solution was also administered to the control groups during each phase. The dosages were prepared immediately prior to each ip injection with a 26 gauge insulin needle.

Each phase was designed to consist of three groups of mice, where a maximum of six mice were assigned to each group. Hence, a maximum of 18 mice were allowed for each phase. Phase 1 investigated **8** at two intermediate starting dosages (3 and 6 μmol/kg) for five consecutive days in comparison with an untreated control group. Phase 2 investigated **17** at two intermediate starting dosages (3 and 6 μmol/kg) for five consecutive days in comparison with a control group. The study proceeded to Phase 3 where the dosage was lowered for both compounds due to the adverse effects observed during Phases 1 and 2. Phase 3 investigated **8** and **17** at a lower dosage (1.5 μmol/kg) for five consecutive days in comparison with a control group. The animals were weighed daily and monitored for pain and distress (behavioural changes). Toxicity was determined by evaluation of reduced food and water intake resulting in weight loss, observation of abnormal movement (particularly as it pertains to the ability of the animal to obtain food and water), ease of breathing and

visible piloerection. Any animal showing signs of pain and distress or a weight loss of more than 20% original weight would have been euthanized immediately by CO_2 overdose. If two or more animals in a group were to show these signs, the whole group would have been euthanized and no further testing of the specific dosage would take place.

After the last day (i.e. day six) of the investigation), the mice were euthanized with isofluorane, whereafter maximum blood was drawn *via* cardiac puncture by a staff member at UPBRC. The department of Pathology at the Faculty of Veterinary Science, University of Pretoria was responsible for heamatological analysis and enzyme level determination. Toxicity was determined by observation of physical parameters as described above. In addition to observed adverse effects, standard liver markers (AST, ALT and GGT) and kidney markers (urea and creatinine) were analysed. A whole blood profile was done on all the blood samples. Statistical evaluation was done by Wilcoxon signed-rank non-parametric test (body weight changes) or Kruskal-Wallis non-parametric test (Liver and kidney markers, haematology and organ weights) with GRAPHAD Statistical software© program.

Acknowledgement

We gratefully thank the Claude Harris Leon Foundation (UEIH), Alexander von Humboldt Stiftung (HGR and SC), NRF (National Research Foundation, South Africa), Harmony Gold Mining Co. Ltd. through Project Autek and the Research Foundation Flanders – FWO (LD) for financial support of this work as well as Mintek for the generous loan of gold, and Prof. V. J. Catalano, Dept. Chemistry, University of Nevada, Reno for allowing CES to work on this paper during his post-doctoral study. Dr. Roland Auer and Ms. Santa Meyer, University of Pretoria Biomedical Research Centre (UPBRC), Onderstepoort, took care of the experimental animals.

Appendix A. Supplementary material

Crystallographic data for compounds **1**, **18** and **26** have been deposited with the Cambridge Crystallographic Data Centre, CCDC No. 855925-855927. These data may be obtained free of charge

via http://www.ccdc.cam.ac.uk/cgi-bin/catreq.cgi (or from CCDC, 12 Union Road, Cambridge CB2 1EZ, UK; fax: +44 1223 336033). Supplementary data associated with this article (Packing diagrams, biological assays: apoptosis, cell division; *in vivo* toxicity as well as complex syntheses and characterization) can be found online at doi:10.1016/j.jinorgbio.2011.0x.0xx.

References

[1] S.P. Fricker, Gold Bull. 29 (1996) 53–60.

[2] Z. Guo, P.J. Sadler, Angew. Chem., Int. Ed. 38 (1999) 1512–1531.

[3] E.R.T. Tiekink, Crit. Rev. Oncol/Hematol. 42 (2002) 225–248.

[4] K. Nomiya, R. Noguchi, K. Ohsawa, K. Tsuda, M. Oda, J. Inorg. Biochem. 78 (2000) 363–370.

[5] C.F. Shaw III, in: H. Schmidbaur (ed.), Gold: Progress in Chemistry, Biochemistry and Technology, Wiley, Chichester, 1999, pp. 259–308.

[6] D. Wang, S.J. Lippard, Nat. Rev. Drug Discovery 4 (2005) 307–320.

[7] M.J. McKeage, L. Maharaj, S. J. Berners-Price, Coord. Chem. Rev. 232 (2002) 127–135.

[8] C. K. Mirabelli, D. T. Hill, L.F. Faucette, F. L. McCabe, G. R. Girard, D. B. Byran, B. M. Sutton, J. O`Leary Bartus, S. T. Crooke, R. K. Johnson, J. Med. Chem. 30 (1987) 2181–2190.

[9] S.J. Berners-Price, C.K. Mirabelli, R.K. Johnson, M.R. Mattern, F.L. McCabe, L.F. Faucette, C. Sung, S. Mong, P.J. Sadler, S.T. Crooke, Cancer Res. 46 (1986) 5486–5493.

[10] C.K. Mirabelli, R.K. Johnson, D.T. Hill, L.F. Faucette, G.R. Girard, G.Y. Kuo, C.M. Sung, S.T. Crooke, J. Med. Chem. 29 (1986) 218–223.

[11] G.F. Rush, P.F. Smith, D.W. Alberts, C.K. Mirabelli, R.M. Snyder, S.T. Crooke, J. Sowinski, H.B. Jones, P.J. Bugelski, Toxicol. Appl. Pharmacol. 90 (1987) 377–390.

[12] P.F. Smith, G.D. Hoke, D.W. Alberts, P.J. Bugelski, S.Lupo, C.K, Mirabelli, G.F. Rush, J. Pharmcol. Exp. Therap. 249 (1989) 944–950.

[13] G.D. Hoke, R.A. Macia, P.C. Meunier, P.J. Bugelski, C.K. Mirabelli, G.F. Rush, W.D. Matthews, Toxicol. Appl. Pharmacol. 100 (1989) 293–306.

[14] S.J. Berners-Price, R.J. Bowen, P. Galettis, P.C. Healy, M.J. McKeage, Coord. Chem. Rev. 185–186 (1999) 823–836.

[15] E. Solary, A. Bettaieb, L. Dubrez-Daloz, L. Coros, Leuk. Lymphoma 44 (2003) 563–574.

[16] C. Zhu, M. Johansson, A. Karlsson, FEBS Lett. 474 (2000) 129–132.

[17] K. Spiegel, A. Magistrato, P. Carloni, J. Reedijk, M.L. Kelin, J. Phys. Chem. B 111 (2007) 11873–11876.

[18] U.E.I. Horvath, G. Bentivoglio, M. Hummel, H. Schottenberger, K. Wurst, M.J. Nell, C.E. Janse van Rensburg, S. Cronje, H.G. Raubenheimer, New J. Chem. 32 (2008) 533–539.

[19] J. Coetzee, S. Cronje, L. Dobrzańska, H.G. Raubenheimer, M.J. Nell, G. Jooné, H. Hoppe, Dalton Trans. 40 (2011) 1471–1483.

[20] R.L. Kieft, W.M. Peterson, G.L. Blundell, S. Horton, R.A. Henry, H.B. Jonassen, Inorg. Chem. 15 (1976) 1721–1722.

[21] D. Leonesi, A-Lorenzotti, A. Cingolarri, F. Bonati, Gazz. Chim. Ital. 111 (1981) 483-487.

[22] F. Bonati, M. Felici, B.R. Pietroni, A. Burini, Gazz. Chim. Ital. 112 (1982) 5–8.

[23] R. Usón. L.A. Oro, J. Gimerio, M.A. Ciriano, J.A. Cabeza, A. Tiripicchio, M. Camellini, J. Chem. Soc., Dalton Trans. (1983) 323–329.

[24] K. Nomiya, S. Yamamoto, R. Naguchi, H. Yokoyama, N. C. Kasuga, K. Ohyama, C. Kato, J. Inorg. Biochem. 95 (2003) 208–220.

[25] U.E.I. Horvath, S. Cronje, J.M. McKenzie, L.J. Barbour, H.G. Raubenheimer, Z. Naturforsch. 59b (2004) 1605–1617.

[26] J. Coetzee, W.F. Gabrielli, K. Coetzee, O. Schuster, S.D. Nogai, S. Cronje, H.G. Raubenheimer, Angew. Chem. Int. Ed. 46 (2007) 2497–2500.

[27] H. Friebolin, Basic One- and Two-Dimensional NMR Spectroscopy, Wiley-VCH, Weinheim, 1998, pp. 124–125.

[28] E. Colacio, R. Cuesta, J.M. Gutiérrez-Zorrilla, A. Luque, P. Román, T. Girali,M.R. Taylor, Inorg. Chem. 35 (1996) 4232–4238.

[29] R. Narayanaswamy, M.A. Young, E. Parkhurst, M. Oullette, M.E. Kerr, D.M. Ho, R.C. Elder, A.E. Bruce, M.R.M. Bruce, Inorg. Chem. 32 (1993) 2506–2517.

[30] H. Schmidbaur, S. Cronje, B. Djordjevic, O. Schuster, Chem. Phys. 311 (2005) 151–161

[31] R. Uson, L.A. Oro, J. Gimeno, M.A. Ciriano, J.A. Cabeza, A. Tiripicchio, M. Tiripicchio Camellini, J. Chem. Soc., Dalton Trans. (1983) 323–330.

[32] M.C. Torralba, P. Ovejero, M.J. Mayoral, M. Cano, J.A. Campo, J.V. Heras, E. Pinilla, M.R. Torres, Helv. Chim. Acta 87 (2004) 250–263.

[33] M.A.Omary, M.A. Rawashdeh-Omary, M.W.A.Gonser, O.Elbjeirami, T.Grimes, T.R.Cundari, H.V.K.Diyabalanage, C.S.P.Gamage, H.V.R.Dias, Inorg.Chem. 44 (2005) 8200–8210.

[34] A.L. Spek, PLATON, A Multipurpose Crystallographic Tool, Utrecht University, Utrecht, The Netherlands, 2001.

[35] M.J. McKeage, S.J. Berners-Price, P. Galettis, R.J. Bowen, W. Brouwer, L. Ding, L. Zhuang, B.C. Baguley, Cancer Chemoth. Pharm. 46 (2000) 343–350.

[36] K.N.J. Burger, R.W.H.M. Staffhorst, H.C. De Vijlder, M.J. Velinova, P.H. Bomans, P.M. Frederik, B. De Kruijff, Nat. Med. 8 (2002) 81–84.

[38] J.A. Yalowitz, K. Pankiewicz, S.E. Patterson, H.N. Jayaram, Cancer Lett. 181 (2002) 31–38.

[38] S. Mahepal, R. Bowen, M.A. Mamo, M. Lay, C.E. Jansen van Rensburg, Met.-Based Drugs (2008) 1–5.

[39] F. Yu, J.K. Megyesi, P.M. Price, Am. J. Physiol. Renal. Physiol. 295 (2008) F44–F52.

[40] R. Ferraresi, L. Troiano, D. Rossi, E. Gualdi, E. Lugli, C. Mussini, A. Cossaizza, Mitochondrion 4 (2004) 271–278.

[41] D.E. Thurston, Chemistry and pharmacology of anticancer drugs, CRC Press, Boca Raton 2007, p. 37–84.

[42] C.X. Zhang, S.J. Lippard, Curr. Opion. Chem. Biol. 7 (2003) 481–489.

[43] E.R. Schiff, M.F. Sorrell, W.C. Maddrey, Schiff's Diseases of the liver, Lippincott Williams & Wilkins, Philadelphia, 2006, p. 47.

[44] J.L. Gross, M.J. de Azevedo, S.P. Silveiro, L.H. Canani, M.L. Caramori, T. Zelmanovitz, Diabetes Care 28 (2005) 164–176.

[45] M. Sinha, P. Manna, P.C. Sil, Pathophysiology, 15 (2008) 147–156.

[46] Y.M. Bishop, The Veterinary Formulary, 6th ed., Pharmaceutical Press, London, 2005, p. 119.

[47] K.D. Pagana, T.J. Pagana, Mosby's Manual of Diagnostic and Laboratory tests, Mosby Inc., St. Louis, 1998.

[48] H.P. Rang, M.M. Dale, J.M. Ritter, R.J. Flower, Rang and Dale's Pharmacology, 6th ed., Churchill, Livingstone, 2007, p. 74 and p. 282.

[49] D.S. Egglestone, D.F. Chodosh, Inorg. Chim. Acta 108 (1985) 221–226.

[50] M.K. Cooper, L.E. Mitchell, K. Hendrick, M. McPartlin, A. Scott, Inorg. Chim. Acta 84 (1984) L9–L10.

[51] H. Schmidbaur, P. Bissinger, J. Lachmann, O. Steiglmann, Z. Naturforsch. 47b (1992) 1711–1716.

[52] J.E. Goldberg, D.F. Mullica, E.L. Sappenfield, F.G.A. Stone, J. Chem. Soc., Dalton Trans. (1992) 2495–2502.

[53] B.M. Sutton, E. McGusty, D.T. Walz, M.J. DiMartino, J. Med. Chem. 15 (1972) 1095–1098.

[54] A. Haas, J. Helmbrecht, U. Niemann, in G. Brauer (Ed.) Handbuch der Präparativen Anorganischen Chemie, Ferdinand Enke Verlag, Stuttgart, 1978, p. 1014.

[55] R. Uson, A. Laguna, Inorg. Synth. 26 (1989) 85–87.

[56] SMART: Data collection software (version 5.629), Bruker AXS Inc., Madison, WI, 2003.

[57] SADABS (version 2.05), Bruker AXS Inc., Madison, WI, 2002.

[58] SAINT: Data reduction software (version 6.45), Bruker AXS Inc., Madison, WI, 2003.

[59] R.H. Blessing, Acta Cryst. A51 (1995), 33–38.

[60] G.M. Sheldrick, Acta Cryst. A64 (2008) 112–122.

[61] L.J. Barbour, J. Supramol. Chem. 1 (2003) 189–191.

[62] P. van der Sluis, A.L. Spek, Acta Cryst. A46 (1990) 194–201.

[63] R.I. Freshney, Culture of Animal Cells: A Manual of Basic Technique, 4th ed. Wiley-Liss Publishers, New York, 2000.

[64] R. Anderson, M.J. Smit, C.E. Janse van Rensburg, Mol. Pharmacol. 44 (1993) 605–619.

[65] R.J. Bowen, Hydrophilic bidentate phosphines and their group 11 complexes: potential anti-tumour agents, Ph.D. Thesis, Griffith University, Australia, 1999, p. 112.

[66] G.D. Hoke, G.F. Rush, G.E. Bossard, J.V. McArdle, B.D. Jensen, C.K. Mirabelli, J. Biol. Chem. 263 (1988) 11203–11210

[67] J. Michie, J. Akudugu, A.. Binder, C.E. Janse Van Rensburg, L. Böhm, Cancer Res. 56 (2003) 544–550.

[68] H. Tuschl, C.E. Schwab, Toxicol. *in vitro* 18 (2003) 483–491.

[69] A. Cossarizza, M. Baccarani-Contri, G. Kalashnikova, C. Franceschi, Biochem. Biophys. Res. Commun. 197(1993) 40–45.

[70] F. Caruso, R.V. Villa, M. Rossi, C. Pettinari, F. Paduano, M. Pennati, M.G. Daidone, N. Zaffaroni, Biochem. Pharmacol. 73 (2007) 773–781.

[71] D.L. Anger, D.J. Crankshaw, W.G. Foster, Reprod. Toxicol. 22 (2006) 760–764.

[72] F. De la Portilla, I. Ynfante, D. Berjarano, J. Conde, A. Fernández, J. Ma Ortega, G. Carranza, Dis. Colon. Rectum 47 (2004) 2157–2161.

LIST OF TABLE CAPTIONS:

Table 1 Selected distances (Å) and angles (º) for compounds 1, 18 and 26.

Table 2 Octanol/water partition coefficients of selected new compounds, $[(dppe)_2Au]Cl$ and cisplatin.

Table 3 Mean drug concentration causing 50% cell death (IC_{50}) and the calculated tumour specificities ($\Sigma[IC_{50}$ of normal cells$]/\Sigma[IC_{50}$ of cancer cells]) of various cells after treatment with the new and control compounds.

Table 4 Mean drug concentration causing 50% cell death (IC_{50}) and the calculated resistance factors (RFs) (RF = [IC_{50} A2780cis / IC_{50} A2780]) of the A2780 and A2780cis cell lines after treatment with selected new and control compounds.

Table 5 Cell death pathway analysis (mean %) of Jurkat cell lines after exposure to three different concentrations (μmol/l) of each selected gold compound after 24 h exposure (average of three experiments).

Table 6 Crystal data, data collection and structure refinement details of **1**, **18** and **26.**

LIST OF FIGURE CAPTIONS:

Scheme 1 Gold(I) complexes of imidazolate (**1–5**), pyrazolate (**5–9**), 1,2,3-triazolate (**10–14**), 1,2,4-triazolate (**15–18**) and pyrrolate (**19**).

Scheme 2 Dinuclear Gold(I) complexes of purine-6-amine-9-ate (**20** and **21**), purine-9-ate (**22, 23** and **24**) and a monomeric imidazolate complex (**25**).

Scheme 3 Cyclic, cationic gold(I) diphosphine complex (**26)**.

Fig. 1. Molecular structure of **1**·MeOH (displacement ellipsoids at 50% probability) showing H-bonding with a methanol molecule by a dashed line

Fig. 2. A fragment of the 1D supramolecular chain formed by aurophilic interactions and weak hydrogen bonds shown as dashed lines (Au···Au interactions shown in gold, C-H···π in blue), consisting of dimeric units with each dimer represented in a single colour; for symmetry operations, see main text. Solvent molecules are omitted for clarity.

Fig. 3. Molecular structure of **18** (displacement ellipsoids at 50% probability). Unlabeled atoms are related to the labeled ones by the symmetry operation: -x, -y, -z.

Fig. 4. The molecular structure of the cyclic, cationic complex **26** with intramolecular Au···Au interactions shown as dashed lines (displacement ellipsoids at 50% probability).

Table 1 Selected distances (Å) and angles (°) for compounds 1, 18 and 26.

	1·MeOH	**18**	**26**
Bond lengths (Å)			
Au1–N1	2.043(3)	2.041(3)	2.00(1)
Au1–P1	2.244(1)	2.2400(8)	2.239(4)
Au2–N21	2.045(3)		
Au2–P2	2.239(1)		
Au1...Au2	3.2913(4)		3.045(1)
Bond angles (°)			
P1–Au1–N1	177.19(9)	174.53(7)	176.7(3)
P2–Au2–N21	176.56(10)		

Table 2 Octanol/water partition coefficients of selected new compounds, [(dppe)2Au]Cl and cisplatin.

Compound	Ligands	Mean log (octanol/water PC)±SEM[a]
3	imidazolate, dpppe	1.16±0.07 [c, d]
8	pyrazolate, dpppe	1.25±0.06 [c, d]
17	1,2,4-triazolate, dpppe	0.81±0.02 [c, d]
20[b]	purine-6-amine-9-ate, dpppe	0.70±0.03 [e, f]
22[b]	purine-9-ate, dppp	0.66±0.11 [e, f]
23[b]	purine-9-ate, dpppe	0.53±0.06 [e, f]
24	purine-9-ate, dpph	0.71±0.24 [e, f]
$[(dppe)_2Au]Cl$	dppe	1.62±0.06 [c]
cisplatin	NH_3, Cl	0.33±0.13 [f]

[a] Average of three experiments, [b] [26], [c] $p \leq 0.05$ when compared to cisplatin, [d] $p \leq 0.05$ when compared to **20**–**24**, [e] $p \leq 0.05$ when compared to **3**, **8** and **17**, [f] $p \leq 0.05$ when compared to $[Au(dppe)_2]Cl$.

Table 3 Mean drug concentration causing 50% cell death (IC50) and the calculated tumour specificities (Σ[IC50 of normal cells]/Σ[IC50 of cancer cells]) of various cells after treatment with the new and control compounds.

Compound	Cells/IC_{50} (μM)±(SEM) (average of three independent experiments)					
	HeLa	Jurkat	CoLo	Human lymphocytes (resting)	Human lymphocytes (PHA stimulated)	Tumour specificity [a]
1	> 50	-	-	-	-	-
2	2.517± 0.072	0.922±0.107	0.602±0.187	1.936±0.135	0.836±0.082	0.69
3	0.063±0.010	0.325±0.060	0.005±0.002	1.708±0.218	1.204±0.244	7.7
4	0.143±0.025	-	-	1.284±0.115	1.033±0.244	8.1[b]
5	> 50	-	-	-	-	-
6	6.739±1.569	0.915±0.166	0.159±0.065	2.509±0.159	1.138±0.152	0.47
8	0.050±0.011	0.119±0.010	0.005±0.000	3.052±0.885	1.559±0.076	26
9	0.140±0.045	0.045±0.009	0.039±0.025	0.691±0.095	0.513±0.122	5.4
11	4.303±1.159	0.277±0.016	0.137±0.043	2.013±0.340	0.887±0.048	0.62
12	2.593±0.044	0.480±0.040	0.348±0.145	1.479±0.159	0.619±0.070	0.61
13	0.082±0.002	0.104±0.009	0.011±0.002	1.344±0.046	1.052±0.166	12
14	0.183±0.037	-	-	1.640±0.360	1.407±0.226	8.3
17	0.065±0.005	0.075±0.030	0.007±0.000	2.095±0.010	1.454±0.085	24
18	0.043±0.004	-	-	1.325±0.251	0.866±0.144	25[b]
20[c]	0.092±0.010	0.376±0.100	0.015±0.001	1.172±0.047	0.715±0.295	3.9
22[c]	2.178±0.398	0.322±0.055	0.138±0.037	1.936±0.123	1.330±0.122	1.2
23[c]	0.081±0.000	0.344±0.115	0.016±0.003	1.390±0.178	1.097±0.120	5.6
24	0.098±0.020	0.219±0.000	0.025±0.001	0.846±0.066	0.594±0.035	4.2
25	3.443±0.681	1.631±0.143	0.368±0.013	2.786±0.083	2.054±0.632	0.89
27	0.572±0.027	0.253±0.031	1.007±0.081	0.808±0.111	7.41±0.405	4.5[d]
$[(dppe)_2 Au]Cl$	0.603±0.084	0.081±0.003	0.156±0.013	1.007±0.300	0.192±0.006	1.4
cisplatin	0.413±0.098	0.962±0.061	0.312±0.037	39.775±4.888	11.650±0.245	30.5

[a] Tumour specificity of HeLa, Jurkat and CoLo cells; [b] tumour specificity of HeLa only calculated from average of normal cells; [c] reference [25]; [d] reference [18].

Table 4 Mean drug concentration causing 50% cell death (IC50) and the calculated resistance factors (RFs) (RF = [IC50 A2780cis / IC50 A2780]) of the A2780 and A2780cis cell lines after treatment with selected new and control compounds.

Compound	Cells/IC_{50} (μM)±(SEM) (average of three independent experiments)							
	MCF7	A2780	A2780cis	Chicken embryo fibroblasts	Human Lymphocytes (resting)	Human Lymphocytes (PHA stimulated)	Tumour specificity [a]	Resistance factor (RF)
3	0.047±0.002	0.015±0.001	0.207±0.006	0.085±0.002	1.708±0.218	1.204±0.244	4.5	14
8	0.077±0.008	0.015±0.001	0.241±0.013	0.169±0.019	3.052±0.885	1.559±0.076	9.4	16
17	0.060±0.004	0.016±0.001	0.200±0.003	0.121±0.007	2.095±0.010	1.454±0.085	8.7	12
23	0.062±0.002	0.016±0.002	0.195±0.016	0.170±0.028	1.390±0.178	1.097±0.120	3.7	12
$[(dppe)_2Au]Cl$	0.333±0.011	0.051±0.013	0.330±0.004	0.200±0.017	1.007±0.300	0.192±0.006	0.9	6.5
cisplatin	0.824±0.010	0.123±0.030	0.371±0.007	0.503±0.070	39.775±4.888	11.650±0.245	17.3	3.0

[a] Tumour specificity includes results of HeLa, Jurkat and CoLo cells in Table 3:$\sum[IC_{50}$(normal cells – human and chicken)]/$\sum[IC_{50}$ of 6 cancer cells].

Table 5 Cell death pathway analysis (mean %) of Jurkat cell lines after exposure to three different concentrations (μmol/l) of each selected gold compound after 24 h exposure (average of three experiments).

Compound	Concen-tration (μM)	Initial apoptosis	Advanced apoptosis	Necrosis	Nonviable cells (%)
		(mean percentage cells ± SEM)			
Control	-	3.31±0.61	1.97±0.22	1.03±0.57	6.31
8	0.119 [a]	5.98±0.24[d]	2.12.±0.13	1.23±0.27	9.33
	0.238 [b]	6.4±0.64[d]	2.25±0.11	1.23±0.17	9.88
	0.595 [c]	3.89±0.19	3.53±0.27[d]	5.39±0.49[d]	12.81
17	0.075 [a]	5.05±0.61[d]	2.44±0.01	1.47±0.17	8.96
	0.150 [b]	7.17±0.35[d]	2.29±0.02	1.33±0.27	10.79
	0.375 [c]	6.50±0.39[d]	3.66±0.10[d]	6.23±0.18[d]	16.39
$[(dppe)_2Au]Cl$	0.081 [a]	3.39±0.58	6.25±0.99[d]	5.75±1.32[d]	15.39
	0.162 [b]	2.75±0.47	6.17±0.60[d]	6.15±0.96[d]	15.07
	0.405 [c]	2.81±0.22	18.13±0.18[d]	17.66±0.09[d]	38.60
cisplatin	0.962 [a]	5.26±0.32[d]	2.03±0.14	1.30±0.05	8.59
	1.924 [b]	4.99±0.59[d]	1.92±0.12	1.22±0.13	8.31
	4.810 [c]	3.4±0.23	1.98±0.08	1.35±0.25	6.73

[a] IC_{50}, [b] $2 \times IC_{50}$ and [c] $5 \times IC_{50}$; [d] $p \leq 0.05$ when compared to the untreated control.

Table 6 Crystal data, data collection and structure refinement details of 1, 18 and 26.

Compound reference	**1**	**18**	**26**
Chemical formula	$C_{13}H_{26}Au_2N_4OP_2$	$C_{34}H_{36}Au_2N_6P_2$	$C_{58}H_{54}Au_4Cl_2N_4P_4$
Formula Mass	710.25	984.56	1789.70
Crystal system	Monoclinic	Triclinic	Monoclinic
a/Å	26.467(4)	8.8411(10)	18.156(5)
b/Å	10.6496(13)	9.8465(11)	21.701(6)
c/Å	17.988(2)	10.7011(12)	12.304(4)
α/°	90.00	70.016(2)	90.00
β/°	129.972(2)	70.623(2)	123.616(4)
γ/°	90.00	78.093(2)	90.00
Unit cell volume/Å^3	3885.6(9)	821.34(16)	4037(2)
Temperature/K	100(2)	100(2)	150(2)
Space group	*C*2/*c*	*P*$\bar{1}$	*C*2/*m*
No. of formula units per unit cell, *Z*	8	1	2
Absorption coefficient, *μ*/mm^{-1}	15.256	9.052	7.478
No. of reflections measured	11840	8662	7563
No. of independent reflections	4507	3351	3348
R_{int}	0.0221	0.0265	0.0580
Final R_1 [a] values ($I > 2\sigma(I)$)	0.0219	0.0196	0.0697
Final wR_2 [b] values ($I > 2\sigma(I)$)	0.0476	0.0505	0.1678
Final R_1 [a] values (all data)	0.0264	0.0199	0.0915
Final wR_2 [b] values (all data)	0.0490	0.0506	0.1756
Goodness of fit on F^2	1.051	1.108	1.068

[a] $R_1 = \sum \| F_o | - | F_c \| / \sum | F_o |$; [b] $wR_2 = \{ \sum [w (F_o^2 - F_c^2)^2] / \sum [w (F_o^2)^2] \}^{1/2}$.

Chart 1

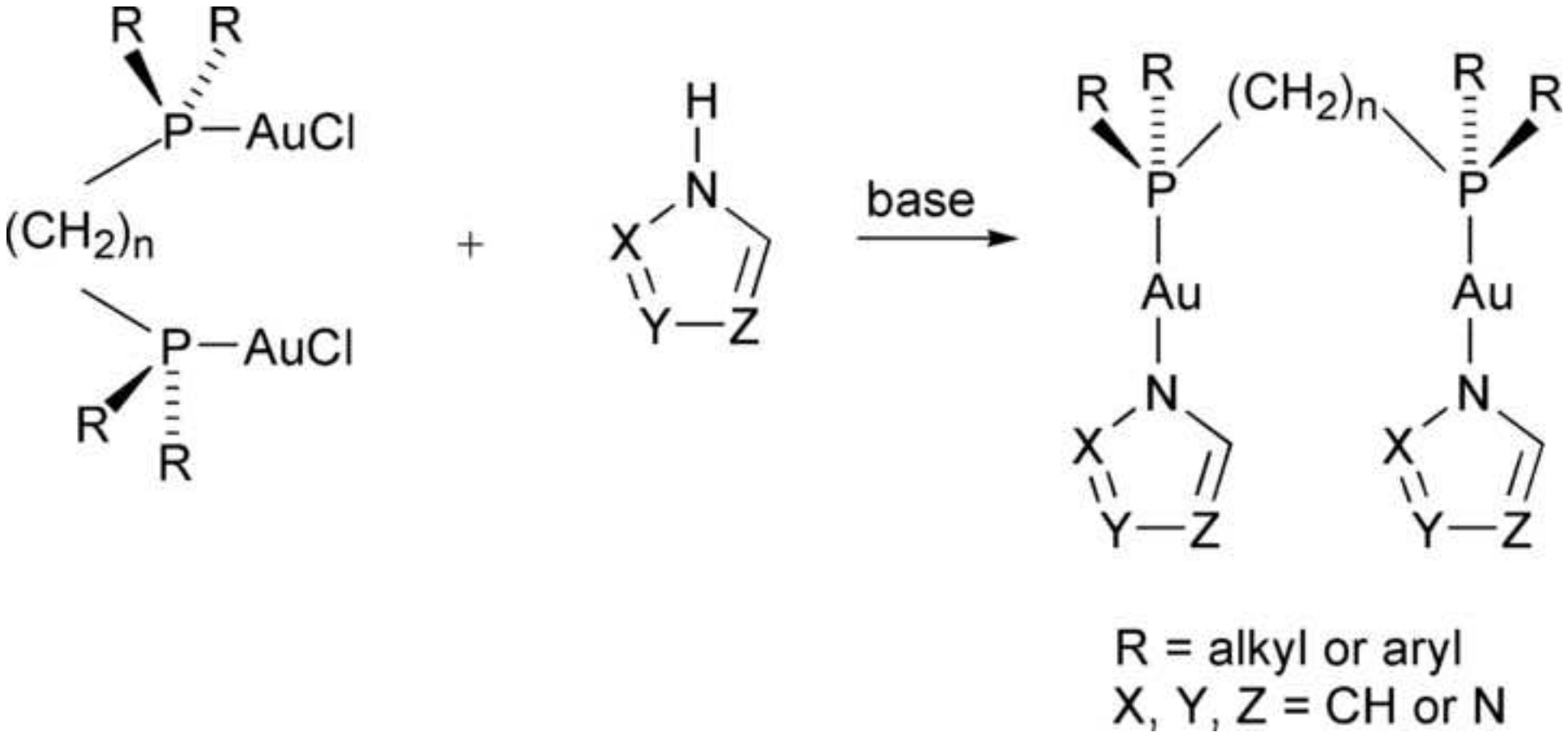
R
R
P—AuCl
(CH2)n
P—AuCl
R
R
+
H
N
X
Y—Z
base
R
R
(CH2)n
R
R
P
P
Au
Au
N
N
X
X
Y—Z
Y—Z
R = alkyl or aryl
X, Y, Z = CH or N

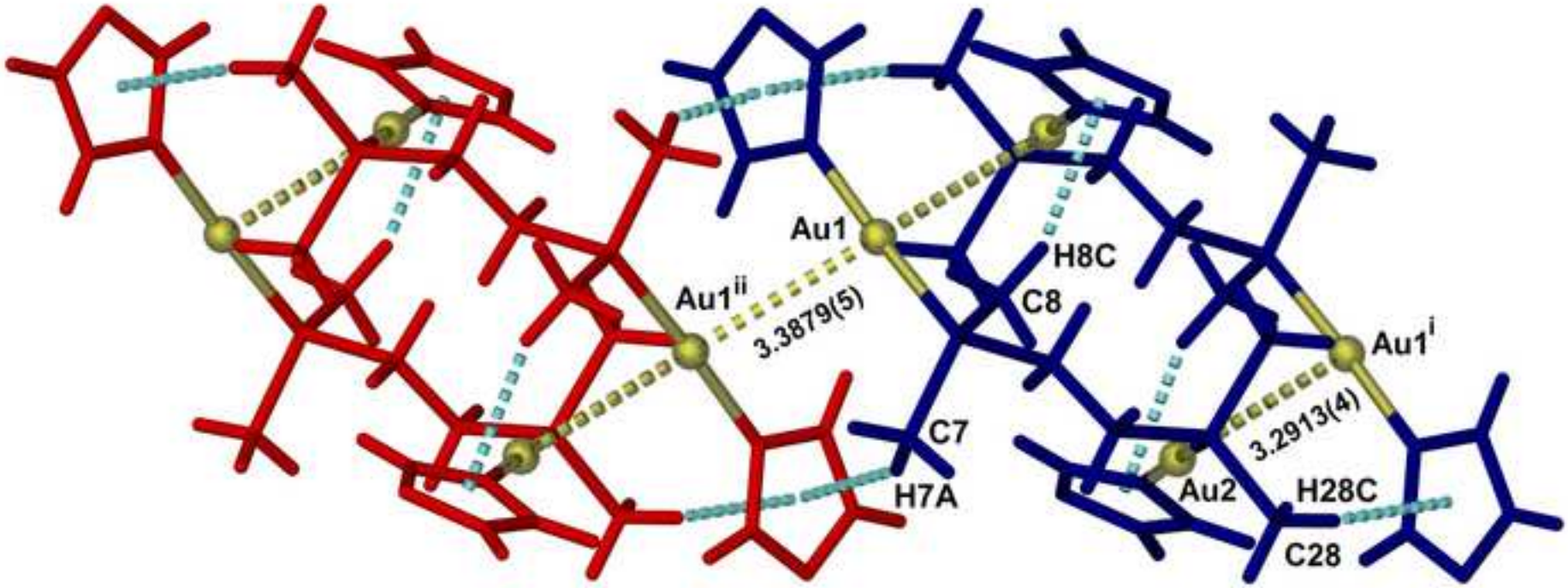

Fig. 2. A fragment of the 1D supramolecular chain formed by aurophilic interactions and weak hydrogen bonds shown as dashed lines (Au…Au interactions shown in gold, Csingle bondH…π in blue), consisting of dimeric units with each dimer represented in a single colour; for symmetry operations, see main text. Solvent molecules are omitted for clarity.

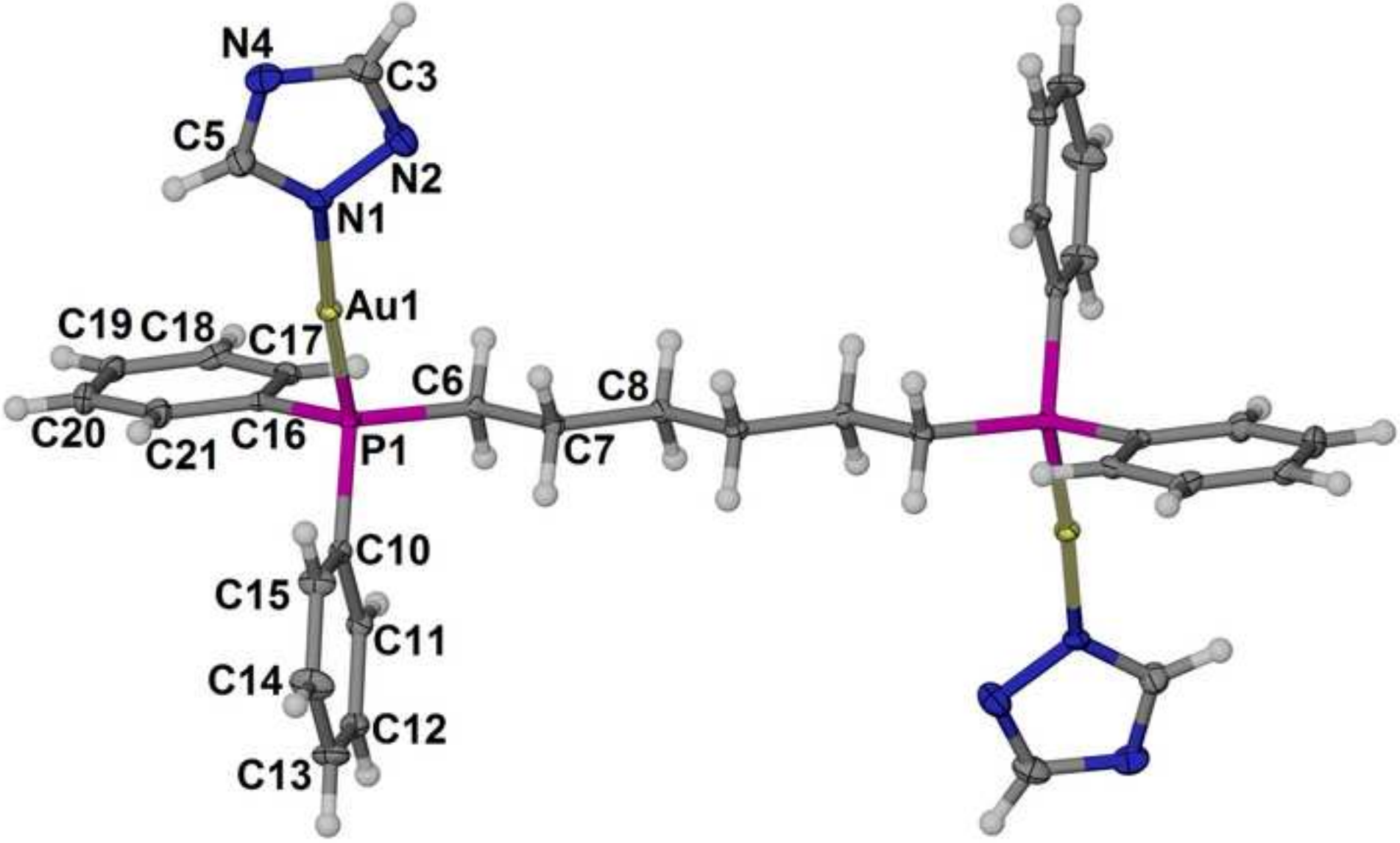

Fig. 3. Molecular structure of 18 (displacement ellipsoids at 50% probability). Unlabeled atoms are related to the labeled ones by the symmetry operation: − x, − y, − z.

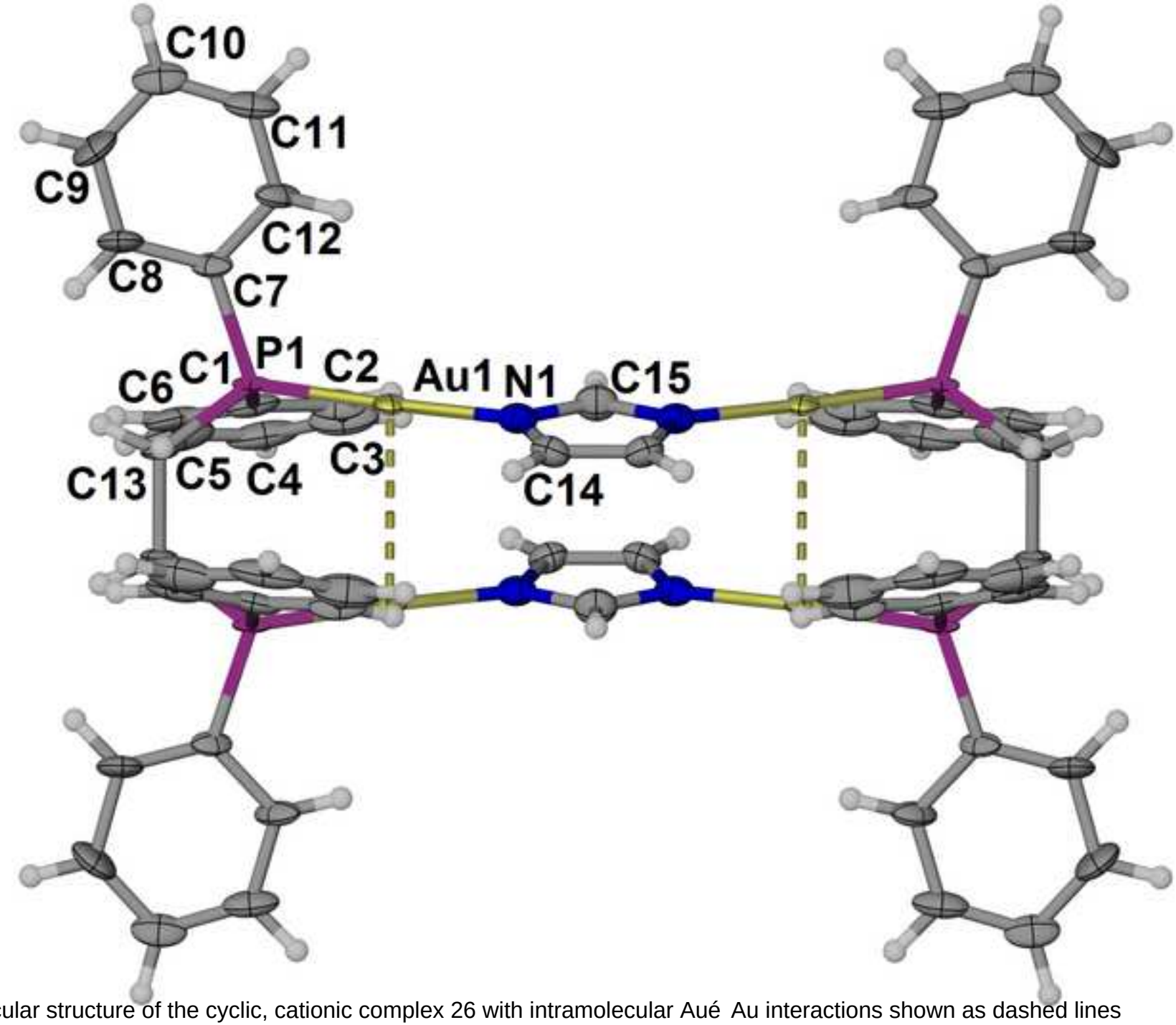

Fig. 4. The molecular structure of the cyclic, cationic complex 26 with intramolecular Aué Au interactions shown as dashed lines (displacement ellipsoids at 50% probability).

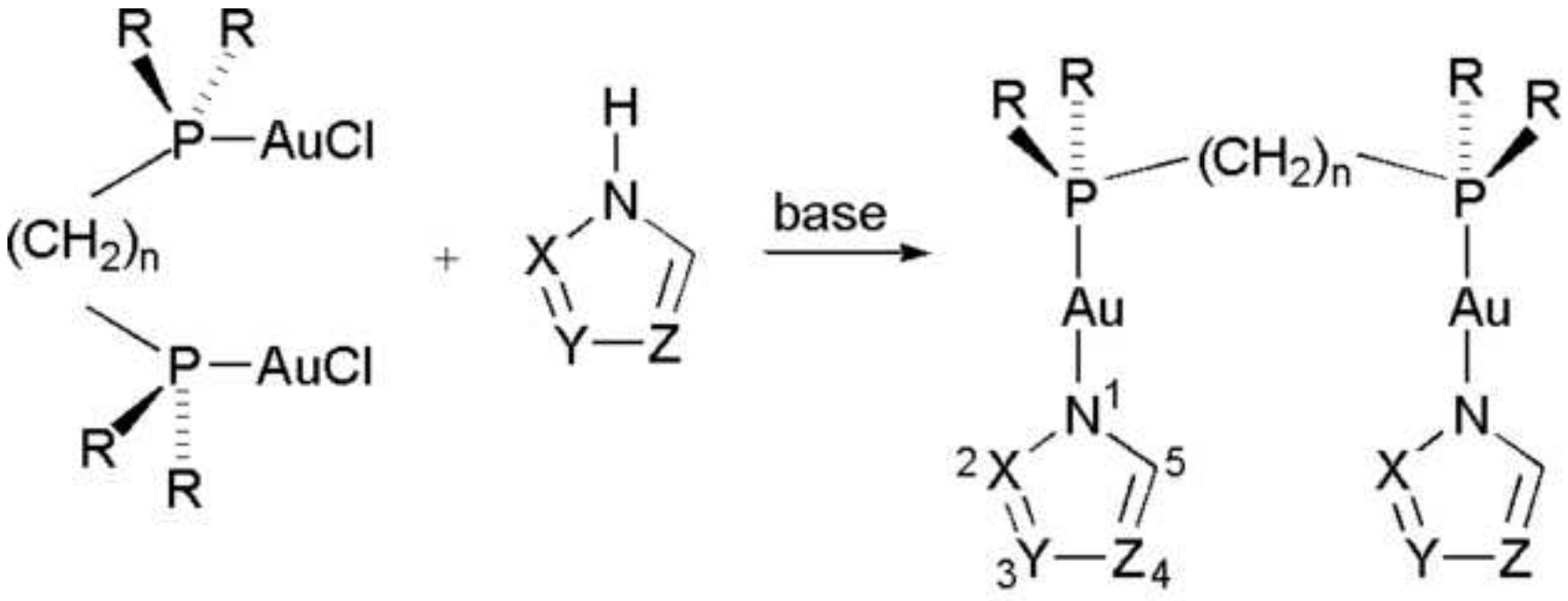

	R	n	X	Y	Z
1	Me	2	CH	N	CH
2	Ph	3	CH	N	CH
3	Ph	5	CH	N	CH
4	Ph	6	CH	N	CH
5	Me	2	N	CH	CH
6	Ph	2	N	CH	CH
7	Ph	3	N	CH	CH
8	Ph	5	N	CH	CH
9	Ph	6	N	CH	CH
10	Me	2	N	N	CH

	R	n	X	Y	Z
11	Ph	2	N	N	CH
12	Ph	2	N	N	CH
13	Ph	2	N	N	CH
14	Ph	2	N	N	CH
15	Ph	2	N	CH	N
16	Ph	3	N	CH	N
17	Ph	5	N	CH	N
18	Ph	6	N	CH	N
19	Me	2	CH	CH	CH

Scheme 1. Gold(I) complexes of imidazolate (1–5), pyrazolate (5–9), 1,2,3-triazolate (10–14), 1,2,4-triazolate (15–18) and pyrrolate (19).

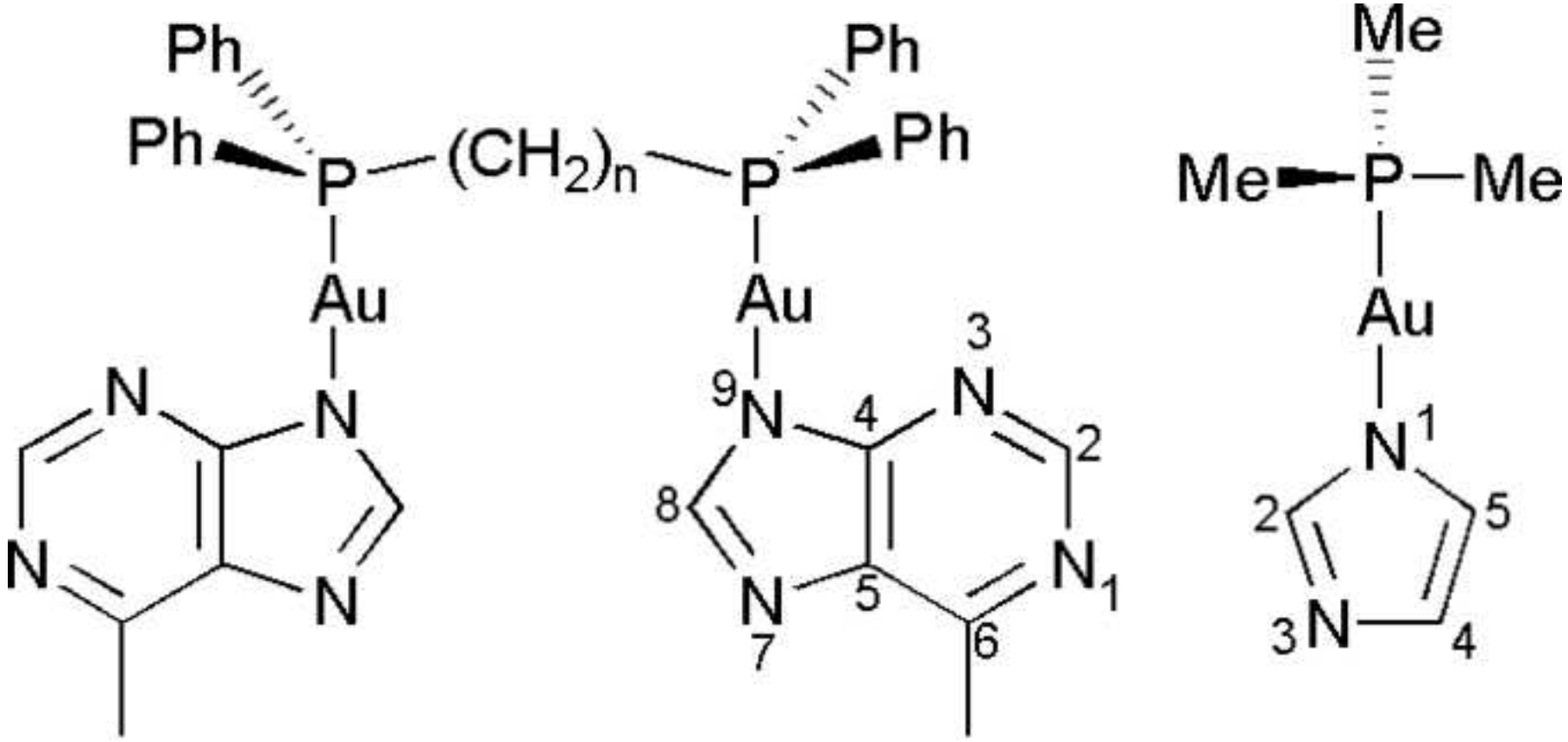

20 n = 5, X = NH_2

21 n = 6, X = NH_2

22 n = 3, X = H

23 n = 5, X = H

24 n = 6, X = H

25

Scheme 2. Dinuclear gold(I) complexes of purine-6-amine-9-ate (20 and 21), purine-9-ate (22, 23 and 24) and a monomeric imidazolate complex (25

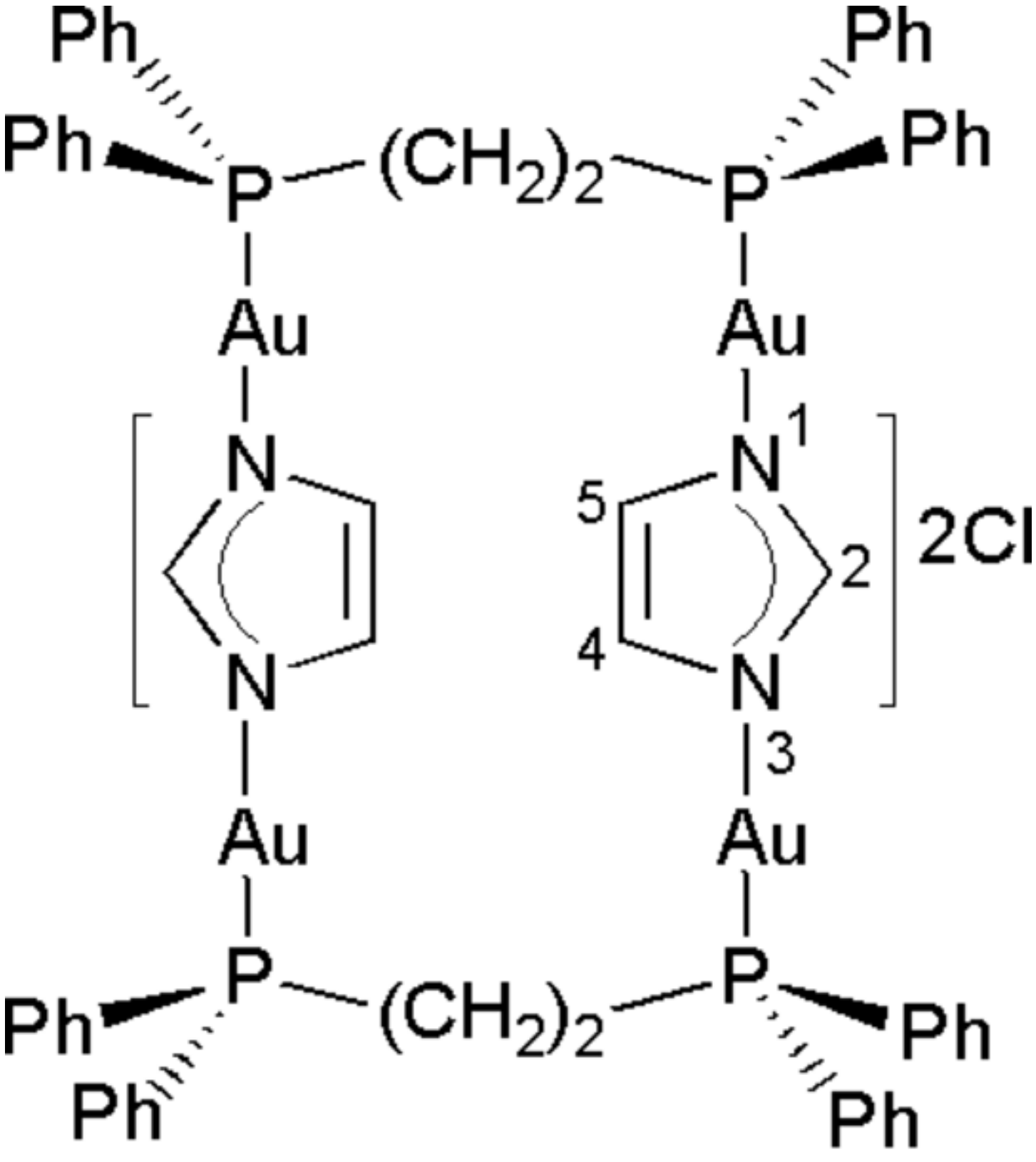

26

Scheme 3. Cyclic, cationic gold(I) diphosphine complex (26).

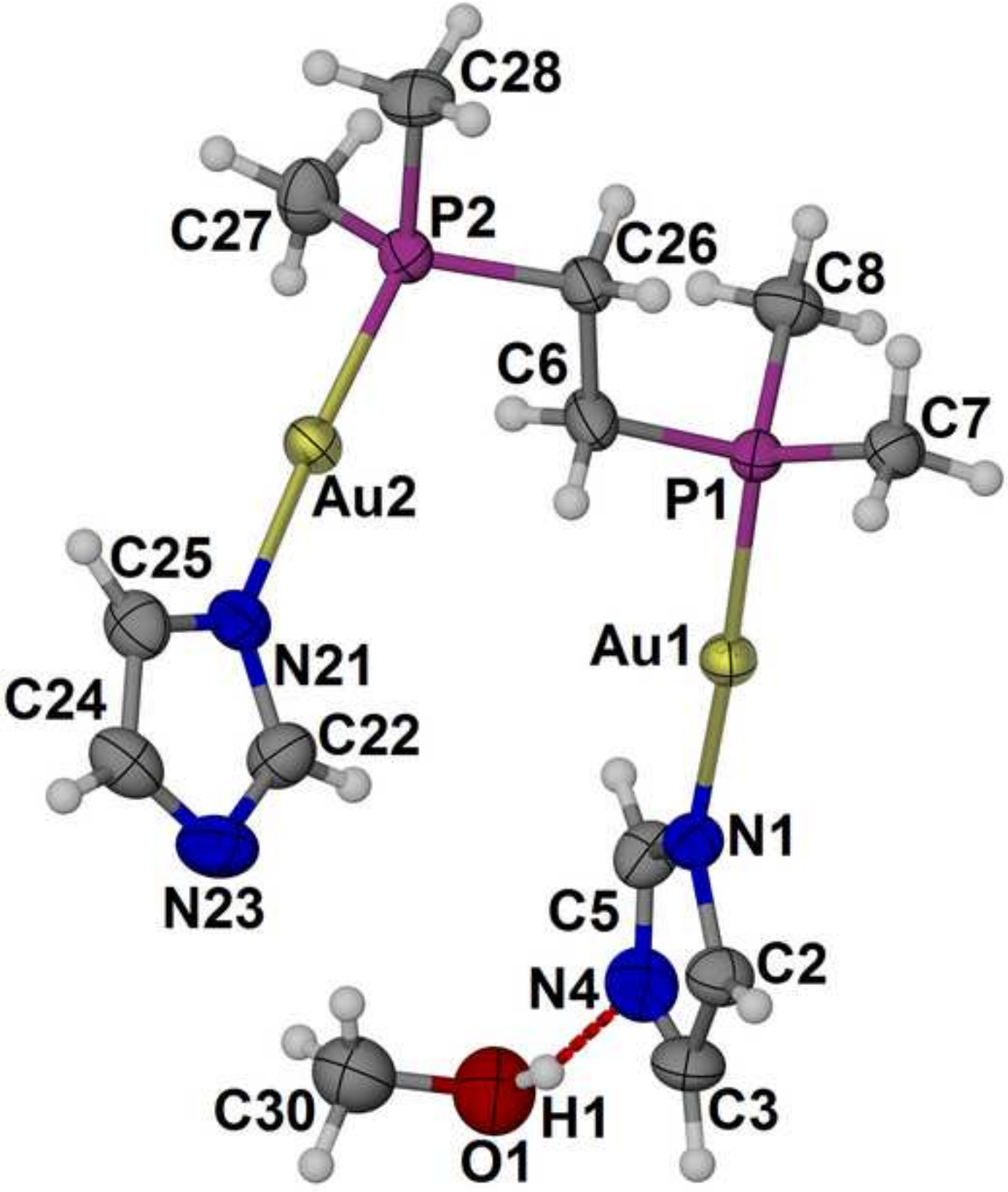

Fig. 1. Molecular structure of 1·MeOH (displacement ellipsoids at 50% probability) showing H-bonding with a methanol molecule by a dashed line.

Amides of gold(I) disphosphines prepared from N-heterocyclic sources and their *in vitro* and *in vivo* screening for anticancer activity

Ulrike E. I. Horvath[a], Liliana Dobrzańska[a,b], Christoph E. Strasser[a], Wilna Bouwer (neé Potgieter)[c], Gisela Joone[c], Constance E. Jansen van Rensburg[c], Stephanie Cronje[a,d] and Helgard G. Raubenheimer[a,*]

[a] *Department of Chemistry and Polymer Science, University of Stellenbosch, Private Bag X1, Matieland, 7602, Stellenbosch, South Africa*
[b] *Department of Chemistry, Katholieke Universiteit Leuven,Celestijnenlaan 200F - bus 2404, B-3001 Heverlee, Belgium,*
[c] *Department of Pharmacology, University of Pretoria, P.O. Box 2034, Pretoria 0001, South Africa*
[d] *Institut für Anorganische und Analytische Chemie, Goethe-Universität Frankfurt, Max-von-Laue-Strasse 7, D-60348 Frankfurt am Main, Germany*
*Corresponding author.
E-mail address: hgr@sun.ac.za (H. G. Raubenheimer)

Supplementary Information

SI 2.2.4 Crystal and molecular structures

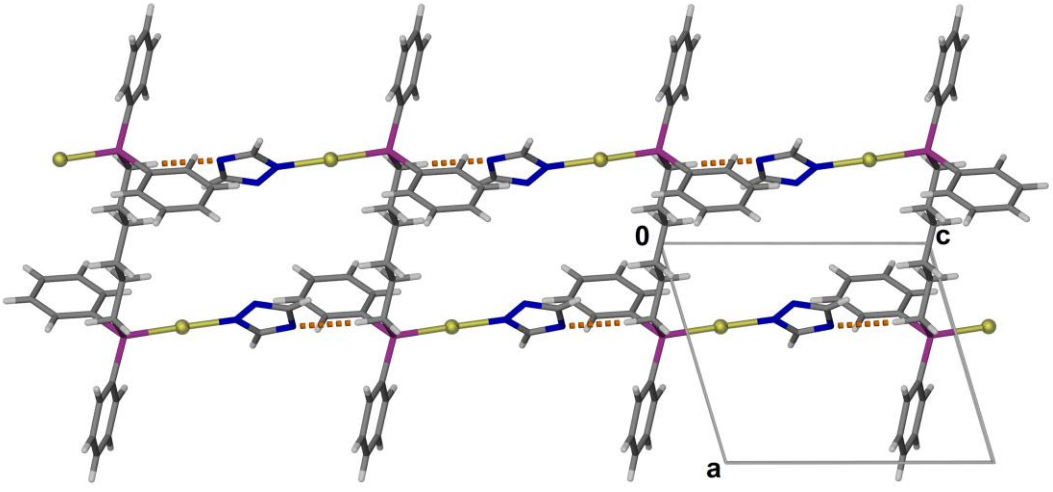

Fig. SI 1. Formation of a 1D railroad-like motif in **18** by C-H…N hydrogen bonds (dashed lines) shown down the b axis.

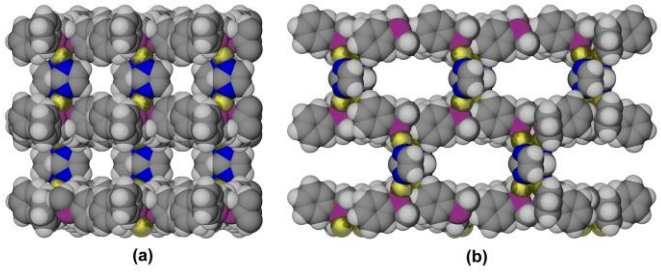

Fig. SI 2. Space filling packing of **26** showing the presence of channels along the a and c axes, (a) and (b), respectively, in which counterions and solvent molecules are located (not shown).

SI 2.5 Apoptosis

Table SI 1

Cell death pathway analysis of Jurkat cell lines after exposure to three different concentrations (μM) of each experimental compound at 48h of exposure (average of three experiments).

Compound	Concen-tration (μM)	Initial apoptosis	Advanced apoptosis	Necrosis	Non-vialble cells (%)
	Incubation time 48 hours, mean percentage (%) cells±SEM				
Control	-	32.9±0.18	7.10±0.30	8.86±0.05	48.86
7	0.119 [a]	27.73±0.09	6.96.±0.15	16.83±0.28*	51.52
	0.238 [b]	25.46±0.13	8.75±0.29	18.72±0.36*	52.93
	0.595 [c]	10.75±0.11*	19.34±0.08*	52.55±0.04*	82.64
17	0.075 [a]	29.59±0.02	9.21±0.14	18.87±0.18*	53.67
	0.150 [b]	28.79±0.17	10.29±0.15	22.58±0.18*	61.66
	0.375 [c]	16.65±0.06*	16.42±0.17*	43.39±0.09*	76.46
[Au(dppe)$_2$Cl]	0.081 [a]	27.36±0.04	8.05±0.21	19.51±0.18*	54.92
	0.162 [b]	25.20±0.11	9.83±0.05	26.46±0.17*	61.49
	0.405 [c]	15.87±0.02	5.92±0.19	38.16±0.02*	59.95
Cisplatin	0.413 [a]	30.08±0.15	7.79±0.15	16.41±0.28*	54.28
	0.826 [b]	32.99±0.09	10.52±0.24	15.17±0.33*	58.68
	2.065 [c]	33.01±0.06	9.78±0.25	15.96±0.30*	58.75

[a] IC_{50}, [b] $2\times IC_{50}$ and [c] $5\times IC_{50}$,* $p\leq 0.05$ when compared to the untreated control.

Results in Table SI 2 represent the ratio between green (FL1, indicating apoptic cells with depolarised MMPs) and orange (FL2, indicating cells with polarised MMPs) fluorescence of JC-1 (mitochondrial membrane stain).

Table SI 2
The mean ratioa between green and orange fluorescence of mitochondrial membrane stain, JC-1±SEM in cells treated for 24 h.

Compound	Concen-tration (μM)	Mean ratio Jurkat cells [FL1/FL2]	Concen-tration (μM)	Mean ratio PHA stimulated human lymphocytes [FL2/FL1]
cisplatin	0.413	460.0±6.8	11.650	765.0±3.2
	0.826	458.0±5.3	23.300	805.2±15.6
	2.065	499.7±42.2	58.250	787.0±17.0
[(dppe)$_2$Au]Cl	0.081	523.3±10.9[b]	0.192	468.4±38.0[b]
	0.162	568.3±5.2[b]	0.384	411.8±43.3[c]
	0.405	679.3±13.5[c]	0.960	407.5±7.5[d]
8	0.119	435.0±2.5	1.559	606.8±73.7
	0.238	421.3±3.2	3.118	526.8±49.7[b]
	0.595	558.7±15.9[b]	7.795	471.0±6.0[b]
17	0.075	427.7±1.5	1.454	613.0±66.6
	0.150	436.3±7.3	2.908	564.3±59.7
	0.375	456.0±13.4	7.270	436.0±13.0
valinomycin	10	737.0±13.1[d]	10.000	459.7±18.7[c]
control untreated	0	430.0±14.0	-	729.3±11.3

[a] Mean of three independent experiments, [b] $p < 0.05$,[c] $p < 0.01$ and [d] $p < 0.001$ compared to the untreated control.

SI 2.7 Effects on cell division

Table SI 3
Cell cycle analysis [a] of Jurkat cell lines after 24 h exposure to different concentrations of each experimental compound.

Compound	Concen-tration (μM)	G1 phase	S phase	G2/M phase
	(mean percentage (%) cells±SEM)			
Control	-	62.02±0.05	33.41±0.03	4.66±0.45
8	0.119 [b]	66.76±0.09	27.45.±0.21	5.76±0.90
	0.238 [c]	64.51±0.04	29.52±0.03[f]	5.99±0.56
	0.595 [d]	69.75±0.08[e]	25.20±0.08[f]	5.06±0.72
17	0.075 [b]	60.31±0.03	32.47±0.08	7.22±0.41
	0.150 [c]	66.62±0.11	27.23±0.15[f]	6.16±0.51
	0.375 [d]	61.18±0.03	32.49±0.09	6.33±0.20
[(dppe)$_2$Au]Cl	0.081 [b]	72.27±0.05[e]	24.64±0.09[f]	3.09±0.54
	0.162 [c]	74.43±0.04[e]	22.56±0.12[f]	2.99±0.03
	0.405 [d]	67.02±0.19	23.05±0.38[f]	9.91±0.90
Cisplatin	0.413 [b]	57.33±0.06	38.95±0.08[e]	3.72±0.86
	0.826 [c]	60.80±0.09	36.15±0.09[e]	3.05±0.73
	2.065 [d]	51.61±0.16	41.22±0.16[e]	7.17±0.70

[a] Average of three independent experiments; [b] IC_{50}, [c] $2 \times IC_{50}$ and [d] $5 \times IC_{50}$,
[e] $p \leq 0.05$ higher value when compared to the untreated control, [f] $p \leq 0.05$ lower value when compared to the untreated control

Table SI 4
Cell cycle analysis of Jurkat cell lines after exposure to different concentrations of each experimental compound after 48 hours exposure.

Compound	Concen-tration (μM)	G1 phase	S phase	G2/M phase
	Incubation time 48 hours, mean percentage (%) cells±SEM (average of three experiments)			
Control	-	55.93±0.10	34.02±0.01	10.05±0.01
7	0.119 [a]	57.78±0.09	37.62.±0.20	4.60±1.01*
	0.238 [b]	64.22±0.08*	31.25±0.10	4.20±0.45*
	0.595 [c]	60.34±0.01*	33.53±0.04	6.13±0.08*
17	0.075 [a]	58.01±0.03	35.56±0.05	5.76±0.20*
	0.150 [b]	59.39±0.06	33.80±0.07	6.80±0.22*
	0.375 [c]	64.62±0.03*	29.27±0.10	5.44±0.16
[Au(dppe)$_2$Cl]	0.081 [a]	62.75±0.07*	32.89±0.14	4.36±0.44*
	0.162 [b]	63.97±0.08*	30.57±0.14*	5.46±0.45*
	0.405 [c]	62.44±0.03*	34.62±0.07	2.42±0.36*
Cisplatin	0.413 [a]	53.94±0.01*	40.46±0.07*	5.60±0.47*
	0.826 [b]	54.13±0.08	39.23±0.02*	6.64±0.51*
	2.065 [c]	51.06±0.06*	42.65±0.05*	6.29±0.35*

[a] IC_{50}, [b] $2\times IC_{50}$ and [c] $5\times IC_{50}$,* $p \leq 0.05$ when compared to the untreated control.

SI 2.7 Assessment of in vivo acute toxicity

Table SI 5
Mean daily body weights (g) of mice that received only the control solvent mixture (DMSO–olive oil), complex **8** or complex **17** (both at 1.5 μmol/kg) for five consecutive days (phase 1).

Day	Control	**8** (1.5 μmol/kg)	**17** (1.5 μmol/kg)
	Body weight (g)±SEM	Body weight (g)±SEM	Body weight (g)±SEM
1	20.27±0.66	18.90±0.35	18.76±0.58
2	20.45±0.73	15.12±0.28[a]	17.31±0.54
3	20.78±0.68	17.89±0.44[b]	17.20±0.66
4	21.35±0.71	17.62±0.39[b]	17.61±0.65
5	21.40±0.68	18.24±0.30	17.54±0.58
6	21.20±0.74	18.27±0.31	17.63±0.51

[a] $p \leq 0.01$ when the mean weight of the group receiving **8** (1.5 μmol/kg) on the relevant day is compared to the mean weight on day 1 of the same group, [b] $p \leq 0.05$ when the mean weight of the group receiving **8** (1.5 μmol/kg) on the relevant day is compared to the mean weight on day 1 of the same group.

Table SI 6
Mean daily body weights (g) of mice that received only the control solvent mixture (DMSO–olive oil) or two different concentrations of complex **8** for five consecutive days (phase 2).

Day	Control	**8** (3 μmol/kg)	**8** (6 μmol/kg)
	Body weight (g)±SEM	Body weight (g)±SEM	Body weight (g)±SEM
1	19.10±0.25	18.92±0.55	19.10±0.75
2	19.88±0.29[a]	19.65±0.49	19.37±0.89
3	20.12±0.34[a]	19.98±0.46	20.10±0.68
4	19.98±0.41[a]	18.48±0.33	18.86±0.65
5	20.17±0.37[a]	18.05±0.29[c]	18.13±0.59
6	20.48±0.32[b]	17.87±0.36[c]	17.80±0.52[d]

[a] $p \leq 0.05$ when the mean weight of the untreated control group on the relevant day is compared to the mean weight on day 1 of the same group; [b] $p \leq 0.01$ when the mean weight of the untreated control group on the relevant day is compared to the mean weight on day 1 of the same group; [c] $p \leq 0.05$ when the mean weight of the group receiving **7** (3 μmol/kg) on the relevant day is compared to the mean weight on day 1 of the same group; [d] $p \leq 0.05$ when the mean weight of the group receiving **7** (6 μmol/kg) on the relevant day is compared to the mean weight on day 1 of the same group.

Table SI 7
Mean daily body weights (g ± SEM) of mice that received only the control solvent mixture (DMSO–olive oil) or two different concentrations of complex **17** for five consecutive days (phase 3).

Day	Control	**17** (3 μmol/kg)	**17** (6 μmol/kg)
	Body weight (g)±SEM	Body weight (g)±SEM	Body weight (g)±SEM
1	17.38±0.65	18.01±0.36	17.66±0.49
2	17.92±0.76	18.56±0.37	17.85±0.45
3	18.41±0.80	17.79±0.31	16.72±0.41
4	18.53±0.77	17.13±0.39	16.21±0.31[b]
5	18.93±0.87	16.44±0.49[a]	16.08±0.58
6	19.18±0.78	16.35±0.51[a]	15.09±0.35[b]

[a] $p \leq 0.05$ when the mean weight of the group receiving **17** (3 μmol/kg) on the relevant day is compared to the mean weight on day 1 of the same group; [b] $p \leq 0.05$ when the mean weight of the group receiving **17** (6 μmol/kg) on the relevant day is compared to the mean weight on day 1 of the same group.

Table SI 8

Average body weights of mice for test phases 1-3 expressed as % of the weight on day one (100)

Phase 1 (%)			Phase 2 (%)			Phase 3 (%)		
Control	**8** (1.5 μmol/kg)	**17** (1.5 μmol/kg)	Control	**8** (3 μmol/kg)	**8** (6 μmol/kg)	Control	**17** (3 μmol/kg)	**17** (6 μmol/kg)
100	100	100	100	100	100	100	100	100
100.87	80.01	92.26	104.06	103.87	101.42	103.11	103.05	101.09
102.50	94.66	91.69	105.32	105.61	105.24	105.89	98.76	94.70
105.32	93.24	93.84	104.58	97.66	98.72	106.60	95.11	91.77
105.58	96.56	93.47	105.60	95.38	94.90	108.92	91.26	91.07
104.58	96.67	93.96	107.21	94.48	93.16	110.35	90.75	85.45

Table SI 9
Mean plasma concentrations of AST, ALT, GGT, creatinine and urea in mouse plasma after administration of three different concentrations of **8** and **17** once daily over a period of five consecutive days.

Mean concentration ± SEM	Control	**8** (1.5 μmol/kg)	**17** (1.5 μmol/kg)	**8** (3 μmol/kg)	**17** (3 μmol/kg)	**8** (6 μmol/kg)	**17** (6 μmol/kg)
AST (U/l)	146.70±24.38	204.70±50.05	195.00 ± 58.81	116.70±13.58	132.70±10.73	102.80±7.86	191.70±33.21
ALT (U/l)	25.46 ±4.76	18.25±2.10	25.50 ± 8.38	19.80±2.33	19.05±6.50	20.33±4.07	26.00±6.00
GGT (U/l)	6.58 ±1.91	3.33±1.84	2.00 ± 2.00	7.80±2.52	12.67±5.49	6.50±0.72	33.33±5.70 [a]
Creatinine (μmol/l)	31.29 ±2.25	29.17±6.65	31.60± 3.70	32.17±2.01	25.33±2.40	33.83±1.42	32.67±2.67
Urea (mmol/l)	6.11 ±0.21	7.23±0.56[a]	6.25± 0.52	7.10±0.53	7.90±0.35 [a]	7.74±0.60	6.73±0.57

[a] $p \leq 0.05$ when compared to the untreated control.

Table SI 10
The effects of **8** and **17** on the organ/body weight ratio.

Compound	Concentration (μmol/kg)	Left kidney	Right kidney	Liver	Heart
		Ratio [(organ weight/body weight) × 1000] ± SEM			
Control (n = 15)	N/A	5.326 ± 0.010	5.863 ± 0.012	45.293 ± 0.123	5.033 ± 0.016
8 (n = 6)	1.5	6.066 ± 0.007[a]	6.503 ± 0.011[a]	51.347 ± 0.054[a]	4.972 ± 0.007
8 (n = 6)	3	6.100 ± 0.013[a]	6.323 ± 0.011[a]	49.301 ± 0.122[a]	5.036 ± 0.007
8 (n = 6)	6	5.900 ± 0.01[a]	6.069 ± 0.015[a]	44.675 ± 0.101	5.170 ± 0.013
17 (n = 6)	1.5	6.214 ± 0.013[a]	6.442 ± 0.011[a]	49.915 ± 0.122[a]	5.131 ± 0.007
17 (n = 3)	3	6.882 ± 0.000[a]	7.061 ± 0.002[a]	47.397 ± 0.046	5.685 ± 0.009[a]
17 (n = 3)	6	6.689 ± 0.009[a]	7.224 ± 0.008[a]	44.816 ± 0.053	7.358 ± 0.005[a]

[a] $p \leq 0.05$ when compared to the untreated control.

Table SI 11
The mean full blood counts of mice that received three different doses of **8** and **17** for five consecutive days; data is expressed as mean ± standard error of the mean (SEM).

	Control (n = 15)	**8** 1.5 μmol/kg (n = 6)	**8** 3 μmol/kg (n = 6)	**8** 6 μmol/kg (n = 6)	**17** 1.5 μmol/kg (n = 6)	**17** 3 μmol/kg (n = 3)	**17** 6 μmol/kg (n = 3)
Hb (g/l)	153.8 ± 16.40	144.5 ± 6.70	165.83 ± 13.00[a]	170.67 ± 15.12[a]	136.67 ± 15.04[a]	145.67 ± 2.89	142.33 ± 3.78
RCC ($\times 10^{12}$/l)	9.10 ± 0.61	8.92 ± 0.41	9.75 ± 0.40[a]	9.69 ± 0.16[a]	8.54 ± 0.97	9.37 ± 0.05	9.25 ± 0.25
HT (l/l)	0.43 ± 0.03	0.42 ± 0.02	0.46 ± 0.02[a]	0.45 ± 0.01[a]	0.40 ± 0.05	0.44 ± 0.01	0.42 ± 0.01
MCV (fl)	47.05 ± 1.29	47.03 ± 0.48	46.75 ± 0.67	46.50 ± 0.55	46.25 ± 0.45[a]	46.40 ± 0.44	45.60 ±1.15[a]
MCH (g/dl)	16.92 ± 1.59	16.17 ± 0.37	17.07 ± 1.55	17.62 ± 1.62	16.00 ± 0.19	15.53 ± 0.23[a]	15.37 ± 0.38[a]
MCHC (g/dl)	35.97 ± 3.24	34.40 ± 0.49	36.42 ± 3.24	37.92 ± 3.53	34.62 ± 0.33	33.43 ± 0.23[a]	33.80 ± 0.10[a]
WCC ($\times 10^9$/l)	5.53 ± 3.50	7.35 ± 6.51	7.26 ± 5.01	4.33 ± 2.03	3.46 ± 0.76	4.23 ± 2.14	7.80 ± 2.35
RDW (%)	18.23 ± 0.97	18.08 ± 1.08	17.48 ± 0.58	17.63 ± 1.19	17.58 ± 0.56	19.43 ± 0.97[a]	20.17 ± 1.12[a]

[a] $p \leq 0.05$ when compared to the untreated control.

SI 4.1 Synthesis and characterization

*SI 4.1.3 Preparation of bis(1H-imidazolato-κN^1){μ-[1,3-propanediylbis(diphenylphosphine-κP)]}digold(I), **2***

The same procedure as for **1**in the main text was followed but using NaOH (0.022 g, 0.55 mmol), imidazole (0.038 g, 0.56 mmol) and (μ-1,3-bis(diphenylphosphino)propane)bis(chlorogold) (0.25 g, 0.28 mmol) to afford **2** as a colourless, microcrystalline material. Yield: 0.15 g, 55%. Mp: 89 °C (dec). IR (KBr, cm^{-1}): ν(aromatic C-H) 3111m, 3051m; ν(aliphatic C-H) 2914m. ^{1}H NMR (300 MHz, CD_2Cl_2): δ = 7.67 (8 H, m, *m*-C_6H_5), 7.56 (4 H, m, *p*-C_6H_5), 7.48 (8 H, m, *o*-C_6H_5), 7.38 (2 H, s, H2), 7.03 (4 H, s, H4, H5), 2.89 (4 H, m, P-CH_2CH_2CH_2-P), 1.99 (2 H, m, P-CH_2CH_2CH_2-P). ^{13}C NMR (75 MHz, CH_2Cl_2): δ = 142.8 (s, C2), 133.9 (d, ^3J = 12.8 Hz, *m*-C_6H_5), 132.9 (d, ^4J = 1.8 Hz, *p*-C_6H_5), 130.1 (d, ^2J = 11.6 Hz, *o*-C_6H_5), 128.9 (d, ^1J = 60.9 Hz, *i*-C_6H_5), 126.0 (bs, C4, C5), 28.1 (dd, ^1J = 37.8 Hz, ^3J = 11.6 Hz, P-*C*H_2CH_2*C*H_2-P), 20.4 (bs, P-

$CH_2CH_2CH_2$-P). ^{31}P NMR (121 MHz, CD_2Cl_2): δ = 24.4 (s). ESI MS: m/z (%): 940 [M^+, 3%], 873 [M^+-imidazol-N-yl, 8]. FAB MS: m/z (%) 873 [M^+-imidazol-N-yl, 4%]. Anal. Calc. for $C_{33}H_{32}Au_2N_4P_2$·: C, 42.14; H, 3.43; N, 5.86, found: C, 41.73; H, 3.32; N, 5.98 %.

SI 4.1.4 Preparation of bis(1H-imidazolato-κN^1){μ-[1,5-pentanediylbis(diphenylphosphine-κP)]}digold(I), ***3***

Preparation of **3** followed the same method as for **1** using NaOH (0.059 g, 1.5 mmol), imidazole (0.10 g, 1.5 mmol) and (μ-1,5-bis(diphenylphosphino)pentane)bis(chlorogold) (0.67 g, 0.74 mmol) to give **3** as a colourless, microcrystalline material. Yield: 0.38 g, 53%. Mp: 68 °C. IR (KBr, cm^{-1}): ν(aromatic C-H) 3113s, 3088s, 3051s; ν(aliphatic C-H) 2924s, 2854m; ν(C=N) 1647w. ^{1}H NMR (300 MHz, CD_2Cl_2): δ = 7.70 (8 H, m, *m*-C_6H_5), 7.54 (12 H, m, *p*- and *o*-C_6H_5), 7.46 (2 H, s, H2), 7.06 (4 H, s, H4, H5), 2.44 (4 H, m, P-CH_2(CH_2)$_3$CH_2-P), 1.70 (6 H, m, P-CH_2(CH_2)$_3$$CH_2$-P). ^{13}C NMR (75 MHz, CD_2Cl_2): δ = 142.7 (s, C2), 133.9 (d, ^3J = 12.8 Hz, *m*-C_6H_5), 132.7 (d, ^4J = 3.1 Hz, *p*-C_6H_5), 130.1 (d, ^2J = 11.6 Hz, *o*-C_6H_5), 129.9 (d, ^1J = 59.7 Hz, *i*-C_6H_5), 125.9 (bs, C4, C5), 31.8 (t, ^3J = 15.9 Hz, P-(CH_2)$_2$CH_2(CH_2)$_2$-P), 27.7 (d, ^1J = 37.8 Hz, P-CH_2(CH_2)$_3$CH_2-P), 25.3 (d, ^2J = 3.1 Hz, P-CH_2C$H_2$$CH_2CH_2$$CH_2$-P). ^{31}P NMR (121 MHz, CD_2Cl_2): δ = 28.1 (s). ESI MS: m/z (%): 901 [M^+-$C_3H_3N_2$, 91%], 637 [(dpppe)Au^+, 22]. FAB MS: m/z (%) 901 [M^+-imidazol-N-yl), 36%], 637 [(dpppe)Au^+, 44]. Anal. calc. for $C_{35}H_{36}Au_2N_4P_2$: C, 43.40; H, 3.75; N, 5.78, found: C, 43.18; H, 3.51; N, 5.82 %.

SI 4.1.5 Preparation of {μ-[1,6-hexanediylbis(diphenylphosphine-κP)]}bis(1H-imidazolato-κN^1)digold(I), ***4***

A suspension of imidazole (0.066 g, 0.97 mmol) and (μ-1,6-bis(diphenylphosphino)hexane)bis(chlorogold) (0.40 g, 0.44 mmol) in DME (20 cm^3) was treated with NaOH (0.039 g, 0.98 mmol) dissolved in H_2O (1 cm^3) and stirred for 1 h at room temperature. The mixture was reduced to dryness *in vacuo*. The crude product was washed with H_2O (2 x 30 cm^3), Et_2O (3 x 15 cm^3), then dissolved in CH_2Cl_2 (20 cm^3), preupitation with ether, filtered and stripped of solvent. The residue was dried *in vacuo*, to give **4** as a beige microcrystalline material. Yield: 0.31 g, 65%. Mp: 102 °C (dec). IR (KBr, cm^{-1}): ν(aromatic C-H) 3117m, 3090m, 3049m; ν(aliphatic C-H) 2924m, 2912s; ν(C=N) 1639m. ^{1}H NMR (300 MHz, CD_2Cl_2): δ = 7.71 (8 H, m, *m*-C_6H_5), 7.54 (12 H, m, *p*- and *o*-C_6H_5), 7.44 (2 H, s, H2), 7.07 (4 H, s, H4, H5), 2.44 (4 H, m, P-CH_2(CH_2)$_4$CH_2-P), 1.58 (8 H, m, P-CH_2(CH_2)$_4$$CH_2$-P). ^{13}C NMR (75 MHz, CD_2Cl_2): δ = 143.1 (s, C2), 133.9 (d, ^3J = 12.7 Hz, *m*-C_6H_5), 132.6 (d, ^4J = 2.5 Hz, *p*-C_6H_5), 130.1 (d, ^1J = 59.3 Hz, *i*-C_6H_5), 129.9 (d, ^2J = 11.3, *o*-C_6H_5), 126.0 (bs, C4, C5), 30.5 (d, ^3J = 15.5 Hz, P-(CH_2)$_2$(CH_2)$_2$(CH_2)$_2$-P), 27.8 (d, ^1J = 37.9 Hz, P-CH_2(CH_2)$_4$CH_2-P), 25.7 (d, ^2J = 2.6 Hz, P-CH_2CH_2(CH_2)$_2$C$H_2$$CH_2$-P). ^{31}P NMR (121 MHz, CD_2Cl_2): δ = 28.6 (s). FAB MS: m/z (%) 915 [M^+-imidazol-N-yl, 29%], 651 [(dpph)Au, 20]. Anal. calc. for $C_{36}H_{38}Au_2N_4P_2$: C, 44.01; H, 3.90; N, 5.70, found: C, 43.87; H, 4.06; N, 5.33 %.

SI 4.1.6 Preparation of {μ-[1,2-ethanediylbis(dimethylphosphine-κP)]}bis(1H-pyrazolato-κN^1)digold(I), ***5***

A mixture of NaOH (0.082 g, 2.1 mmol), pyrazole (0.14 g, 2.1 mmol) and (μ-1,2-bis(dimethylphosphino)ethane)bis(chlorogold) (0.62 g, 1.0 mmol) in MeOH (20 cm^3) was stirred for 1 h at room temperature, followed by filtration through Na_2SO_4. The filtrate was reduced to dryness *in vacuo*. The crude product was treated with CH_2Cl_2 (30 cm^3), followed by filtration through Na_2SO_4, preupitation with ether, filtration and solvent removal. The residue was dried *in vacuo*, to give **5** as a colourless, microcrystalline material. Yield: 0.46 g, 68%. Mp: 74-85 °C. IR (KBr, cm^{-1}): ν(aromatic C-H) 3082m;

ν(aliphatic C-H) 2970m, 2902m; ν(C=N) 1635m. ^{1}H NMR (300 MHz, CD_2Cl_2): δ = 7.59 (4 H, d, ^{3}J = 1.8 Hz, H3, H5), 6.31 (2 H, t, ^{3}J = 1.8 Hz, H4), 2.12 (4 H, s, P-$(CH_2)_2$-P), 1.57 (12 H, bs, CH_3). ^{13}C NMR (75 MHz, CD_2Cl_2): δ = 138.3 (bs, C3, C5), 103.6 (s, C4), 25.1 (t, ^{1}J = 19.2 Hz, P-$(CH_2)_2$-P), 13.6 (t, ^{3}J = 18.6 Hz, CH_3). ^{31}P NMR (121 MHz, CD_2Cl_2): δ = 20.4 (s). FAB MS: m/z (%) 875 [M^++Au, 8%], 611 [M^+-pyrazol-N-yl), 100]. Anal. calc. for $C_{12}H_{22}Au_2N_4P_2$: C, 21.25; H, 3.27; N, 8.26, found: C, 21.20; H, 2.87; N, 8.48 %.

SI 4.1.7 Preparation of {μ-[1,2-ethanediylbis(diphenylphosphine-κP)]}bis(1H-pyrazolato-κN^1)digold(I), ***6***

The procedure used for **5** was followed using pyrazole (0.054 g, 0.79 mmol), NaOH (0.032 g, 0.80 mmol) and (μ-1,2-bis(diphenylphosphino)ethane)bis(chlorogold) (0.35 g, 0.41 mmol) to obtain **6** as a colourless, microcrystalline material. Yield: 0.21 g, 57%. Mp: 95-102 °C. IR (KBr, cm^{-1}): ν(aromatic C-H) 3118s, 3082s; ν(aliphatic C-H) 2958m, 2906m; ν(C=N) 1647w. ^{1}H NMR (600 MHz, CD_2Cl_2): δ = 7.65 (8 H, m, *m*-C_6H_5), 7.52 (4 H, m, *p*-C_6H_5), 7.44 (12 H, m, *o*-C_6H_5, H3, H5), 6.34 (2 H, s, H4), 2.75 (4 H, s, P-$(CH_2)_2$-P). ^{13}C NMR (151 MHz, CD_2Cl_2): δ = 137.7 (bs, C3, C5), 133.7 ("t", ^{3}J = 6.7 Hz, *m*-C_6H_5), 132.6 (s, *p*-C_6H_5), 129.8 ("t", ^{2}J = 5.5 Hz, *o*-C_6H_5), 129.8 ("t", ^{1}J = 29.9 Hz, *i*-C_6H_5), 103.3 (s, C4), 24.0 (t, ^{1}J = 20.2 Hz, P-$(CH_2)_2$-P). ^{31}P NMR (121 MHz; CD_2Cl_2): δ = 29.8 (s). FAB MS m/z (%): 859 [M^+-pyrazole, 9%]. Anal. calc. for $C_{32}H_{30}Au_2N_4P_2$·: C, 41.45; H, 3.26; N, 6.05, found: C, 40.96; H, 3.30; N, 5.88 %.

SI 4.1.8 Preparation of {μ-[1,3-propanediylbis(diphenylphosphine-κP)]}bis(1H-pyrazolato-κN^1)digold(I), ***7***

The same procedure as described for **5** was followed using pyrazole (0.078 g, 1.2 mmol), NaOH (0.046 g, 1.2 mmol) and (μ-1,3-bis(diphenylphosphino)propane)bis(chlorogold) (0.50 g, 0.57 mmol) to attain **7** as a colourless, microcrystalline material. Yield: 0.39 g, 52%. Mp: 82 °C (dec). IR (KBr, cm^{-1}): ν(aromatic C-H) 3117m, 3074m; ν(aliphatic C-H) 2906m; ν(C=N) 1628m. ^{1}H NMR (300 MHz, CD_2Cl_2): δ = 7.69 (12 H, m, *m*-C_6H_5, H3, H5), 7.52 (4 H, m, *p*-C_6H_5), 7.43 (8 H, m, *o*-C_6H_5), 6.35 (2 H, s, H4), 2.90 (4 H, m, P-CH_2CH$_2$CH_2-P), 1.97 (2 H, m, P-CH$_2$CH_2CH$_2$-P). ^{13}C NMR (75 MHz, CD_2Cl_2): δ = 138.0 (bs, C3, C5), 134.1 (d, ^{3}J = 12.8 Hz, *m*-C_6H_5), 132.6 (d, ^{4}J = 1.9 Hz, *p*-C_6H_5), 130.0 (d, ^{2}J = 11.5 Hz, *o*-C_6H_5), 129.1 (d, ^{1}J = 60.2 Hz, *i*-C_6H_5), 103.6 (s, C4), 28.1 (dd, ^{1}J = 37.8, ^{3}J = 11.5 Hz, P-*C*H$_2$CH$_2$*C*H$_2$-P), 20.3 (bs, P-CH$_2$*C*H$_2$CH$_2$-P). ^{31}P NMR (121 MHz, CD_2Cl_2): δ = 24.8 (s). FAB MS: m/z (%) 873 [M^+-pyrazol-N-yl, 100%]. Anal. calc. for $C_{33}H_{32}Au_2N_4P_2$·0.50CH_2Cl_2: C, 40.93; H, 3.38; N, 5.70, found: C, 40.79; H, 2.98; N, 6.08 %.

SI 4.1.9 Preparation of {μ-[1,5-pentanediylbis(diphenylphosphine-κP)]}bis(1H-pyrazolato-κN^1)digold(I), ***8***

Using pyrazole (0.068 g, 1.0 mmol), (μ-1,5-bis(diphenylphosphino)pentane)bis(chlorogold) (0.45 g, 0.50 mmol) and NaOH (0.040 g, 1.0 mmol) dissolved in H_2O (1 cm^3) and DME (20 cm^3) instead of MeOH in the method as described for **5**, **8** was acquired as a beige, microcrystalline material. Yield: 0.29 g, 60%. Mp: 51-55 °C. IR (KBr, cm^{-1}): ν(aromatic C-H) 3118w, 3051s; ν(aliphatic C-H) 2964s, 2921s. ^{1}H NMR (300 MHz, CD_2Cl_2): δ = 7.72 (8 H, m, *m*-C_6H_5), 7.62 (4 H, d, ^{3}J = 1.9 Hz, H3, H5), 7.61 (12 H, m, *p*- and *o*-C_6H_5), 6.34 (2 H, t, ^{3}J = 1.9 Hz, H4), 2.46 (4 H, m, P-CH_2(CH$_2$)$_3$CH_2-P), 1.70 (6 H, m, P-CH$_2$(CH_2)$_3$CH$_2$-P). ^{13}C NMR (75 MHz, CD_2Cl_2): δ = 137.5 (C3, C5), 133.9 (d, ^{3}J = 13.4 Hz, *m*-C_6H_5), 132.5 (s, *p*-C_6H_5), 129.9 (d, ^{1}J = 59.7 Hz, *i*-C_6H_5), 129.8 (d, ^{2}J = 11.6 Hz, *o*-C_6H_5), 103.7 (s, C4), 31.5 (t, ^{3}J = 15.2 Hz, P-$(CH_2)_2$*C*H$_2$(CH$_2$)$_2$-P), 27.5 (d, ^{1}J = 37.2 Hz, P-*C*H$_2$(CH$_2$)$_3$*C*H$_2$-P), 25.0 (d, ^{2}J = 1.2 Hz, P-CH$_2$*C*H$_2$CH$_2$*C*H$_2$CH$_2$-P). ^{31}P NMR

(121 MHz, CD_2Cl_2): δ = 27.6 (s). FAB MS: m/z (%) 901 [M^+-pyrazol-N-yl, 4%], 637 [(dpppe)Au^+, 2]. Anal. calc. for $C_{35}H_{36}Au_2N_4P_2$ requires C, 43.40; H, 3.75; N, 5.78, found: C, 43.34; H, 3.69; N, 6.04 %.

SI 4.1.10 Preparation of {μ-[1,6-hexanediylbis(diphenylphosphine-κP)]}bis(1H-pyrazolato-κN^1)digold(I), ***9***

According to the description for **4**, deprotonation of pyrazole (0.063 g, 0.93 mmol) with NaOH (0.037 g, 0.93 mmol) in the presence of (μ-1,6-bis(diphenylphosphino)hexane)bis(chlorogold) (0.40 g, 0.44 mmol) yielded **9** as a beige, microcrystalline material. Yield: 0.23 g, 53%. Mp: 61-64 °C. IR (KBr, cm^{-1}): ν(aromatic C-H) 3118m, 3076m, 3049m; ν(aliphatic C-H) 2966m, 2924m. ^{1}H NMR (300 MHz, CD_2Cl_2): δ = 7.73 (8 H, m, *m*-C_6H_5), 7.62 (4 H, d, ^3J = 1.8 Hz, H3, H5), 7.51 (12 H, m, *p*- and *o*-C_6H_5), 6.35 (2 H, t, ^3J = 1.8 Hz, H4), 2.44 (4 H, m, P-C$H_2$$(CH_2)_4CH_2$-P), 1.63 (4 H, m, P-$CH_2CH_2$$(CH_2)_2CH_2$$CH_2$-P), 1.48 (4 H, m, P-$(CH_2)_2$$(CH_2)_2$$(CH_2)_2$-P). ^{13}C NMR (75 MHz, CD_2Cl_2): δ = 138.7 (s, C3, C5), 133.9 (d, ^3J = 12.7 Hz, *m*-C_6H_5), 132.5 (d, ^4J = 2.4 Hz, *p*-C_6H_5), 130.2 (d, ^1J = 60.0 Hz, *i*-C_6H_5), 129.9 (d, ^2J = 11.3 Hz, *o*-C_6H_5), 103.0 (s, C4), 30.3 (d, ^3J = 15.2 Hz, P-$(CH_2)_2$$(CH_2)_2$$(CH_2)_2$-P), 27.7 (d, ^1J = 37.7 Hz, P-$CH_2$$(CH_2)_4$$CH_2$-P), 25.6 (s, P-$CH_2$$CH_2$$(CH_2)_2$$CH_2$$CH_2$-P). ^{31}P NMR (121 MHz, CD_2Cl_2): δ = 28.0 (s). FAB MS: m/z (%) 915 [M^+-pyrazol-N-yl, 32%], 651 [(dpph)Au^+, 4]. Anal. calc. for $C_{36}H_{38}Au_2N_4P_2$: C, 44.01; H, 3.90; N, 5.70, found: C, 44.35; H, 3.76; N, 5.54 %.

SI 4.1.11 Preparation of {μ-[1,2-ethanediylbis(dimethylphosphine-κP)]}bis(1H-1,2,3-triazolato-κN^1)digold(I), ***10***

As described for **1**, 1,2,3-triazole (0.10 mL, 1.7 mmol), (μ-1,2-bis(dimethylphosphino)ethane)bis(chlorogold) (0.48 g, 0.78 mmol) and NaOH (0.064 g, 1.6 mmol) reacted in a methanol (20 cm^3) suspension to afford **10** as a colourless, microcrystalline material after work-up. Yield: 0.29 g, 55%. Mp: 60-62 °C. IR (ATR, cm^{-1}): ν(aromatic C-H) 3112s; ν(aliphatic C-H) 2990s, 2963s; ν(C=N) 1652w. ^{1}H NMR (300 MHz, MeOH-d_4): δ = 7.71 (4 H, d, H4, H5), 2.36 (4 H, d, ^3J = 7.3 Hz, P-$(CH_2)_2$-P), 1.74 (12 H, t, ^2J = 5.6 Hz, CH_3). ^{13}C NMR (75 MHz, MeOH-d_4): δ = 132.0 (s, C4, C5), 25.1 (t, ^1J = 18.8 Hz, P-$(CH_2)_2$-P), 13.2 ("t", ^3J = 19.9 Hz, CH_3). ^{31}P NMR (121 MHz, MeOH-d_4): δ = 0.75 (s). FAB MS: m/z (%) 612 [M^+-triazol-N-yl, 100%]. Anal. calc. for $C_{10}H_{20}Au_2N_6P_2$: C, 17.66; H, 2.96; N, 12.36, found: C, 17.86; H, 3.05; N, 12.14 %.

SI 4.1.12 Preparation of {μ-[1,2-ethanediylbis(diphenylphosphine-κP)]}bis(1H-1,2,3-triazolato-κN^1)digold(I), ***11***

A suspension of 1,2,3-triazole (0.06 mL, 1.0 mmol) and (μ-1,2-bis(diphenylphosphino)ethane)bis(chlorogold) (0.45 g, 0.50 mmol) in DME (20 cm^3) was treated with NaOH (0.041 g, 1.0 mmol) dissolved in H_2O (1 cm^3) was treated according to the procedure for **4** to obtain **11** as a beige, microcrystalline material. Yield: 0.29 g, 64%. Mp: 98-104 °C. IR (KBr, cm^{-1}): ν(aromatic C-H) 3117s, 3074s, 3053s; ν(aliphatic C-H) 2987s, 2953s; ν(C=N) 1637s. ^{1}H NMR (300 MHz, CD_2Cl_2): δ = 7.74 (4 H, s, H4, H5), 7.69 (8 H, m, *m*-C_6H_5), 7.53 (12 H, m, *p*- and *o*-C_6H_5), 2.80 (4 H, m, P-$(CH_2)_2$-P). ^{13}C NMR (75 MHz, CD_2Cl_2): δ = 134.0 ("t", ^3J = 6.7 Hz, *m*-C_6H_5), 133.1 (s, *p*-C_6H_5), 131.9 (bs, C4, C5), 130.2 ("t", ^2J = 5.5 Hz, *o*-C_6H_5), 128.2 (d, ^1J = 61.5 Hz, *i*-C_6H_5), 24.1 (t, ^1J = 21.3 Hz, P-$(CH_2)_2$-P). ^{31}P NMR (121 MHz, CD_2Cl_2): δ = 29.4 (s). FAB MS: m/z (%) 860 [M^+-triazol-N-yl, 10%]. Anal. calc. for $C_{30}H_{28}Au_2N_6P_2$: C, 38.81; H, 3.04; N, 9.05, found: C, 38.92; H, 2.91; N, 9.45 %.

SI 4.1.13 Preparation of {μ-[1,3-propanediylbis(diphenylphosphine-κP)]}bis(1H-1,2,3-triazolato-κN^1)digold(I), ***12***

Colourless, microcrystalline, compound **12** was prepared from 1,2,3-triazole (0.06 mL, 1.1 mmol), NaOH (0.044 g, 1.1 mmol) and (μ-1,3-bis(diphenylphosphino)propane)bis(chlorogold) (0.45 g, 0.51 mmol) in a similar fashion as **4**, but not treated with diethyl ether and filtered through $MgSO_4$. Yield: 0.33 g, 68%. Mp: 40-51 °C. IR (KBr, cm^{-1}): ν(aromatic C-H) 3109m, 3053m; ν(aliphatic C-H) 2974m, 2928m; ν(C=N) 1637w. ^{1}H NMR (300 MHz, CD_2Cl_2): δ = 7.76 (4 H, s, H4, H5), 7.68 (8 H, m, *m*-C_6H_5), 7.48 (12 H, m, *p*- and *o*-C_6H_5), 2.94 (4 H, m, P-C*H*$_2$CH$_2$C*H*$_2$-P), 1.97 (2 H, m, P-CH$_2$C*H*$_2$CH$_2$-P). ^{13}C NMR (75 MHz, CD_2Cl_2): δ = 134.0 (d, ^3J = 13.0 Hz, *m*-C_6H_5), 132.8 (d, ^4J = 2.5 Hz, *p*-C_6H_5), 131.9 (bs, C4, C5), 130.3 (d, ^2J = 11.6 Hz, *o*-C_6H_5), 128.5 (d, ^1J = 61.0 Hz, *i*-C_6H_5), 28.2 (dd, ^1J = 39.4 Hz, ^3J = 12.6 Hz, P-*C*H$_2$CH$_2$*C*H$_2$-P), 20.1 (bs, P-CH$_2$*C*H$_2$CH$_2$-P). ^{31} P NMR (121 MHz, CD_2Cl_2): δ = 24.1 (s). ESI MS: m/z (%) 874 [M^+-triazol-N-yl, 100%]. Anal. calc. for $C_{31}H_{30}Au_2N_6P_2$: C, 39.51; H, 3.21; N, 8.92, found: C, 39.34; H, 2.96; N, 9.13 %.

SI 4.1.14 Preparation of {μ-[1,5-pentanediylbis(diphenylphosphine-κP)]}bis(1H-1,2,3-triazolato-κN^1)digold(I), ***13***

Again, 1,2,3-triazole (0.05 cm^3, 0.86 mmol), NaOH (0.034 g, 0.85 mmol) and (μ-1,5-bis(diphenylphosphino)pentane)bis(chlorogold) (0.35 g, 0.39 mmol) were reacted according to a method similar to the synthesis of **4**, to afford **13** as colourless, microcrystalline material. Yield: 0.15 g, 40%. Mp: 138 °C (dec). IR (KBr, cm^{-1}): ν(aromatic C-H) 3051w; ν(aliphatic C-H) 2923m, 2856w. ^{1}H NMR (400 MHz, CD_2Cl_2): δ = 7.72 (12 H, m, H4, H5, *m*-C_6H_5), 7.51 (12 H, m, *p*- and *o*-C_6H_5), 2.50 (4 H, m, P-C*H*$_2$(CH$_2$)$_3$C*H*$_2$-P), 1.75 (6 H, m, P-CH$_2$(C*H*$_2$)$_3$CH$_2$-P). ^{13}C NMR (101 MHz, CD_2Cl_2): δ = 133.6 (d, ^3J = 12.9 Hz, *m*-C_6H_5), 132.3 (d, ^4J = 2.6 Hz, *p*-C_6H_5), 131.4 (bs, C4, C5), 129.6 (d, ^2J = 11.5 Hz, *o*-C_6H_5), 129.2 (d, ^1J = 61.8 Hz, *i*-C_6H_5), 31.7 (t, ^3J = 15.8 Hz, P-(CH$_2$)$_2$*C*H$_2$(CH$_2$)$_2$-P), 27.5 (d, ^1J = 38.5, P-*C*H$_2$(CH$_2$)$_3$CH$_2$-P), 25.1 (d, ^2J = 2.9, P-CH$_2$*C*H$_2$CH$_2$*C*H$_2$CH$_2$-P). ^{31} P NMR (162 MHz, CD_2Cl_2): δ = 27.2 (s). FAB MS: m/z (%) 902 [M^+-triazol-N-yl, 42%], 637 [(dpppe)Au^+, 6]. Anal. calc. for $C_{33}H_{34}Au_2N_6P_2$: C, 40.84; H, 3.53; N, 8.66, found: C, 40.53; H, 3.67; N, 8.99 %.

SI 4.1.15 Preparation of {μ-[1,6-hexanediylbis(diphenylphosphine-κP)]}bis(1H-1,2,3-triazolato-κN^1)digold(I) , ***14***

Colourless, slightly hygroscopic, microcrystalline **14** was prepared as described above from 1,2,3-triazole (0.05 cm^3, 0.86 mmol), NaOH (0.037 g, 0.93 mmol) and (μ-1,6-bis(diphenylphosphino)hexane)bis(chlorogold) (0.40 g, 0.44 mmol), but stirred for 2h. Yield 0.26 g, 60%. Mp: 38-41 °C. IR (ATR, cm^{-1}): ν(aromatic C-H) 3114s, 3087s; ν(aliphatic C-H) 2988s, 2967s. ^{1}H NMR (300 MHz, CD_2Cl_2): δ = 7.71 (12 H, m, H4, H5, *m*-C_6H_5), 7.52 (12 H, m, *p*- and *o*-C_6H_5), 2.46 (4 H, m, P-C*H*$_2$(CH$_2$)$_4$C*H*$_2$-P), 1.54 (8 H, m, P-CH$_2$(C*H*$_2$)$_4$CH$_2$-P). ^{13}C NMR (75 MHz, CD_2Cl_2): δ = 133.9 (d, ^3J = 12.6 Hz, *m*-C_6H_5), 132.6 (d, ^4J = 2.1 Hz, *p*-C_6H_5), 131.7 (bs, C4, C5), 129.9 (d, ^2J = 11.4 Hz, *o*-C_6H_5), 129.5 (d, ^1J = 60.8 Hz, *i*-C_6H_5), 30.2 (d, ^3J = 15.5 Hz, P-(CH$_2$)$_2$(*C*H$_2$)$_2$(CH$_2$)$_2$-P), 27.6 (d, ^1J = 38.3 Hz, P-*C*H$_2$(CH$_2$)$_4$*C*H$_2$-P), 25.5 (d, ^2J = 2.0 Hz, P-CH$_2$*C*H$_2$(CH$_2$)$_2$*C*H$_2$CH$_2$-P). ^{31}P NMR (121 MHz, CD_2Cl_2): δ = 27.4 (s). FAB MS: m/z (%) 916 [M^+-triazol-N-yl, 100%], 651 [(dpph)Au, 26]. Anal. calc. for $C_{34}H_{36}Au_2N_6P_2$: C, 41.48; H, 3.69; N, 8.54, found: C, 41.43; H, 3.78; N, 8.26 %.

SI 4.1.16 Preparation of {μ-[1,2-ethanediylbis(diphenylphosphine-κP)]}bis(1H-1,2,4-triazolato-κN^1)digold(I), ***15***

Complex **15** was prepared by treating 1,2,4-triazole (0.075 g, 1.1 mmol), NaOH (0.044 g, 1.1 mmol) and (μ-1,2-bis(diphenylphosphino)ethane)bis(chlorogold) (0.45 g, 0.52 mmol) in the manner as described for **5**. The obtained residue was triturated with n-pentane (2 x 20 cm^3) and dried *in vacuo*, to afford **15** as slightly pinkish, microcrystalline material. Yield 0.29 g, 60%. Mp: 95 °C (dec). IR (ATR, cm^{-1}) ν(aromatic C-H) 3098m, 3050m; ν(aliphatic C-H) 2972s, 2930s. ^{1}H NMR (300 MHz, CD_2Cl_2): δ = 8.05 (4 H, s, H3, H5), 7.71 (8 H, m, *m*-C_6H_5), 7.54 (12 H, m, *p*- and *o*-C_6H_5), 2.81 (4 H, d, ^3J = 3.2 Hz, P-$(CH_2)_2$-P). ^{13}C NMR (75 MHz, CD_2Cl_2): δ = 151.0 (s, C3, C5), 134.0 ("t", ^3J = 6.5 Hz, *m*-C_6H_5), 133.2 (s, *p*-C_6H_5), 130.3 ("t", ^2J = 5.7 Hz, *o*-C_6H_5), 128.2 ("t", ^1J = 30.4 Hz, *i*-C_6H_5), 24.1 (t, ^1J = 19.9 Hz, P-$(CH_2)_2$-P). ^{31}P NMR (121 MHz, CD_2Cl_2): δ = 28.2 (s). FAB MS: m/z (%) 860 [M^+-triazol-N-yl, 63%]. Anal. calc. for $C_{30}H_{28}Au_2N_6P_2$: C, 38.81; H, 3.04; N, 9.05, found: C, 39.07; H, 2.99; N, 9.34 %.

SI 4.1.17 Preparation of {μ-[1,3-propanediylbis(diphenylphosphine-κP)]}bis(1H-1,2,4-triazolato-κN^1)digold(I), ***16***

Similar to the preparation of **4**, 1,2,4-triazole (0.071 g, 1.0 mmol), NaOH (0.041 g, 1.0 mmol) and (μ-1,3-bis(diphenylphosphino)propane)bis(chlorogold) (0.45 g, 0.51 mmol) were used to prepare **16** as a colourless, microcrystalline material. Yield: 0.31 g, 64%. Mp: 105 °C (dec). IR (KBr, cm^{-1}): ν(aromatic C-H) 3109m, 3091s; ν(aliphatic C-H) 2939m; ν(C=N) 1635w. ^{1}H NMR (300 MHz, CD_2Cl_2): δ = 8.08 (4 H, s, H3, H5), 7.67 (8 H, m, *m*-C_6H_5), 7.50 (12 H, m, *p*- and *o*-C_6H_5), 2.90 (4 H, m, P-C*H*$_2$CH$_2$C*H*$_2$-P), 1.96 (2 H, m, P-CH$_2$C*H*$_2$CH$_2$-P). ^{13}C NMR (75 MHz, CD_2Cl_2): δ = 151.0 (s, C3, C5), 134.0 (d, ^3J = 13.0 Hz, *m*-C_6H_5), 132.9 (d, ^4J = 2.0 Hz, *p*-C_6H_5), 130.1 (d, ^2J = 11.6 Hz, *o*-C_6H_5), 128.6 (d, ^1J = 61.0 Hz, *i*-C_6H_5), 28.1 (dd, ^1J = 37.9, ^3J = 11.5 Hz, P-*C*H$_2$CH$_2$*C*H$_2$-P), 20.0 (bs, P-CH$_2$*C*H$_2$CH$_2$-P). ^{31}P NMR (121 MHz, CD_2Cl_2): δ = 25.2 (s). FAB MS: m/z (%) 874 [M^+-triazol-N-yl, 53%], 609 [(dppp)Au, 1]. Anal.calc. for $C_{31}H_{30}Au_2N_6P_2$: C, 38.51; H, 3.21; N, 8.92, found: C, 39.25; H, 3.34; N, 8.59 %.

SI 4.1.18 Preparation of {μ-[1,5-pentanediylbis(diphenylphosphine-κP)]}bis(1H-1,2,4-triazolato-κN^1)digold(I), ***17***

Compound **17** was prepared similarly to **4** using 1,2,4-triazole (0.070 g, 1.0 mmol), NaOH (0.040 g, 1.0 mmol) and (μ-1,5-bis(diphenylphosphino)pentane)bis(chlorogold) (0.45 g, 0.50 mmol), but filtered through $MgSO_4$, to yield **17** as colourless, microcrystalline material after solvent removal. Yield: 0.33 g, 68%. Mp: 48-53 °C. IR (KBr, cm^{-1}): ν(aromatic C-H) 3053s; ν(aliphatic C-H) 2964s, 2924s. ^{1}H NMR (300 MHz, CD_2Cl_2): δ = 8.09 (4 H, s, H3, H5), 7.70 (8 H, m, *m*-C_6H_5), 7.53 (12 H, m, *p*- and *o*-C_6H_5), 2.45 (4 H, m, P-C*H*$_2$(CH$_2$)$_3$C*H*$_2$-P), 1.66 (6 H, m, P-CH$_2$(C*H*$_2$)$_3$CH$_2$-P). ^{13}C NMR (75 MHz, CD_2Cl_2): δ = 150.2 (s, C3, C5), 133.9 (d, ^3J = 12.8 Hz, *m*-C_6H_5), 132.7 (d, ^4J = 2.6 Hz, *p*-C_6H_5), 130.0 (d, ^2J = 11.5 Hz, *o*-C_6H_5), 129.7 (d, ^1J = 60.2 Hz, *i*-C_6H_5), 31.6 (t, ^3J = 15.4 Hz, P-(CH$_2$)$_2$*C*H$_2$(CH$_2$)$_2$-P), 27.6 (d, ^1J = 37.8 Hz, P-*C*H$_2$(CH$_2$)$_3$*C*H$_2$-P), 25.1 (d, ^2J = 2.6 Hz, P-CH$_2$*C*H$_2$CH$_2$*C*H$_2$CH$_2$-P). ^{31}P NMR (121 MHz, CD_2Cl_2): δ = 28.3 (s). FAB MS: m/z (%) 902 [M^+-triazol-N-yl, 15%], 637 [(dpppe)Au, 8]. Anal. calc. for $C_{33}H_{34}Au_2N_6P_2$: C, 40.84; H, 3.53; N, 8.66, found: C, 40.48; H, 3.52; N, 8.44 %.

SI 4.1.19 Preparation of {μ-[1,6-hexanediylbis(diphenylphosphine-κP)]}bis(1H-1,2,4-triazolato-κN^1)digold(I), ***18***

Colourless, microcrystalline **18** was prepared as described above for **4** from 1,2,4-triazole (0.067 g, 0.97 mmol), NaOH (0.39 g, 0.98 mmol) and (μ-1,6-bis(diphenylphosphino)hexane)bis(chlorogold) (0.40 g, 0.44

mmol). Yield: 0.15 g, 40%. Mp: 79-80 °C. IR (KBr, cm^{-1}): ν(aromatic C-H) 3091m, 3052m; ν(aliphatic C-H) 2970m, 2924m. ^{1}H NMR (300 MHz, CD_2Cl_2): δ = 8.05 (4 H, s, H3, H5), 7.71 (8 H, m, *m*-C_6H_5), 7.52 (12 H, m, *p*- and *o*-C_6H_5), 2.45 (4 H, m, P-CH_2(CH_2)$_4$CH_2-P), 1.56 (8 H, m, P-CH_2(CH_2)$_4$$CH_2$-P). ^{13}C NMR (75 MHz, CD_2Cl_2): δ = 151.1 (s, C3, C5), 133.9 (d, ^{3}J = 12.7 Hz, *m*-C_6H_5), 132.7 (d, ^{4}J = 2.5 Hz, *p*-C_6H_5), 130.0 (d, ^{2}J = 11.4 Hz, *o*-C_6H_5), 129.8 (d, ^{1}J = 61.1 Hz, *i*-C_6H_5), 30.4 (d, ^{3}J = 15.6 Hz, P-(CH_2)$_2$(CH_2)$_2$(CH_2)$_2$-P), 27.7 (d, ^{1}J = 38.1 Hz, P-CH_2(CH_2)$_4$CH_2-P), 25.6 (d, ^{2}J = 2.4, P-CH_2CH_2(CH_2)$_2$C$H_2$$CH_2$-P). ^{31}P NMR (121 MHz, CD_2Cl_2): δ = 28.1 (s). FAB MS: m/z (%) 916 [M^+-triazol-N-yl, 54%], 651 [(dpph)Au^+, 8]. Anal. calc. for $C_{34}H_{36}Au_2N_6P_2$ requires C, 41.48; H, 3.69; N, 8.54, found: C, 41.69; H, 3.54; N, 8.64 %.

SI 4.1.20 Preparation of {μ-[1,2-ethanediylbis(dimethylphosphine-κP)]}bis(1H-pyrrolato-κN)digold(I), ***19***

Complex **19** was obtained from NaOH (0.081 g, 2.0 mmol), pyrrole (0.14 cm^3, 2.0 mmol) and (μ-1,2-bis(dimethylphosphino)ethane)bis(chlorogold) (0.62 g, 1.0 mmol) in MeOH (20 cm^3). The mixture was stirred for 1 h at 50 °C and filtered through celite. After solvent removal the residue was treated with CH_2Cl_2 (20 cm^3), filtered through Na_2SO_4 and dried *in vacuo*, to give **19** as a colourless, microcrystalline material. Yield: 0.33 g, 49%. Mp: 86 °C (dec). IR (KBr, cm^{-1}): ν(aromatic C-H) 3091m; ν(aliphatic C-H) 2972m, 2901m; ν(C=N) 1633m. ^{1}H NMR (300 MHz, CD_2Cl_2): δ = 6.80 (4 H, s, H2, H5), 6.21 (4 H, m, H3, H4), 2.03 (4 H, m, P-(CH_2)$_2$-P), 1.52 (12 H, t, ^{2}J = 10.1 Hz, CH_3). ^{13}C NMR (75 MHz, CD_2Cl_2): δ = 127.7 (s, C2, C5), 107.3 (s, C3, C4), 25.5 (t, ^{1}J = 18.9 Hz, P-(CH_2)$_2$-P), 13.8 (t, ^{1}J = 18.9 Hz, CH_3). ^{31}P NMR (121 MHz, CD_2Cl_2): δ = 2.8 (s). ESI MS: m/z (%) 610 [M^+-triazol-N-yl, 100%]. FAB MS: m/z (%) 610 [M^+-pyrrole, 2%]. Anal. calc. for $C_{14}H_{24}Au_2N_2P_2$: C, 24.87; H, 3.58; N, 4.14, found: C, 25.04; H, 3.18; N, 4.01 %.

SI 4.1.21 Preparation of {μ-[1,6-hexanediylbis(diphenylphosphine-κP)]}bis(9H-purin-6-aminato-κN^9)digold(I), ***24***

Complex **24** was prepared according to the method previously described for **20** [26]. A suspension of adenine (0.15 g, 1.1 mmol) and (μ-1,6-bis(diphenylphosphino)hexane)bis(chlorogold) (0.50 g, 0.54 mmol) in DME (20 cm^3) was treated with NaOH (0.048 g, 1.2 mmol) dissolved in H_2O (1 cm^3) and stirred for 2 h at 50 °C. The mixture was reduced to dryness *in vacuo*. The crude product was treated with a mixture of CH_2Cl_2/MeOH (20 cm^3, 1:1), followed by filtration through $MgSO_4$ and solvent removal. The residue was washed with H_2O (3 x 15 cm^3) and Et_2O (3 x 25 cm^3) and then dried *in vacuo*, to give **21** as a colourless, microcrystalline material. Yield: 0.41 g, 68%. Mp: 106 °C (dec). IR (KBr, cm^{-1}): ν(N-H) 3323s, 3124s; ν(aromatic C-H) 3055s; ν(aliphatic C-H) 2928s, 2854s; ν(C=N) 1633s. ^{1}H NMR (300 MHz, CD_2Cl_2/MeOH-d_4) δ = 8.11 (2 H, s, H2), 7.83 (2 H, s, H8), 7.70 (8 H, m, *m*-C_6H_5), 7.48 (12 H, m, *p*- and *o*-C_6H_5), 2.50 (4 H, m, P-CH_2(CH_2)$_4$CH_2-P), 1.56 (8 H, m, P-CH_2(CH_2)$_4$$CH_2$-P). ^{13}C NMR (75 MHz, CD_2Cl_2/MeOH-d_4): δ = 157.8 (s, C4), 156.1 (s, C2), 151.6 (s, C8), 149.6 (s, C6), 134.0 (d, ^{3}J = 12.2 Hz, *m*-C_6H_5, C5), 132.8 (s, *p*-C_6H_5), 130.0 (d, ^{2}J = 11.2 Hz, *o*-C_6H_5), 129.9 (d, ^{1}J = 60.2, *i*-C_6H_5), 30.3 (d, ^{3}J = 14.7 Hz, P-(CH_2)$_2$(CH_2)$_2$(CH_2)$_2$-P), 27.6 (d, ^{1}J = 38.0 Hz, P-CH_2(CH_2)$_4$CH_2-P), 25.6 (bs, P-$CH_2$$CH_2$($CH_2$)$_2$$CH_2$$CH_2$-P). ^{31}P NMR (121 MHz, CD_2Cl_2/MeOH-d_4): δ = 28.9 (s). FAB MS: m/z (%) 982 [M^+-purine-6-amine-N-yl, 37%], 651 [(dpph)Au^+, 41]. Anal. calc. for $C_{40}H_{40}Au_2N_{10}P_2$: C, 43.02; H, 3.61; N, 12.54, found: C, 42.85; H, 3.82; N, 12.17 %.

SI 4.1.22 Preparation of {μ-[1,6-hexanediylbis(diphenylphosphine-κP)]}bis(9H-purinato-κN^9)digold(I), ***24***

Compound **24** was prepared similarly to **22** and **23**, as previously described [26]. A suspension of purine (0.13 g, 1.1 mmol) and (μ-1,6-bis(diphenylphosphino)hexane)bis(chlorogold) (0.50 g, 0.54 mmol) in DME (20 cm^3) was treated with NaOH (0.048 g, 1.2 mmol) dissolved in H_2O (1 cm^3) and stirred for 1 h at 50 °C. The mixture was reduced to dryness *in vacuo*. The crude product was treated with CH_2Cl_2 (20 cm^3), followed by filtration through $MgSO_4$ and solvent removal. The residue was dried *in vacuo*, to afford **21** as a colourless, microcrystalline material. Yield: 0.45 g, 77%. Mp: 121 °C (dec). IR (KBr, cm^{-1}): ν(aromatic C-H) 3084s, 3053s; ν(aliphatic C-H) 2997m, 2966s; ν(C=N) 1653m. ^{1}H NMR (300 MHz, CD_2Cl_2): δ = 9.03 (2 H, s, H6), 8.13 (2 H, s, H8), 7.73 (8 H, m, *m*-C_6H_5), 7.54 (12 H, m, *p*- and *o*-C_6H_5), 6.82 (2 H, s, H2), 2.50 (4 H, m, P-C*H*$_2$(CH$_2$)$_4$C*H*$_2$-P), 1.67 (8 H, m, P-CH$_2$(C*H*$_2$)$_4$CH$_2$-P). ^{13}C NMR (75 MHz, CD_2Cl_2): δ = 160.7 (C4), 154.6 (C2), 151.9 (C8), 146.4 (C6), 134.9 (C5), 133.9 (d, ^3J = 12.7 Hz, *m*-C_6H_5), 132.8 (d, ^4J = 2.5 Hz, *p*-C_6H_5), 130.0 (d, ^2J = 11.4 Hz, *o*-C_6H_5), 129.7 (d, ^1J = 60.2 Hz, *i*-C_6H_5), 30.4 (d, ^3J = 11.4 Hz, P-(CH$_2$)$_2$(*C*H$_2$)$_2$(CH$_2$)$_2$-P), 27.8 (d, ^1J = 38.5 Hz, P-*C*H$_2$(CH$_2$)$_4$*C*H$_2$-P), 25.7 (d, ^2J = 2.4 Hz, P-CH$_2$*C*H$_2$(CH$_2$)$_2$*C*H$_2$CH$_2$-P). ^{31}P NMR (121 MHz, CD_2Cl_2): δ = 28.2 (s). FAB MS: m/z (%) 967 [M^+-purine-6-amine-N-yl, 41%], 651 [(dpph)Au^+, 33]. Anal. calc. for $C_{40}H_{38}Au_2N_8P_2$: C, 44.21; H, 3.52; N, 10.31, found: C, 44.33; H, 3.27; N, 10.51 %.

SI 4.1.23 Preparation of bis(1H-imidazolato-κN^1)(trimethylphosphane)gold(I), ***25***

Colourless, microcrystalline material of **25** was obtained from NaOH (0.059 g, 1.5 mmol), imidazole (0.10 g, 1.5 mmol) and chloro(trimethylphosphine)gold (0.45 g, 1.5 mmol) in MeOH (20 cm^3) after stirring for 2h and treatment as described for **5**. Yield: 0.34 g, 69%. Mp: 121 °C (dec). IR (KBr, cm^{-1}): ν(aromatic C-H) 3113vw, 3082vw; ν(C=N) 1645m. ^{1}H NMR (300 MHz, CD_2Cl_2): δ = 7.37 (1 H, s, H2), 7.00 (2 H, s, H4, H5), 1.58 (9 H, d, ^2J = 11.1 Hz, CH_3). ^{13}C NMR (75 MHz, CD_2Cl_2): δ = 143.0 (s, C2), 125.9 (s, C4, C5), 15.6 (d, ^1J = 40.8 Hz, CH_3). ^{31}P NMR (121 MHz, CD_2Cl_2): δ = -10.9 (s). ESI MS: m/z (%) m/z 613 [M^++AuP(CH$_3$)$_3$, 95%], 341 [M^+, 20], 273 [M^+-imidazol-N-yl, 83]. FAB MS: m/z (%) 613 [M^++AuP(CH$_3$)$_3$, 100%], 341 [M^+, 24], 273 [M^+-imidazol-N-yl, 46]. EI MS: m/z (%) 341 [M^+, 1%], 76 [P(CH$_3$)$^+_3$, 66]. Anal. calc. for $C_6H_{12}AuN_2P$: C, 21.19; H, 3.56; N, 8.24, found: C, 21.41; H, 3.16; N, 8.49 %.

SI 4.1.24 Preparation of cyclo-{bis{μ-[1,2-ethanediylbis(diphenylphosphine-κP)]}bis(μ-1H-imidazolato-κ^{2}N^1:N^3)tetragold(I) chloride, ***26***

Following the same procedure as in the preparation of **5** using NaOH (0.046 g, 1.2 mmol), imidazole (0.079 g, 1.2 mmol) and (μ-1,2-bis(diphenylphosphino)ethane)bis(chlorogold) (0.50 g, 0.58 mmol) **26** was obtained as a colourless, microcrystalline material. Yield: 0.12 g, 23%. Mp: 126-129 °C. IR (KBr, cm^{-1}): ν(aromatic C-H) 3051s; ν(aliphatic C-H) 2902s. ^{1}H NMR (300 MHz, CD_2Cl_2) δ = 7.71 (8 H, m, *m*-C_6H_5), 7.55 (12 H, m, *p*- and *o*-C_6H_5), 7.42 (1 H, s, H2), 7.07 (2 H, s, H4, H5), 2.85 (4 H, d, ^3J = 3.3 Hz, P-(CH$_2$)$_2$-P). ^{13}C NMR (75 MHz, CH_2Cl_2): δ = 143.3 (C2), 133.9 ("t", ^3J = 6.7 Hz, *m*-C_6H_5), 133.1 (s, *p*-C_6H_5), 130.1 ("t", ^2J = 6.1 Hz, *o*-C_6H_5), 128.6 ("t", ^1J = 29.8 Hz, *i*-C_6H_5), 126.2 (s, C4, C5), 24.1 (t, ^1J = 20.7 Hz, P-(CH$_2$)$_2$-P). ^{31}P NMR (121 MHz, CD_2Cl_2): δ = 29.7 (s). ESI MS: m/z (%) 859 [M-2Cl]$^{2+}$, 100%]. FAB MS: m/z 989 [M-2Cl]$^{2+}$. Anal. calc. for $C_{58}H_{54}Au_4Cl_2N_4P_4 \cdot 0.5CH_2Cl_2$: C, 38.35; H, 3.03; N, 3.06, found: C, 38.32; H, 3.25; N, 3.45 %.

```
data_Compound1.MeOH

_audit_creation_method          SHELXL-97
_chemical_name_systematic
;
[\m-1,2-bis(diphenylphosphino)ethane]bis(imidazolido-\kN)digold(I)
 methanol solvate
;
_chemical_name_common
(\m-dppe)~2~Au~2~(C~3~H~3~N)~2~.CH~3~OH
_chemical_melting_point         ?
_chemical_formula_moiety         'C12 H22 Au2 N4 P2, C H4 O'
_chemical_formula_sum           'C13 H26 Au2 N4 O P2'
_chemical_formula_weight         710.25

loop_
 _atom_type_symbol
 _atom_type_description
 _atom_type_scat_dispersion_real
 _atom_type_scat_dispersion_imag
 _atom_type_scat_source
'C'  'C'   0.0033   0.0016
 'International Tables Vol C Tables 4.2.6.8 and 6.1.1.4'
'H'  'H'   0.0000   0.0000
 'International Tables Vol C Tables 4.2.6.8 and 6.1.1.4'
'N'  'N'   0.0061   0.0033
 'International Tables Vol C Tables 4.2.6.8 and 6.1.1.4'
'P'  'P'   0.1023   0.0942
 'International Tables Vol C Tables 4.2.6.8 and 6.1.1.4'
'O'  'O'   0.0106   0.0060
 'International Tables Vol C Tables 4.2.6.8 and 6.1.1.4'
'Au'  'Au'  -2.0133   8.8022
 'International Tables Vol C Tables 4.2.6.8 and 6.1.1.4'

_symmetry_cell_setting          monoclinic
_symmetry_space_group_name_H-M    'C 2/c'
_symmetry_space_group_name_Hall   '-C 2yc'
_symmetry_int_tables_number      15

loop_
 _symmetry_equiv_pos_as_xyz
 'x, y, z'
 '-x, y, -z+1/2'
 'x+1/2, y+1/2, z'
 '-x+1/2, y+1/2, -z+1/2'
 '-x, -y, -z'
 'x, -y, z-1/2'
 '-x+1/2, -y+1/2, -z'
 'x+1/2, -y+1/2, z-1/2'

_cell_length_a                 26.467(4)
_cell_length_b                 10.6496(13)
```

```
_cell_length_c                  17.988(2)
_cell_angle_alpha               90.00
_cell_angle_beta                129.972(2)
_cell_angle_gamma               90.00
_cell_volume                    3885.6(9)
_cell_formula_units_Z           8
_cell_measurement_temperature     100(2)
_cell_measurement_reflns_used     5940
_cell_measurement_theta_min       2.223
_cell_measurement_theta_max       23.158

_exptl_crystal_description        prism
_exptl_crystal_colour             colourless
_exptl_crystal_size_max           0.22
_exptl_crystal_size_mid           0.13
_exptl_crystal_size_min           0.12
_exptl_crystal_density_meas       ?
_exptl_crystal_density_diffrn     2.428
_exptl_crystal_density_method     'not measured'
_exptl_crystal_F_000              2624
_exptl_absorpt_coefficient_mu     15.256
_exptl_absorpt_correction_type    multi-scan
_exptl_absorpt_correction_T_min   0.127
_exptl_absorpt_correction_T_max   0.26
_exptl_absorpt_process_details    'SADABS (Bruker, 2002)'

_exptl_special_details            ?

_diffrn_ambient_temperature       100(2)
_diffrn_radiation_wavelength      0.71073
_diffrn_radiation_type            MoK\a
_diffrn_radiation_source          'fine-focus sealed tube'
_diffrn_radiation_monochromator   graphite
_diffrn_measurement_device_type   'Bruker APEX CCD area detector'
_diffrn_measurement_method        \w-scans
_diffrn_detector_area_resol_mean  ?
_diffrn_reflns_number             11840
_diffrn_reflns_av_R_equivalents   0.0221
_diffrn_reflns_av_sigmaI/netI     0.0273
_diffrn_reflns_limit_h_min        -33
_diffrn_reflns_limit_h_max        34
_diffrn_reflns_limit_k_min        -14
_diffrn_reflns_limit_k_max        9
_diffrn_reflns_limit_l_min        -23
_diffrn_reflns_limit_l_max        21
_diffrn_reflns_theta_min          2.27
_diffrn_reflns_theta_max          28.25
_reflns_number_total              4507
_reflns_number_gt                 3983
_reflns_threshold_expression      I>2\s(I)

_computing_data_collection        'SMART (Bruker, 2002)'
```

```
_computing_cell_refinement       'SAINT (Bruker, 2003)'
_computing_data_reduction        SAINT
_computing_structure_solution    'SHELXS-97 (Sheldrick, 2008)'
_computing_structure_refinement  'SHELXL-97 (Sheldrick, 2008)'
_computing_molecular_graphics
 'X-Seed (Barbour, 2001; Atwood & Barbour, 2003)'
_computing_publication_material  X-Seed

_refine_special_details
;
 Refinement of F^2^ against ALL reflections.  The weighted R-factor wR and
 goodness of fit S are based on F^2^, conventional R-factors R are based
 on F, with F set to zero for negative F^2^. The threshold expression of
 F^2^ > 2\s(F^2^) is used only for calculating R-factors(gt) etc. and is
 not relevant to the choice of reflections for refinement.  R-factors based
 on F^2^ are statistically about twice as large as those based on F, and R-
 factors based on ALL data will be even larger.
;

_refine_ls_structure_factor_coef  Fsqd
_refine_ls_matrix_type           full
_refine_ls_weighting_scheme      calc
_refine_ls_weighting_details
 'calc w=1/[\s^2^(Fo^2^)+(0.0194P)^2^+4.2628P] where P=(Fo^2^+2Fc^2^)/3'
_atom_sites_solution_primary     direct
_atom_sites_solution_secondary   difmap
_atom_sites_solution_hydrogens   geom
_refine_ls_hydrogen_treatment    constr
_refine_ls_extinction_method     none
_refine_ls_extinction_coef       ?
_refine_ls_number_reflns         4507
_refine_ls_number_parameters     205
_refine_ls_number_restraints     0
_refine_ls_R_factor_all          0.0264
_refine_ls_R_factor_gt           0.0219
_refine_ls_wR_factor_ref         0.0490
_refine_ls_wR_factor_gt          0.0476
_refine_ls_goodness_of_fit_ref   1.051
_refine_ls_restrained_S_all      1.051
_refine_ls_shift/su_max          0.002
_refine_ls_shift/su_mean         0.000

loop_
 _atom_site_label
 _atom_site_type_symbol
 _atom_site_fract_x
 _atom_site_fract_y
 _atom_site_fract_z
 _atom_site_U_iso_or_equiv
 _atom_site_adp_type
 _atom_site_occupancy
 _atom_site_symmetry_multiplicity
```

_atom_site_calc_flag
_atom_site_refinement_flags
_atom_site_disorder_assembly
_atom_site_disorder_group
Au1 Au 0.431066(7) 0.428493(14) 0.631684(10) 0.03494(5) Uani 1 1 d . . .
Au2 Au 0.193895(8) 0.180142(15) 0.583832(11) 0.03746(5) Uani 1 1 d . . .
P2 P 0.17050(5) 0.38269(10) 0.54133(7) 0.0339(2) Uani 1 1 d . . .
P1 P 0.36606(5) 0.53113(10) 0.65087(7) 0.0339(2) Uani 1 1 d . . .
N1 N 0.48621(16) 0.3329(3) 0.6075(2) 0.0364(7) Uani 1 1 d . . .
N21 N 0.21928(17) -0.0015(3) 0.6311(2) 0.0423(8) Uani 1 1 d . . .
C28 C 0.1161(2) 0.4506(4) 0.5582(3) 0.0480(11) Uani 1 1 d . . .
H28A H 0.1352 0.4403 0.6259 0.072 Uiso 1 1 calc R . .
H28C H 0.0732 0.4082 0.5157 0.072 Uiso 1 1 calc R . .
H28B H 0.1102 0.5402 0.5421 0.072 Uiso 1 1 calc R . .
N4 N 0.5282(2) 0.2733(4) 0.5381(3) 0.0557(10) Uani 1 1 d . . .
C26 C 0.24305(18) 0.4836(4) 0.6087(3) 0.0374(9) Uani 1 1 d . . .
H26A H 0.2301 0.5697 0.5818 0.045 Uiso 1 1 calc R . .
H26B H 0.2624 0.4876 0.6775 0.045 Uiso 1 1 calc R . .
C7 C 0.3999(2) 0.5682(4) 0.7726(3) 0.0421(10) Uani 1 1 d . . .
H7C H 0.3688 0.6211 0.7707 0.063 Uiso 1 1 calc R . .
H7B H 0.4416 0.6132 0.8057 0.063 Uiso 1 1 calc R . .
H7A H 0.4077 0.4904 0.8077 0.063 Uiso 1 1 calc R . .
C5 C 0.4844(2) 0.3414(5) 0.5316(3) 0.0458(10) Uani 1 1 d . . .
H5 H 0.4535 0.3931 0.4771 0.055 Uiso 1 1 calc R . .
C8 C 0.3360(2) 0.6769(4) 0.5863(3) 0.0475(10) Uani 1 1 d . . .
H8A H 0.3120 0.7220 0.6026 0.071 Uiso 1 1 calc R . .
H8C H 0.3064 0.6604 0.5164 0.071 Uiso 1 1 calc R . .
H8B H 0.3733 0.7280 0.6045 0.071 Uiso 1 1 calc R . .
C6 C 0.2941(2) 0.4327(4) 0.6024(3) 0.0442(10) Uani 1 1 d . . .
H6B H 0.2715 0.4157 0.5333 0.053 Uiso 1 1 calc R . .
H6A H 0.3101 0.3512 0.6368 0.053 Uiso 1 1 calc R . .
C27 C 0.1300(2) 0.4148(5) 0.4157(3) 0.0525(12) Uani 1 1 d . . .
H27B H 0.1291 0.5057 0.4062 0.079 Uiso 1 1 calc R . .
H27C H 0.0848 0.3825 0.3746 0.079 Uiso 1 1 calc R . .
H27A H 0.1542 0.3737 0.3982 0.079 Uiso 1 1 calc R . .
C2 C 0.5357(2) 0.2504(4) 0.6679(3) 0.0450(10) Uani 1 1 d . . .
H2 H 0.5501 0.2227 0.7290 0.054 Uiso 1 1 calc R . .
C3 C 0.5612(2) 0.2145(5) 0.6251(4) 0.0545(12) Uani 1 1 d . . .
H3 H 0.5966 0.1572 0.6519 0.065 Uiso 1 1 calc R . .
C22 C 0.2773(2) -0.0580(5) 0.6766(3) 0.0506(11) Uani 1 1 d . . .
H22 H 0.3143 -0.0161 0.6904 0.061 Uiso 1 1 calc R . .
C25 C 0.1807(2) -0.0932(4) 0.6265(3) 0.0490(11) Uani 1 1 d . . .
H25 H 0.1358 -0.0850 0.5983 0.059 Uiso 1 1 calc R . .
N23 N 0.2799(2) -0.1756(4) 0.7009(3) 0.0604(11) Uani 1 1 d . . .
C24 C 0.2185(3) -0.1971(4) 0.6695(3) 0.0527(12) Uani 1 1 d . . .
H24 H 0.2040 -0.2742 0.6767 0.063 Uiso 1 1 calc R . .
O1 O 0.53090(19) 0.2015(4) 0.3898(3) 0.0694(10) Uani 1 1 d . . .
H1 H 0.5371 0.2200 0.4405 0.083 Uiso 1 1 calc R . .
C30 C 0.4770(3) 0.1229(6) 0.3331(4) 0.0775(16) Uani 1 1 d . . .
H30A H 0.4917 0.0353 0.3487 0.116 Uiso 1 1 calc R . .
H30C H 0.4543 0.1387 0.2644 0.116 Uiso 1 1 calc R . .
H30B H 0.4467 0.1389 0.3459 0.116 Uiso 1 1 calc R . .

```
loop_
 _atom_site_aniso_label
 _atom_site_aniso_U_11
 _atom_site_aniso_U_22
 _atom_site_aniso_U_33
 _atom_site_aniso_U_23
 _atom_site_aniso_U_13
 _atom_site_aniso_U_12
Au1 0.03309(9) 0.03650(9) 0.03840(8) -0.00217(6) 0.02441(7) 0.00107(6)
Au2 0.03990(9) 0.03372(9) 0.03903(9) -0.00124(6) 0.02548(7) 0.00011(6)
P2 0.0342(5) 0.0335(5) 0.0338(5) -0.0019(4) 0.0218(4) -0.0005(4)
P1 0.0300(5) 0.0348(5) 0.0346(5) -0.0043(4) 0.0196(4) 0.0008(4)
N1 0.0364(18) 0.0411(19) 0.0365(17) -0.0007(15) 0.0256(15) 0.0020(15)
N21 0.048(2) 0.0345(19) 0.0444(19) -0.0001(16) 0.0299(17) 0.0014(16)
C28 0.044(2) 0.053(3) 0.060(3) 0.004(2) 0.039(2) 0.009(2)
N4 0.059(3) 0.069(3) 0.059(2) -0.012(2) 0.047(2) -0.003(2)
C26 0.036(2) 0.033(2) 0.042(2) -0.0070(18) 0.0250(18) -0.0036(17)
C7 0.043(2) 0.044(2) 0.038(2) -0.0049(19) 0.0249(19) 0.0040(19)
C5 0.041(2) 0.058(3) 0.040(2) 0.000(2) 0.027(2) -0.001(2)
C8 0.052(3) 0.041(2) 0.050(2) 0.005(2) 0.033(2) 0.008(2)
C6 0.040(2) 0.042(2) 0.055(2) -0.018(2) 0.032(2) -0.0079(18)
C27 0.055(3) 0.051(3) 0.038(2) 0.000(2) 0.024(2) -0.007(2)
C2 0.047(3) 0.046(3) 0.043(2) 0.003(2) 0.030(2) 0.007(2)
C3 0.049(3) 0.052(3) 0.065(3) -0.004(2) 0.038(3) 0.012(2)
C22 0.043(2) 0.054(3) 0.048(2) 0.004(2) 0.026(2) 0.003(2)
C25 0.052(3) 0.046(3) 0.057(3) -0.004(2) 0.039(2) -0.006(2)
N23 0.064(3) 0.048(2) 0.065(3) 0.013(2) 0.039(2) 0.016(2)
C24 0.073(3) 0.041(3) 0.056(3) 0.001(2) 0.047(3) 0.002(2)
O1 0.076(3) 0.086(3) 0.070(2) -0.007(2) 0.057(2) -0.008(2)
C30 0.077(4) 0.067(4) 0.079(4) -0.001(3) 0.046(3) 0.007(3)

_geom_special_details
;
 All esds (except the esd in the dihedral angle between two l.s. planes)
 are estimated using the full covariance matrix.  The cell esds are taken
 into account individually in the estimation of esds in distances, angles
 and torsion angles; correlations between esds in cell parameters are only
 used when they are defined by crystal symmetry.  An approximate (isotropic)
 treatment of cell esds is used for estimating esds involving l.s. planes.
;

loop_
 _geom_bond_atom_site_label_1
 _geom_bond_atom_site_label_2
 _geom_bond_distance
 _geom_bond_site_symmetry_2
 _geom_bond_publ_flag
Au1 N1 2.043(3) . ?
Au1 P1 2.2443(10) . ?
Au1 Au2 3.2913(4) 7_556 ?
Au1 Au1 3.3879(5) 2_656 ?
```

```
data_Compound1.MeOH

_audit_creation_method          SHELXL-97
_chemical_name_systematic
;
[\m-1,2-bis(diphenylphosphino)ethane]bis(imidazolido-\kN)digold(I)
 methanol solvate
;
_chemical_name_common
(\m-dppe)~2~Au~2~(C~3~H~3~N)~2~.CH~3~OH
_chemical_melting_point         ?
_chemical_formula_moiety        'C12 H22 Au2 N4 P2, C H4 O'
_chemical_formula_sum           'C13 H26 Au2 N4 O P2'
_chemical_formula_weight        710.25

loop_
 _atom_type_symbol
 _atom_type_description
 _atom_type_scat_dispersion_real
 _atom_type_scat_dispersion_imag
 _atom_type_scat_source
'C'  'C'   0.0033   0.0016
 'International Tables Vol C Tables 4.2.6.8 and 6.1.1.4'
'H'  'H'   0.0000   0.0000
 'International Tables Vol C Tables 4.2.6.8 and 6.1.1.4'
'N'  'N'   0.0061   0.0033
 'International Tables Vol C Tables 4.2.6.8 and 6.1.1.4'
'P'  'P'   0.1023   0.0942
 'International Tables Vol C Tables 4.2.6.8 and 6.1.1.4'
'O'  'O'   0.0106   0.0060
 'International Tables Vol C Tables 4.2.6.8 and 6.1.1.4'
'Au'  'Au'  -2.0133   8.8022
 'International Tables Vol C Tables 4.2.6.8 and 6.1.1.4'

_symmetry_cell_setting          monoclinic
_symmetry_space_group_name_H-M    'C 2/c'
_symmetry_space_group_name_Hall   '-C 2yc'
_symmetry_int_tables_number      15

loop_
 _symmetry_equiv_pos_as_xyz
 'x, y, z'
 '-x, y, -z+1/2'
 'x+1/2, y+1/2, z'
 '-x+1/2, y+1/2, -z+1/2'
 '-x, -y, -z'
 'x, -y, z-1/2'
 '-x+1/2, -y+1/2, -z'
 'x+1/2, -y+1/2, z-1/2'

_cell_length_a                 26.467(4)
_cell_length_b                 10.6496(13)
```

_geom_angle_site_symmetry_1
_geom_angle_site_symmetry_3
_geom_angle_publ_flag
N1 Au1 P1 177.19(9) . . ?
N1 Au1 Au2 83.60(9) . 7_556 ?
P1 Au1 Au2 93.60(3) . 7_556 ?
N1 Au1 Au1 85.85(9) . 2_656 ?
P1 Au1 Au1 96.90(3) . 2_656 ?
Au2 Au1 Au1 159.419(5) 7_556 2_656 ?
N21 Au2 P2 176.56(10) . . ?
N21 Au2 Au1 88.32(10) . 7_556 ?
P2 Au2 Au1 95.06(3) . 7_556 ?
C28 P2 C27 103.8(2) . . ?
C28 P2 C26 105.4(2) . . ?
C27 P2 C26 104.2(2) . . ?
C28 P2 Au2 113.88(16) . . ?
C27 P2 Au2 114.92(17) . . ?
C26 P2 Au2 113.50(14) . . ?
C8 P1 C7 105.5(2) . . ?
C8 P1 C6 107.2(2) . . ?
C7 P1 C6 104.9(2) . . ?
C8 P1 Au1 112.76(15) . . ?
C7 P1 Au1 117.57(14) . . ?
C6 P1 Au1 108.27(13) . . ?
C5 N1 C2 104.2(3) . . ?
C5 N1 Au1 128.4(3) . . ?
C2 N1 Au1 127.3(3) . . ?
C22 N21 C25 103.6(4) . . ?
C22 N21 Au2 128.5(3) . . ?
C25 N21 Au2 127.8(3) . . ?
P2 C28 H28A 109.5 . . ?
P2 C28 H28C 109.5 . . ?
H28A C28 H28C 109.5 . . ?
P2 C28 H28B 109.5 . . ?
H28A C28 H28B 109.5 . . ?
H28C C28 H28B 109.5 . . ?
C5 N4 C3 103.7(4) . . ?
C6 C26 P2 110.2(3) . . ?
C6 C26 H26A 109.6 . . ?
P2 C26 H26A 109.6 . . ?
C6 C26 H26B 109.6 . . ?
P2 C26 H26B 109.6 . . ?
H26A C26 H26B 108.1 . . ?
P1 C7 H7C 109.5 . . ?
P1 C7 H7B 109.5 . . ?
H7C C7 H7B 109.5 . . ?
P1 C7 H7A 109.5 . . ?
H7C C7 H7A 109.5 . . ?
H7B C7 H7A 109.5 . . ?
N4 C5 N1 115.0(4) . . ?
N4 C5 H5 122.5 . . ?
N1 C5 H5 122.5 . . ?

P1 C8 H8A 109.5 . . ?
P1 C8 H8C 109.5 . . ?
H8A C8 H8C 109.5 . . ?
P1 C8 H8B 109.5 . . ?
H8A C8 H8B 109.5 . . ?
H8C C8 H8B 109.5 . . ?
C26 C6 P1 117.5(3) . . ?
C26 C6 H6B 107.9 . . ?
P1 C6 H6B 107.9 . . ?
C26 C6 H6A 107.9 . . ?
P1 C6 H6A 107.9 . . ?
H6B C6 H6A 107.2 . . ?
P2 C27 H27B 109.5 . . ?
P2 C27 H27C 109.5 . . ?
H27B C27 H27C 109.5 . . ?
P2 C27 H27A 109.5 . . ?
H27B C27 H27A 109.5 . . ?
H27C C27 H27A 109.5 . . ?
N1 C2 C3 107.6(4) . . ?
N1 C2 H2 126.2 . . ?
C3 C2 H2 126.2 . . ?
N4 C3 C2 109.6(4) . . ?
N4 C3 H3 125.2 . . ?
C2 C3 H3 125.2 . . ?
N23 C22 N21 115.3(5) . . ?
N23 C22 H22 122.4 . . ?
N21 C22 H22 122.4 . . ?
C24 C25 N21 107.4(4) . . ?
C24 C25 H25 126.3 . . ?
N21 C25 H25 126.3 . . ?
C22 N23 C24 103.4(4) . . ?
C25 C24 N23 110.4(4) . . ?
C25 C24 H24 124.8 . . ?
N23 C24 H24 124.8 . . ?
C30 O1 H1 109.5 . . ?
O1 C30 H30A 109.5 . . ?
O1 C30 H30C 109.5 . . ?
H30A C30 H30C 109.5 . . ?
O1 C30 H30B 109.5 . . ?
H30A C30 H30B 109.5 . . ?
H30C C30 H30B 109.5 . . ?

loop_
 _geom_torsion_atom_site_label_1
 _geom_torsion_atom_site_label_2
 _geom_torsion_atom_site_label_3
 _geom_torsion_atom_site_label_4
 _geom_torsion
 _geom_torsion_site_symmetry_1
 _geom_torsion_site_symmetry_2
 _geom_torsion_site_symmetry_3
 _geom_torsion_site_symmetry_4

_geom_torsion_publ_flag
Au1 Au2 P2 C28 89.78(17) 7_556 . . . ?
Au1 Au2 P2 C27 -29.79(18) 7_556 . . . ?
Au1 Au2 P2 C26 -149.61(14) 7_556 . . . ?
Au2 Au1 P1 C8 -79.03(17) 7_556 . . . ?
Au1 Au1 P1 C8 118.71(17) 2_656 . . . ?
Au2 Au1 P1 C7 157.95(17) 7_556 . . . ?
Au1 Au1 P1 C7 -4.31(17) 2_656 . . . ?
Au2 Au1 P1 C6 39.37(16) 7_556 . . . ?
Au1 Au1 P1 C6 -122.90(16) 2_656 . . . ?
Au2 Au1 N1 C5 53.9(4) 7_556 . . . ?
Au1 Au1 N1 C5 -143.8(4) 2_656 . . . ?
Au2 Au1 N1 C2 -129.9(4) 7_556 . . . ?
Au1 Au1 N1 C2 32.4(3) 2_656 . . . ?
Au1 Au2 N21 C22 127.1(4) 7_556 . . . ?
Au1 Au2 N21 C25 -55.4(4) 7_556 . . . ?
C28 P2 C26 C6 178.3(3) . . . . ?
C27 P2 C26 C6 -72.8(3) . . . . ?
Au2 P2 C26 C6 53.0(3) . . . . ?
C3 N4 C5 N1 0.5(6) . . . . ?
C2 N1 C5 N4 -0.5(5) . . . . ?
Au1 N1 C5 N4 176.4(3) . . . . ?
P2 C26 C6 P1 171.8(2) . . . . ?
C8 P1 C6 C26 -58.7(4) . . . . ?
C7 P1 C6 C26 53.0(4) . . . . ?
Au1 P1 C6 C26 179.4(3) . . . . ?
C5 N1 C2 C3 0.4(5) . . . . ?
Au1 N1 C2 C3 -176.6(3) . . . . ?
C5 N4 C3 C2 -0.2(6) . . . . ?
N1 C2 C3 N4 -0.1(6) . . . . ?
C25 N21 C22 N23 0.4(5) . . . . ?
Au2 N21 C22 N23 178.3(3) . . . . ?
C22 N21 C25 C24 0.1(5) . . . . ?
Au2 N21 C25 C24 -177.8(3) . . . . ?
N21 C22 N23 C24 -0.7(6) . . . . ?
N21 C25 C24 N23 -0.5(5) . . . . ?
C22 N23 C24 C25 0.7(5) . . . . ?

loop_
_geom_hbond_atom_site_label_D
_geom_hbond_atom_site_label_H
_geom_hbond_atom_site_label_A
_geom_hbond_distance_DH
_geom_hbond_distance_HA
_geom_hbond_distance_DA
_geom_hbond_angle_DHA
_geom_hbond_site_symmetry_A
O1 H1 N4 0.84 2.00 2.820(5) 165.9 .

_diffrn_measured_fraction_theta_max 0.939
_diffrn_reflns_theta_full 26.00
_diffrn_measured_fraction_theta_full 0.998

_refine_diff_density_max 0.732
_refine_diff_density_min -0.843
_refine_diff_density_rms 0.123

```
data_Compound18

_audit_creation_method          SHELXL-97
_chemical_name_systematic
;
Bis(1,2,4-triazolido-\kN^1^)[\m-1,6-bis(diphenylphosphino-\kP)hexane]
digold(I)
;
_chemical_name_common           ?
_chemical_melting_point         ?
_chemical_formula_moiety        'C34 H36 Au2 N6 P2'
_chemical_formula_sum           'C34 H36 Au2 N6 P2'
_chemical_formula_weight        984.56

loop_
 _atom_type_symbol
 _atom_type_description
 _atom_type_scat_dispersion_real
 _atom_type_scat_dispersion_imag
 _atom_type_scat_source
'C'  'C'   0.0033   0.0016
 'International Tables Vol C Tables 4.2.6.8 and 6.1.1.4'
'H'  'H'   0.0000   0.0000
 'International Tables Vol C Tables 4.2.6.8 and 6.1.1.4'
'N'  'N'   0.0061   0.0033
 'International Tables Vol C Tables 4.2.6.8 and 6.1.1.4'
'P'  'P'   0.1023   0.0942
 'International Tables Vol C Tables 4.2.6.8 and 6.1.1.4'
'Au'  'Au'  -2.0133   8.8022
 'International Tables Vol C Tables 4.2.6.8 and 6.1.1.4'

_symmetry_cell_setting          triclinic
_symmetry_space_group_name_H-M    'P -1'
_symmetry_space_group_name_Hall   '-P 1'
_symmetry_int_tables_number       2

loop_
 _symmetry_equiv_pos_as_xyz
'x, y, z'
'-x, -y, -z'

_cell_length_a                  8.8411(10)
_cell_length_b                  9.8465(11)
_cell_length_c                  10.7011(12)
_cell_angle_alpha               70.016(2)
_cell_angle_beta                70.623(2)
_cell_angle_gamma               78.093(2)
_cell_volume                    821.34(16)
_cell_formula_units_Z           1
_cell_measurement_temperature     100(2)
_cell_measurement_reflns_used     7901
```

_cell_measurement_theta_min 2.456
_cell_measurement_theta_max 26.465

_exptl_crystal_description prism
_exptl_crystal_colour colourless
_exptl_crystal_size_max 0.30
_exptl_crystal_size_mid 0.25
_exptl_crystal_size_min 0.15
_exptl_crystal_density_meas ?
_exptl_crystal_density_diffrn 1.991
_exptl_crystal_density_method 'not measured'
_exptl_crystal_F_000 470
_exptl_absorpt_coefficient_mu 9.052
_exptl_absorpt_correction_type multi-scan
_exptl_absorpt_correction_T_min 0.127
_exptl_absorpt_correction_T_max 0.344
_exptl_absorpt_process_details 'SADABS (Bruker, 2002)'

_exptl_special_details ?

_diffrn_ambient_temperature 100(2)
_diffrn_radiation_wavelength 0.71073
_diffrn_radiation_type MoK\a
_diffrn_radiation_source 'fine-focus sealed tube'
_diffrn_radiation_monochromator graphite
_diffrn_measurement_device_type 'Bruker APEX CCD area-detector'
_diffrn_measurement_method \w-scans
_diffrn_detector_area_resol_mean ?
_diffrn_reflns_number 8662
_diffrn_reflns_av_R_equivalents 0.0265
_diffrn_reflns_av_sigmaI/netI 0.0294
_diffrn_reflns_limit_h_min -11
_diffrn_reflns_limit_h_max 11
_diffrn_reflns_limit_k_min -12
_diffrn_reflns_limit_k_max 12
_diffrn_reflns_limit_l_min -13
_diffrn_reflns_limit_l_max 13
_diffrn_reflns_theta_min 2.11
_diffrn_reflns_theta_max 26.46
_reflns_number_total 3351
_reflns_number_gt 3311
_reflns_threshold_expression I>2\s(I)

_computing_data_collection 'SMART (Bruker, 2001)'
_computing_cell_refinement 'SAINT (Bruker, 2002)'
_computing_data_reduction SAINT
_computing_structure_solution 'SHELXS-97 (Sheldrick, 2008)'
_computing_structure_refinement 'SHELXL-97 (Sheldrick, 2008)'
_computing_molecular_graphics
'X-Seed (Atwood & Barbour, 2003; Barbour, 2001)'
_computing_publication_material X-Seed

```
_refine_special_details
;
 Refinement of F^2^ against ALL reflections.  The weighted R-factor wR and
 goodness of fit S are based on F^2^, conventional R-factors R are based
 on F, with F set to zero for negative F^2^. The threshold expression of
 F^2^ > 2\s(F^2^) is used only for calculating R-factors(gt) etc. and is
 not relevant to the choice of reflections for refinement.  R-factors based
 on F^2^ are statistically about twice as large as those based on F, and R-
 factors based on ALL data will be even larger.
;

_refine_ls_structure_factor_coef  Fsqd
_refine_ls_matrix_type          full
_refine_ls_weighting_scheme      calc
_refine_ls_weighting_details
 'calc w=1/[\s^2^(Fo^2^)+(0.0282P)^2^+0.3300P] where P=(Fo^2^+2Fc^2^)/3'
_atom_sites_solution_primary     direct
_atom_sites_solution_secondary    difmap
_atom_sites_solution_hydrogens    geom
_refine_ls_hydrogen_treatment    constr
_refine_ls_extinction_method     none
_refine_ls_extinction_coef       ?
_refine_ls_number_reflns         3351
_refine_ls_number_parameters     199
_refine_ls_number_restraints     0
_refine_ls_R_factor_all          0.0199
_refine_ls_R_factor_gt           0.0196
_refine_ls_wR_factor_ref         0.0506
_refine_ls_wR_factor_gt          0.0505
_refine_ls_goodness_of_fit_ref    1.108
_refine_ls_restrained_S_all      1.108
_refine_ls_shift/su_max          0.006
_refine_ls_shift/su_mean         0.000

loop_
 _atom_site_label
 _atom_site_type_symbol
 _atom_site_fract_x
 _atom_site_fract_y
 _atom_site_fract_z
 _atom_site_U_iso_or_equiv
 _atom_site_adp_type
 _atom_site_occupancy
 _atom_site_symmetry_multiplicity
 _atom_site_calc_flag
 _atom_site_refinement_flags
 _atom_site_disorder_assembly
 _atom_site_disorder_group
Au1 Au 0.379810(12) 0.242362(10) 1.131178(9) 0.01434(6) Uani 1 1 d . . .
P1 P 0.42010(9) 0.27136(8) 0.90599(8) 0.01150(15) Uani 1 1 d . . .
N1 N 0.3464(3) 0.1951(3) 1.3390(3) 0.0174(5) Uani 1 1 d . . .
N4 N 0.3774(4) 0.1686(3) 1.5425(3) 0.0232(6) Uani 1 1 d . . .
```

C14 C 0.1523(5) 0.6623(4) 0.8014(4) 0.0275(8) Uani 1 1 d . . .
H14 H 0.0913 0.7340 0.8446 0.033 Uiso 1 1 calc R . .
C10 C 0.3201(3) 0.4350(3) 0.8123(3) 0.0139(5) Uani 1 1 d . . .
C7 C 0.1640(3) 0.1226(3) 0.9644(3) 0.0145(5) Uani 1 1 d . . .
H7A H 0.1495 0.1150 1.0623 0.017 Uiso 1 1 calc R . .
H7B H 0.1057 0.2159 0.9236 0.017 Uiso 1 1 calc R . .
N2 N 0.2739(4) 0.0729(3) 1.4279(3) 0.0263(6) Uani 1 1 d . . .
C13 C 0.1638(4) 0.6808(4) 0.6650(3) 0.0235(7) Uani 1 1 d . . .
H13 H 0.1102 0.7649 0.6148 0.028 Uiso 1 1 calc R . .
C6 C 0.3436(3) 0.1247(3) 0.8864(3) 0.0132(5) Uani 1 1 d . . .
H6A H 0.3594 0.1390 0.7869 0.016 Uiso 1 1 calc R . .
H6B H 0.4032 0.0307 0.9239 0.016 Uiso 1 1 calc R . .
C15 C 0.2293(4) 0.5391(4) 0.8760(3) 0.0221(7) Uani 1 1 d . . .
H15 H 0.2201 0.5261 0.9703 0.027 Uiso 1 1 calc R . .
C8 C 0.0892(3) -0.0012(3) 0.9609(3) 0.0145(6) Uani 1 1 d . . .
H8A H 0.1463 -0.0948 1.0025 0.017 Uiso 1 1 calc R . .
H8B H 0.1029 0.0060 0.8633 0.017 Uiso 1 1 calc R . .
C5 C 0.4064(4) 0.2462(4) 1.4111(3) 0.0219(7) Uani 1 1 d . . .
H5 H 0.4639 0.3295 1.3719 0.026 Uiso 1 1 calc R . .
C11 C 0.3307(4) 0.4548(3) 0.6737(3) 0.0156(6) Uani 1 1 d . . .
H11 H 0.3914 0.3835 0.6299 0.019 Uiso 1 1 calc R . .
C3 C 0.2961(4) 0.0635(4) 1.5467(3) 0.0247(7) Uani 1 1 d . . .
H3 H 0.2578 -0.0115 1.6295 0.030 Uiso 1 1 calc R . .
C12 C 0.2535(4) 0.5771(3) 0.6006(3) 0.0188(6) Uani 1 1 d . . .
H12 H 0.2616 0.5905 0.5065 0.023 Uiso 1 1 calc R . .
C16 C 0.6314(3) 0.2731(3) 0.8097(3) 0.0138(5) Uani 1 1 d . . .
C17 C 0.7158(4) 0.1681(3) 0.7443(3) 0.0165(6) Uani 1 1 d . . .
H17 H 0.6610 0.0938 0.7458 0.020 Uiso 1 1 calc R . .
C21 C 0.7125(4) 0.3837(3) 0.8043(3) 0.0192(6) Uani 1 1 d . . .
H21 H 0.6556 0.4553 0.8488 0.023 Uiso 1 1 calc R . .
C18 C 0.8797(4) 0.1717(4) 0.6767(3) 0.0208(6) Uani 1 1 d . . .
H18 H 0.9376 0.0989 0.6340 0.025 Uiso 1 1 calc R . .
C19 C 0.9591(4) 0.2836(3) 0.6722(3) 0.0200(6) Uani 1 1 d . . .
H19 H 1.0710 0.2867 0.6260 0.024 Uiso 1 1 calc R . .
C20 C 0.8748(4) 0.3898(4) 0.7347(3) 0.0237(7) Uani 1 1 d . . .
H20 H 0.9284 0.4665 0.7298 0.028 Uiso 1 1 calc R . .

loop_
 _atom_site_aniso_label
 _atom_site_aniso_U_11
 _atom_site_aniso_U_22
 _atom_site_aniso_U_33
 _atom_site_aniso_U_23
 _atom_site_aniso_U_13
 _atom_site_aniso_U_12
Au1 0.01921(8) 0.01449(8) 0.01115(8) -0.00410(5) -0.00610(5) -0.00218(5)
P1 0.0133(3) 0.0117(4) 0.0108(3) -0.0036(3) -0.0048(3) -0.0012(3)
N1 0.0261(14) 0.0159(13) 0.0128(12) -0.0006(10) -0.0114(11) -0.0046(10)
N4 0.0285(15) 0.0268(15) 0.0165(13) -0.0095(12) -0.0087(12) 0.0015(12)
C14 0.037(2) 0.0190(17) 0.0235(17) -0.0100(14) -0.0079(15) 0.0089(14)
C10 0.0127(13) 0.0137(14) 0.0151(13) -0.0032(11) -0.0047(11) -0.0018(10)
C7 0.0158(14) 0.0133(13) 0.0160(13) -0.0053(11) -0.0053(11) -0.0021(11)

N2 0.0332(16) 0.0205(14) 0.0238(14) -0.0048(11) -0.0057(12) -0.0067(12)
C13 0.0283(17) 0.0182(16) 0.0227(16) -0.0030(13) -0.0132(14) 0.0050(13)
C6 0.0141(14) 0.0126(13) 0.0132(12) -0.0042(10) -0.0039(11) -0.0014(10)
C15 0.0273(17) 0.0218(16) 0.0167(14) -0.0082(12) -0.0061(13) 0.0028(13)
C8 0.0169(15) 0.0137(14) 0.0138(13) -0.0026(11) -0.0061(11) -0.0032(11)
C5 0.0258(17) 0.0240(17) 0.0178(14) -0.0065(13) -0.0064(13) -0.0061(13)
C11 0.0179(14) 0.0156(14) 0.0145(13) -0.0057(11) -0.0050(11) -0.0017(11)
C3 0.0303(18) 0.0213(16) 0.0162(14) -0.0016(12) -0.0039(13) -0.0008(13)
C12 0.0214(15) 0.0186(15) 0.0166(14) -0.0023(12) -0.0081(12) -0.0029(12)
C16 0.0159(14) 0.0141(14) 0.0111(13) -0.0008(10) -0.0065(11) -0.0017(11)
C17 0.0212(15) 0.0130(14) 0.0157(13) -0.0016(11) -0.0081(12) -0.0023(11)
C21 0.0210(15) 0.0186(15) 0.0214(14) -0.0081(12) -0.0077(12) -0.0026(12)
C18 0.0181(15) 0.0268(17) 0.0182(14) -0.0080(13) -0.0080(12) 0.0032(12)
C19 0.0132(14) 0.0239(16) 0.0197(14) -0.0017(12) -0.0058(12) -0.0019(12)
C20 0.0211(16) 0.0234(17) 0.0287(16) -0.0041(13) -0.0101(13) -0.0081(13)

_geom_special_details
;
All esds (except the esd in the dihedral angle between two l.s. planes)
are estimated using the full covariance matrix. The cell esds are taken
into account individually in the estimation of esds in distances, angles
and torsion angles; correlations between esds in cell parameters are only
used when they are defined by crystal symmetry. An approximate (isotropic)
treatment of cell esds is used for estimating esds involving l.s. planes.
;

loop_
_geom_bond_atom_site_label_1
_geom_bond_atom_site_label_2
_geom_bond_distance
_geom_bond_site_symmetry_2
_geom_bond_publ_flag
Au1 N1 2.041(3) . ?
Au1 P1 2.2400(8) . ?
P1 C16 1.810(3) . ?
P1 C10 1.811(3) . ?
P1 C6 1.814(3) . ?
N1 C5 1.333(4) . ?
N1 N2 1.376(4) . ?
N4 C5 1.317(4) . ?
N4 C3 1.357(5) . ?
C14 C13 1.379(5) . ?
C14 C15 1.389(5) . ?
C14 H14 0.9500 . ?
C10 C15 1.391(4) . ?
C10 C11 1.401(4) . ?
C7 C8 1.518(4) . ?
C7 C6 1.530(4) . ?
C7 H7A 0.9900 . ?
C7 H7B 0.9900 . ?
N2 C3 1.320(4) . ?
C13 C12 1.389(5) . ?

C13 H13 0.9500 . ?
C6 H6A 0.9900 . ?
C6 H6B 0.9900 . ?
C15 H15 0.9500 . ?
C8 C8 1.519(6) 2_557 ?
C8 H8A 0.9900 . ?
C8 H8B 0.9900 . ?
C5 H5 0.9500 . ?
C11 C12 1.378(4) . ?
C11 H11 0.9500 . ?
C3 H3 0.9500 . ?
C12 H12 0.9500 . ?
C16 C17 1.395(4) . ?
C16 C21 1.398(4) . ?
C17 C18 1.390(4) . ?
C17 H17 0.9500 . ?
C21 C20 1.383(4) . ?
C21 H21 0.9500 . ?
C18 C19 1.403(5) . ?
C18 H18 0.9500 . ?
C19 C20 1.386(5) . ?
C19 H19 0.9500 . ?
C20 H20 0.9500 . ?

loop_
 _geom_angle_atom_site_label_1
 _geom_angle_atom_site_label_2
 _geom_angle_atom_site_label_3
 _geom_angle
 _geom_angle_site_symmetry_1
 _geom_angle_site_symmetry_3
 _geom_angle_publ_flag
N1 Au1 P1 174.53(7) . . ?
C16 P1 C10 105.32(13) . . ?
C16 P1 C6 108.13(13) . . ?
C10 P1 C6 104.34(13) . . ?
C16 P1 Au1 112.25(9) . . ?
C10 P1 Au1 116.20(10) . . ?
C6 P1 Au1 110.02(9) . . ?
C5 N1 N2 107.8(3) . . ?
C5 N1 Au1 131.9(2) . . ?
N2 N1 Au1 119.1(2) . . ?
C5 N4 C3 101.6(3) . . ?
C13 C14 C15 120.2(3) . . ?
C13 C14 H14 119.9 . . ?
C15 C14 H14 119.9 . . ?
C15 C10 C11 119.4(3) . . ?
C15 C10 P1 121.5(2) . . ?
C11 C10 P1 119.1(2) . . ?
C8 C7 C6 113.7(2) . . ?
C8 C7 H7A 108.8 . . ?
C6 C7 H7A 108.8 . . ?

C8 C7 H7B 108.8 . . ?
C6 C7 H7B 108.8 . . ?
H7A C7 H7B 107.7 . . ?
C3 N2 N1 102.6(3) . . ?
C14 C13 C12 120.4(3) . . ?
C14 C13 H13 119.8 . . ?
C12 C13 H13 119.8 . . ?
C7 C6 P1 109.27(19) . . ?
C7 C6 H6A 109.8 . . ?
P1 C6 H6A 109.8 . . ?
C7 C6 H6B 109.8 . . ?
P1 C6 H6B 109.8 . . ?
H6A C6 H6B 108.3 . . ?
C14 C15 C10 119.8(3) . . ?
C14 C15 H15 120.1 . . ?
C10 C15 H15 120.1 . . ?
C7 C8 C8 112.0(3) . 2_557 ?
C7 C8 H8A 109.2 . . ?
C8 C8 H8A 109.2 2_557 . ?
C7 C8 H8B 109.2 . . ?
C8 C8 H8B 109.2 2_557 . ?
H8A C8 H8B 107.9 . . ?
N4 C5 N1 112.7(3) . . ?
N4 C5 H5 123.7 . . ?
N1 C5 H5 123.7 . . ?
C12 C11 C10 120.3(3) . . ?
C12 C11 H11 119.8 . . ?
C10 C11 H11 119.8 . . ?
N2 C3 N4 115.4(3) . . ?
N2 C3 H3 122.3 . . ?
N4 C3 H3 122.3 . . ?
C11 C12 C13 119.8(3) . . ?
C11 C12 H12 120.1 . . ?
C13 C12 H12 120.1 . . ?
C17 C16 C21 119.4(3) . . ?
C17 C16 P1 123.0(2) . . ?
C21 C16 P1 117.7(2) . . ?
C18 C17 C16 120.3(3) . . ?
C18 C17 H17 119.9 . . ?
C16 C17 H17 119.9 . . ?
C20 C21 C16 120.7(3) . . ?
C20 C21 H21 119.7 . . ?
C16 C21 H21 119.7 . . ?
C17 C18 C19 119.6(3) . . ?
C17 C18 H18 120.2 . . ?
C19 C18 H18 120.2 . . ?
C20 C19 C18 120.3(3) . . ?
C20 C19 H19 119.9 . . ?
C18 C19 H19 119.9 . . ?
C21 C20 C19 119.8(3) . . ?
C21 C20 H20 120.1 . . ?
C19 C20 H20 120.1 . . ?

```
loop_
 _geom_torsion_atom_site_label_1
 _geom_torsion_atom_site_label_2
 _geom_torsion_atom_site_label_3
 _geom_torsion_atom_site_label_4
 _geom_torsion
 _geom_torsion_site_symmetry_1
 _geom_torsion_site_symmetry_2
 _geom_torsion_site_symmetry_3
 _geom_torsion_site_symmetry_4
 _geom_torsion_publ_flag
C16 P1 C10 C15 -122.2(3) . . . . ?
C6 P1 C10 C15 124.0(3) . . . . ?
Au1 P1 C10 C15 2.7(3) . . . . ?
C16 P1 C10 C11 59.6(3) . . . . ?
C6 P1 C10 C11 -54.1(3) . . . . ?
Au1 P1 C10 C11 -175.44(19) . . . . ?
C5 N1 N2 C3 0.8(4) . . . . ?
Au1 N1 N2 C3 170.1(2) . . . . ?
C15 C14 C13 C12 -0.5(6) . . . . ?
C8 C7 C6 P1 -177.12(19) . . . . ?
C16 P1 C6 C7 -178.85(19) . . . . ?
C10 P1 C6 C7 -67.1(2) . . . . ?
Au1 P1 C6 C7 58.2(2) . . . . ?
C13 C14 C15 C10 0.7(6) . . . . ?
C11 C10 C15 C14 -0.9(5) . . . . ?
P1 C10 C15 C14 -179.0(3) . . . . ?
C6 C7 C8 C8 -179.8(3) . . . 2_557 ?
C3 N4 C5 N1 0.8(4) . . . . ?
N2 N1 C5 N4 -1.0(4) . . . . ?
Au1 N1 C5 N4 -168.4(2) . . . . ?
C15 C10 C11 C12 0.7(4) . . . . ?
P1 C10 C11 C12 178.9(2) . . . . ?
N1 N2 C3 N4 -0.3(4) . . . . ?
C5 N4 C3 N2 -0.3(4) . . . . ?
C10 C11 C12 C13 -0.4(4) . . . . ?
C14 C13 C12 C11 0.3(5) . . . . ?
C10 P1 C16 C17 -116.1(2) . . . . ?
C6 P1 C16 C17 -5.0(3) . . . . ?
Au1 P1 C16 C17 116.6(2) . . . . ?
C10 P1 C16 C21 65.3(2) . . . . ?
C6 P1 C16 C21 176.4(2) . . . . ?
Au1 P1 C16 C21 -62.0(2) . . . . ?
C21 C16 C17 C18 1.3(4) . . . . ?
P1 C16 C17 C18 -177.3(2) . . . . ?
C17 C16 C21 C20 0.1(4) . . . . ?
P1 C16 C21 C20 178.7(2) . . . . ?
C16 C17 C18 C19 -1.4(4) . . . . ?
C17 C18 C19 C20 0.1(5) . . . . ?
C16 C21 C20 C19 -1.4(5) . . . . ?
C18 C19 C20 C21 1.3(5) . . . . ?
```

_diffrn_measured_fraction_theta_max 0.990
_diffrn_reflns_theta_full 26.00
_diffrn_measured_fraction_theta_full 0.994
_refine_diff_density_max 1.437
_refine_diff_density_min -1.353
_refine_diff_density_rms 0.125

```
data_I

_audit_creation_method          SHELXL-97
_chemical_name_systematic
;
 ?
;
_chemical_name_common           ?
_chemical_melting_point         ?
_chemical_formula_moiety        'C58 H54 Au4 N4 P4, 2Cl'
_chemical_formula_sum
'C58 H54 Au4 Cl2 N4 P4'
_chemical_formula_weight        1789.70

loop_
 _atom_type_symbol
 _atom_type_description
 _atom_type_scat_dispersion_real
 _atom_type_scat_dispersion_imag
 _atom_type_scat_source
'C'  'C'   0.0033   0.0016
 'International Tables Vol C Tables 4.2.6.8 and 6.1.1.4'
'H'  'H'   0.0000   0.0000
 'International Tables Vol C Tables 4.2.6.8 and 6.1.1.4'
'N'  'N'   0.0061   0.0033
 'International Tables Vol C Tables 4.2.6.8 and 6.1.1.4'
'P'  'P'   0.1023   0.0942
 'International Tables Vol C Tables 4.2.6.8 and 6.1.1.4'
'Au'  'Au'  -2.0133   8.8022
 'International Tables Vol C Tables 4.2.6.8 and 6.1.1.4'

_symmetry_cell_setting          monoclinic
_symmetry_space_group_name_H-M    C2/m
_symmetry_space_group_name_Hall   '-C 2y'

loop_
 _symmetry_equiv_pos_as_xyz
 'x, y, z'
 '-x, y, -z'
 'x+1/2, y+1/2, z'
 '-x+1/2, y+1/2, -z'
 '-x, -y, -z'
 'x, -y, z'
 '-x+1/2, -y+1/2, -z'
 'x+1/2, -y+1/2, z'

_cell_length_a                 18.156(5)
_cell_length_b                 21.701(6)
_cell_length_c                 12.304(4)
_cell_angle_alpha               90.00
_cell_angle_beta                123.616(4)
```

```
_cell_angle_gamma                90.00
_cell_volume                     4037(2)
_cell_formula_units_Z            2
_cell_measurement_temperature    150(2)
_cell_measurement_reflns_used    2935
_cell_measurement_theta_min      2.695
_cell_measurement_theta_max      27.153

_exptl_crystal_description       'prism'
_exptl_crystal_colour            'yellow'
_exptl_crystal_size_max          0.32
_exptl_crystal_size_mid          0.28
_exptl_crystal_size_min          0.17
_exptl_crystal_density_meas      ?
_exptl_crystal_density_diffrn    1.484
_exptl_crystal_density_method    'not measured'
_exptl_crystal_F_000             1680
_exptl_absorpt_coefficient_mu    7.478
_exptl_absorpt_correction_type   'multi-scan'
_exptl_absorpt_correction_T_min  0.2019
_exptl_absorpt_correction_T_max  0.3679
_exptl_absorpt_process_details   'SADABS (Sheldrick, 1997)'

_exptl_special_details
;
 ?
;

_diffrn_ambient_temperature      150(2)
_diffrn_radiation_wavelength     0.71073
_diffrn_radiation_type           MoK\a
_diffrn_radiation_source         'fine-focus sealed tube'
_diffrn_radiation_monochromator  'graphite'
_diffrn_measurement_device_type  'Bruker APEX CCD area-detector'
_diffrn_measurement_method       '\w'
_diffrn_detector_area_resol_mean  ?
_diffrn_standards_number         ?
_diffrn_standards_interval_count  ?
_diffrn_standards_interval_time   ?
_diffrn_standards_decay_%        ?
_diffrn_reflns_number            7563
_diffrn_reflns_av_R_equivalents  0.0580
_diffrn_reflns_av_sigmaI/netI    0.0888
_diffrn_reflns_limit_h_min       -19
_diffrn_reflns_limit_h_max       21
_diffrn_reflns_limit_k_min       -25
_diffrn_reflns_limit_k_max       23
_diffrn_reflns_limit_l_min       -10
_diffrn_reflns_limit_l_max       14
_diffrn_reflns_theta_min         1.64
_diffrn_reflns_theta_max         24.71
_reflns_number_total             3348
```

```
_reflns_number_gt               2256
_reflns_threshold_expression     >2sigma(I)

_computing_data_collection       'SMART (Bruker, 2001)'
_computing_cell_refinement       'SAINT (Bruker, 2002)'
_computing_data_reduction        'SAINT'
_computing_structure_solution    'SHELXS-97 (Sheldrick, 1990)'
_computing_structure_refinement  'SHELXL-97 (Sheldrick, 1997)'
_computing_molecular_graphics    'X-Seed (Barbour 2001)'
_computing_publication_material  ?

_refine_special_details
;
 Refinement of F^2^ against ALL reflections.  The weighted R-factor wR and
 goodness of fit S are based on F^2^, conventional R-factors R are based
 on F, with F set to zero for negative F^2^. The threshold expression of
 F^2^ > 2sigma(F^2^) is used only for calculating R-factors(gt) etc. and is
 not relevant to the choice of reflections for refinement.  R-factors based
 on F^2^ are statistically about twice as large as those based on F, and R-
 factors based on ALL data will be even larger.
;

_refine_ls_structure_factor_coef  Fsqd
_refine_ls_matrix_type           full
_refine_ls_weighting_scheme      calc
_refine_ls_weighting_details
 'calc w=1/[\s^2^(Fo^2^)+(0.0980P)^2^] where P=(Fo^2^+2Fc^2^)/3'
_atom_sites_solution_primary     direct
_atom_sites_solution_secondary    difmap
_atom_sites_solution_hydrogens    geom
_refine_ls_hydrogen_treatment    constr
_refine_ls_extinction_method     none
_refine_ls_extinction_coef       ?
_refine_ls_number_reflns         3348
_refine_ls_number_parameters     160
_refine_ls_number_restraints     37
_refine_ls_R_factor_all          0.0915
_refine_ls_R_factor_gt           0.0697
_refine_ls_wR_factor_ref         0.1756
_refine_ls_wR_factor_gt          0.1678
_refine_ls_goodness_of_fit_ref   1.068
_refine_ls_restrained_S_all      1.068
_refine_ls_shift/su_max          0.000
_refine_ls_shift/su_mean         0.000

loop_
 _atom_site_label
 _atom_site_type_symbol
 _atom_site_fract_x
 _atom_site_fract_y
 _atom_site_fract_z
 _atom_site_U_iso_or_equiv
```

_atom_site_adp_type
_atom_site_occupancy
_atom_site_symmetry_multiplicity
_atom_site_calc_flag
_atom_site_refinement_flags
_atom_site_disorder_assembly
_atom_site_disorder_group
Au1 Au 0.41280(3) 0.36177(2) 0.49063(5) 0.0255(2) Uani 1 1 d . . .
P1 P 0.3797(2) 0.26885(17) 0.3958(3) 0.0213(8) Uani 1 1 d . . .
N1 N 0.4369(7) 0.4471(5) 0.5657(11) 0.030(2) Uani 1 1 d U . .
C1 C 0.3736(9) 0.2704(6) 0.2425(14) 0.042(4) Uani 1 1 d DU . .
C2 C 0.3618(9) 0.3265(8) 0.1788(13) 0.045(5) Uani 1 1 d D . .
H2 H 0.3586 0.3631 0.2184 0.054 Uiso 1 1 calc R . .
C3 C 0.3545(11) 0.3315(9) 0.0612(14) 0.063(5) Uani 1 1 d DU . .
H3 H 0.3462 0.3703 0.0200 0.076 Uiso 1 1 calc R . .
C4 C 0.3599(11) 0.2777(8) 0.0066(18) 0.068(5) Uani 1 1 d DU . .
H4 H 0.3575 0.2796 -0.0724 0.082 Uiso 1 1 calc R . .
C5 C 0.3687(11) 0.2209(9) 0.0635(15) 0.070(5) Uani 1 1 d DU . .
H5 H 0.3707 0.1845 0.0223 0.084 Uiso 1 1 calc R . .
C6 C 0.3746(9) 0.2167(8) 0.1818(14) 0.051(4) Uani 1 1 d DU . .
H6 H 0.3793 0.1777 0.2200 0.062 Uiso 1 1 calc R . .
C7 C 0.2705(9) 0.2422(7) 0.3487(14) 0.029(4) Uani 1 1 d . . .
C8 C 0.2497(9) 0.1809(8) 0.3437(18) 0.049(5) Uani 1 1 d . . .
H8 H 0.2939 0.1503 0.3694 0.059 Uiso 1 1 calc R . .
C9 C 0.1624(12) 0.1635(9) 0.300(2) 0.066(6) Uani 1 1 d . . .
H9 H 0.1480 0.1210 0.2935 0.079 Uiso 1 1 calc R . .
C10 C 0.0974(10) 0.2071(9) 0.2668(15) 0.044(4) Uani 1 1 d . . .
H10 H 0.0388 0.1954 0.2381 0.053 Uiso 1 1 calc R . .
C11 C 0.1219(10) 0.2685(9) 0.2774(16) 0.048(5) Uani 1 1 d . . .
H11 H 0.0784 0.2994 0.2541 0.057 Uiso 1 1 calc R . .
C12 C 0.2062(9) 0.2864(8) 0.3201(15) 0.039(4) Uani 1 1 d . . .
H12 H 0.2209 0.3290 0.3303 0.047 Uiso 1 1 calc R . .
C13 C 0.4539(8) 0.2071(7) 0.4920(15) 0.030(4) Uani 1 1 d . . .
H13B H 0.4645 0.2087 0.5801 0.036 Uiso 1 1 calc R . .
H13A H 0.4240 0.1675 0.4518 0.036 Uiso 1 1 calc R . .
C14 C 0.4861(9) 0.4687(6) 0.6937(14) 0.035(3) Uani 1 1 d U . .
H14 H 0.5152 0.4434 0.7695 0.042 Uiso 1 1 calc R . .
C15 C 0.4123(13) 0.5000 0.497(2) 0.038(4) Uani 1 2 d SU . .
H15 H 0.3793 0.5000 0.4040 0.046 Uiso 1 2 calc SR . .

loop_
_atom_site_aniso_label
_atom_site_aniso_U_11
_atom_site_aniso_U_22
_atom_site_aniso_U_33
_atom_site_aniso_U_23
_atom_site_aniso_U_13
_atom_site_aniso_U_12
Au1 0.0173(3) 0.0315(4) 0.0350(3) 0.0007(3) 0.0191(2) 0.0006(2)
P1 0.0098(16) 0.039(2) 0.0214(18) 0.0017(16) 0.0123(15) -0.0001(13)
N1 0.026(4) 0.041(4) 0.029(4) 0.005(3) 0.018(3) 0.002(3)
C1 0.017(7) 0.074(12) 0.035(9) -0.008(8) 0.014(7) -0.014(7)

C2 0.028(8) 0.090(14) 0.025(8) 0.007(9) 0.020(7) 0.003(8)
C3 0.033(9) 0.126(13) 0.036(9) 0.004(9) 0.022(8) -0.008(10)
C4 0.026(9) 0.143(13) 0.038(9) -0.019(7) 0.020(8) -0.024(9)
C5 0.034(10) 0.127(12) 0.051(10) -0.034(9) 0.023(9) -0.023(11)
C6 0.020(8) 0.087(11) 0.049(8) -0.027(8) 0.021(8) -0.021(8)
C7 0.020(7) 0.045(10) 0.030(8) 0.012(7) 0.018(7) 0.002(6)
C8 0.015(7) 0.058(12) 0.066(12) -0.002(9) 0.017(8) -0.001(7)
C9 0.049(11) 0.051(12) 0.111(18) -0.002(12) 0.053(12) -0.023(9)
C10 0.032(9) 0.081(14) 0.028(8) -0.002(9) 0.022(7) -0.004(9)
C11 0.023(8) 0.085(15) 0.040(10) -0.001(9) 0.020(8) 0.006(8)
C12 0.020(8) 0.055(11) 0.043(9) -0.023(8) 0.019(7) -0.003(7)
C13 0.010(7) 0.038(9) 0.043(9) 0.007(7) 0.015(6) 0.000(6)
C14 0.027(5) 0.041(5) 0.035(5) 0.004(4) 0.016(4) 0.006(4)
C15 0.032(6) 0.049(6) 0.029(5) 0.000 0.013(5) 0.000

_geom_special_details
;
All esds (except the esd in the dihedral angle between two l.s. planes)
are estimated using the full covariance matrix. The cell esds are taken
into account individually in the estimation of esds in distances, angles
and torsion angles; correlations between esds in cell parameters are only
used when they are defined by crystal symmetry. An approximate (isotropic)
treatment of cell esds is used for estimating esds involving l.s. planes.
;

loop_
_geom_bond_atom_site_label_1
_geom_bond_atom_site_label_2
_geom_bond_distance
_geom_bond_site_symmetry_2
_geom_bond_publ_flag
Au1 N1 2.007(12) . ?
Au1 P1 2.239(4) . ?
Au1 Au1 3.0448(14) 2_656 ?
P1 C13 1.802(13) . ?
P1 C7 1.825(14) . ?
P1 C1 1.827(16) . ?
N1 C15 1.347(15) . ?
N1 C14 1.393(18) . ?
C1 C6 1.39(2) . ?
C1 C2 1.40(2) . ?
C2 C3 1.38(2) . ?
C2 H2 0.9500 . ?
C3 C4 1.38(3) . ?
C3 H3 0.9500 . ?
C4 C5 1.38(3) . ?
C4 H4 0.9500 . ?
C5 C6 1.40(2) . ?
C5 H5 0.9500 . ?
C6 H6 0.9500 . ?
C7 C8 1.37(2) . ?
C7 C12 1.40(2) . ?

C8 C9 1.41(2) . ?
C8 H8 0.9500 . ?
C9 C10 1.38(3) . ?
C9 H9 0.9500 . ?
C10 C11 1.39(2) . ?
C10 H10 0.9500 . ?
C11 C12 1.37(2) . ?
C11 H11 0.9500 . ?
C12 H12 0.9500 . ?
C13 C13 1.58(2) 2_656 ?
C13 H13B 0.9900 . ?
C13 H13A 0.9900 . ?
C14 C14 1.36(3) 6_565 ?
C14 H14 0.9500 . ?
C15 N1 1.347(15) 6_565 ?
C15 H15 0.9500 . ?

loop_
 _geom_angle_atom_site_label_1
 _geom_angle_atom_site_label_2
 _geom_angle_atom_site_label_3
 _geom_angle
 _geom_angle_site_symmetry_1
 _geom_angle_site_symmetry_3
 _geom_angle_publ_flag
N1 Au1 P1 176.7(3) . . ?
N1 Au1 Au1 90.7(3) . 2_656 ?
P1 Au1 Au1 90.42(9) . 2_656 ?
C13 P1 C7 105.0(6) . . ?
C13 P1 C1 106.7(7) . . ?
C7 P1 C1 104.1(7) . . ?
C13 P1 Au1 116.1(5) . . ?
C7 P1 Au1 112.5(5) . . ?
C1 P1 Au1 111.5(4) . . ?
C15 N1 C14 102.0(13) . . ?
C15 N1 Au1 125.7(10) . . ?
C14 N1 Au1 132.0(10) . . ?
C6 C1 C2 118.1(16) . . ?
C6 C1 P1 121.9(12) . . ?
C2 C1 P1 119.8(11) . . ?
C3 C2 C1 123.4(17) . . ?
C3 C2 H2 118.3 . . ?
C1 C2 H2 118.3 . . ?
C4 C3 C2 116.9(19) . . ?
C4 C3 H3 121.6 . . ?
C2 C3 H3 121.6 . . ?
C3 C4 C5 122(2) . . ?
C3 C4 H4 119.1 . . ?
C5 C4 H4 119.1 . . ?
C4 C5 C6 120(2) . . ?
C4 C5 H5 119.8 . . ?
C6 C5 H5 119.8 . . ?

C1 C6 C5 119.3(17) . . ?
C1 C6 H6 120.4 . . ?
C5 C6 H6 120.4 . . ?
C8 C7 C12 118.9(14) . . ?
C8 C7 P1 123.0(11) . . ?
C12 C7 P1 118.1(12) . . ?
C7 C8 C9 119.8(15) . . ?
C7 C8 H8 120.1 . . ?
C9 C8 H8 120.1 . . ?
C10 C9 C8 121.6(17) . . ?
C10 C9 H9 119.2 . . ?
C8 C9 H9 119.2 . . ?
C9 C10 C11 116.8(16) . . ?
C9 C10 H10 121.6 . . ?
C11 C10 H10 121.6 . . ?
C12 C11 C10 122.6(16) . . ?
C12 C11 H11 118.7 . . ?
C10 C11 H11 118.7 . . ?
C11 C12 C7 120.1(16) . . ?
C11 C12 H12 119.9 . . ?
C7 C12 H12 119.9 . . ?
C13 C13 P1 116.0(9) 2_656 . ?
C13 C13 H13B 108.3 2_656 . ?
P1 C13 H13B 108.3 . . ?
C13 C13 H13A 108.3 2_656 . ?
P1 C13 H13A 108.3 . . ?
H13B C13 H13A 107.4 . . ?
C14 C14 N1 109.6(8) 6_565 . ?
C14 C14 H14 125.2 6_565 . ?
N1 C14 H14 125.2 . . ?
N1 C15 N1 116.7(18) 6_565 . ?
N1 C15 H15 121.7 6_565 . ?
N1 C15 H15 121.7 . . ?

loop_
 _geom_torsion_atom_site_label_1
 _geom_torsion_atom_site_label_2
 _geom_torsion_atom_site_label_3
 _geom_torsion_atom_site_label_4
 _geom_torsion
 _geom_torsion_site_symmetry_1
 _geom_torsion_site_symmetry_2
 _geom_torsion_site_symmetry_3
 _geom_torsion_site_symmetry_4
 _geom_torsion_publ_flag
Au1 Au1 P1 C13 62.1(5) 2_656 . . . ?
Au1 Au1 P1 C7 -177.0(5) 2_656 . . . ?
Au1 Au1 P1 C1 -60.5(5) 2_656 . . . ?
Au1 Au1 N1 C15 90.6(14) 2_656 . . . ?
Au1 Au1 N1 C14 -83.7(14) 2_656 . . . ?
C13 P1 C1 C6 36.9(13) . . . . ?
C7 P1 C1 C6 -73.8(13) . . . . ?

Au1 P1 C1 C6 164.7(10) . . . . ?
C13 P1 C1 C2 -147.3(11) . . . . ?
C7 P1 C1 C2 102.0(12) . . . . ?
Au1 P1 C1 C2 -19.5(13) . . . . ?
C6 C1 C2 C3 -3(2) . . . . ?
P1 C1 C2 C3 -178.5(12) . . . . ?
C1 C2 C3 C4 0(2) . . . . ?
C2 C3 C4 C5 2(2) . . . . ?
C3 C4 C5 C6 -2(3) . . . . ?
C2 C1 C6 C5 3(2) . . . . ?
P1 C1 C6 C5 179.2(12) . . . . ?
C4 C5 C6 C1 -1(2) . . . . ?
C13 P1 C7 C8 -23.3(17) . . . . ?
C1 P1 C7 C8 88.7(15) . . . . ?
Au1 P1 C7 C8 -150.5(13) . . . . ?
C13 P1 C7 C12 154.8(13) . . . . ?
C1 P1 C7 C12 -93.2(14) . . . . ?
Au1 P1 C7 C12 27.7(14) . . . . ?
C12 C7 C8 C9 5(3) . . . . ?
P1 C7 C8 C9 -176.9(15) . . . . ?
C7 C8 C9 C10 -3(3) . . . . ?
C8 C9 C10 C11 0(3) . . . . ?
C9 C10 C11 C12 -1(3) . . . . ?
C10 C11 C12 C7 3(3) . . . . ?
C8 C7 C12 C11 -5(3) . . . . ?
P1 C7 C12 C11 176.4(13) . . . . ?
C7 P1 C13 C13 160.8(13) . . . 2_656 ?
C1 P1 C13 C13 50.7(14) . . . 2_656 ?
Au1 P1 C13 C13 -74.3(14) . . . 2_656 ?
C15 N1 C14 C14 1.5(13) . . . 6_565 ?
Au1 N1 C14 C14 176.7(9) . . . 6_565 ?
C14 N1 C15 N1 -3(2) . . . 6_565 ?
Au1 N1 C15 N1 -178.3(8) . . . 6_565 ?

_diffrn_measured_fraction_theta_max 0.941
_diffrn_reflns_theta_full 24.71
_diffrn_measured_fraction_theta_full 0.941
_refine_diff_density_max 7.410
_refine_diff_density_min -2.764
_refine_diff_density_rms 0.368

loop_
_platon_squeeze_void_nr
_platon_squeeze_void_average_x
_platon_squeeze_void_average_y
_platon_squeeze_void_average_z
_platon_squeeze_void_volume
_platon_squeeze_void_count_electrons
1 -0.022 0.000 -0.028 868 430
2 -0.004 0.500 -0.030 868 430
_platon_squeeze_details
;

The structure contains large channels wherein chloride ions and solvent molecules (dichloromethane, methanol) are located
with a high degree of disorder. Attempts to assign these
molecules were unsuccesful. Therefore the electron density in this area was accounted for by the SQUEEZE instruction of the PLATON program suite.
;

checkCIF/PLATON report

You have not supplied any structure factors. As a result the full set of tests cannot be run.

No syntax errors found. CIF dictionary Interpreting this report

Datablock: Compound1.MeOH

No errors found in this datablock

It is advisable to attempt to resolve as many as possible of the alerts in all categories. Often the minor alerts point to easily fixed oversights, errors and omissions in your CIF or refinement strategy, so attention to these fine details can be worthwhile. In order to resolve some of the more serious problems it may be necessary to carry out additional measurements or structure refinements. However, the purpose of your study may justify the reported deviations and the more serious of these should normally be commented upon in the discussion or experimental section of a paper or in the "special_details" fields of the CIF. checkCIF was carefully designed to identify outliers and unusual parameters, but every test has its limitations and alerts that are not important in a particular case may appear. Conversely, the absence of alerts does not guarantee there are no aspects of the results needing attention. It is up to the individual to critically assess their own results and, if necessary, seek expert advice.

Publication of your CIF in IUCr journals

A basic structural check has been run on your CIF. These basic checks will be run on all CIFs submitted for publication in IUCr journals (*Acta Crystallographica, Journal of Applied Crystallography, Journal of Synchrotron Radiation*); however, if you intend to submit to *Acta Crystallographica Section C* or *E*, you should make sure that full publication checks are run on the final version of your CIF prior to submission.

Publication of your CIF in other journals

Please refer to the *Notes for Authors* of the relevant journal for any special instructions relating to CIF submission.

PLATON version of 30/05/2011; check.def file version of 24/05/2011

Datablock Compound1.MeOH - ellipsoid plot

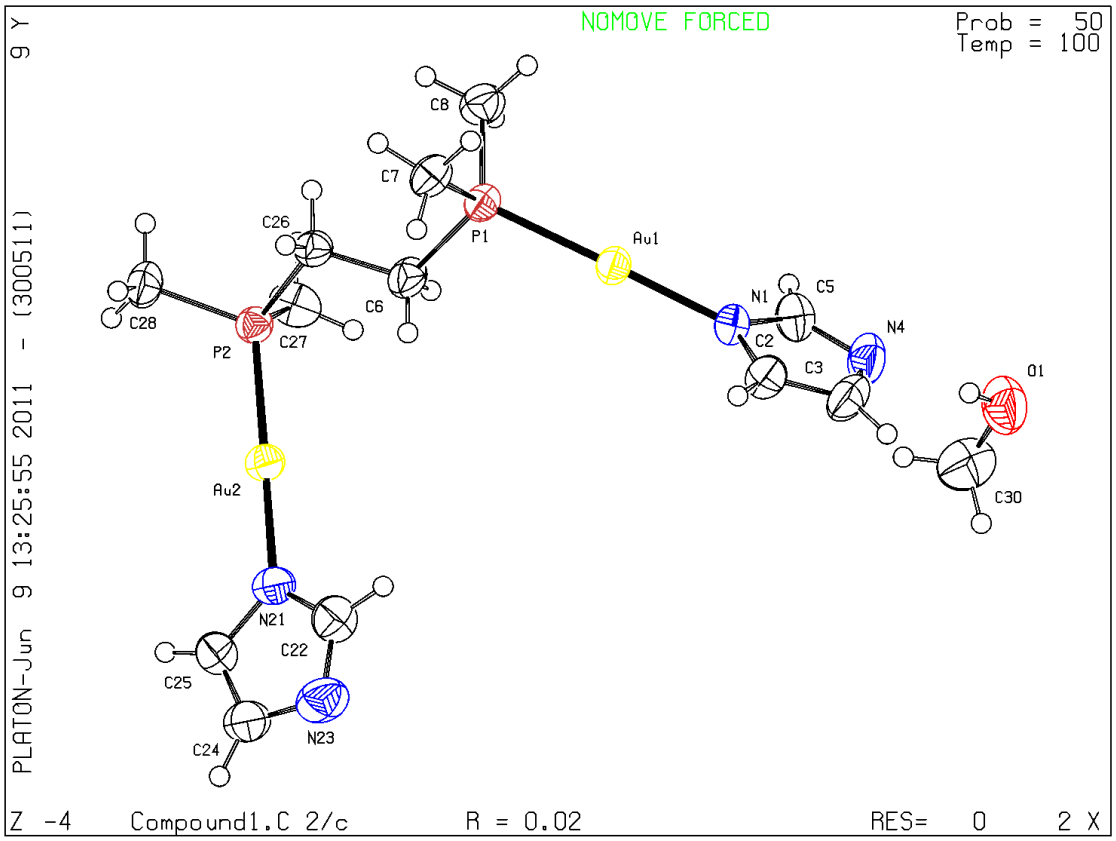

checkCIF/PLATON report

You have not supplied any structure factors. As a result the full set of tests cannot be run.

No syntax errors found. CIF dictionary Interpreting this report

Datablock: Compound18

Bond precision: C-C = 0.0047 A Wavelength=0.71073

Cell: a=8.8411(10) b=9.8465(11) c=10.7011(12)
alpha=70.016(2) beta=70.623(2) gamma=78.093(2)
Temperature: 100 K

	Calculated	Reported
Volume	821.34(16)	821.34(16)
Space group	P -1	P -1
Hall group	-P 1	-P 1
Moiety formula	C34 H36 Au2 N6 P2	C34 H36 Au2 N6 P2
Sum formula	C34 H36 Au2 N6 P2	C34 H36 Au2 N6 P2
Mr	984.57	984.56
Dx,g cm-3	1.991	1.991
Z	1	1
Mu (mm-1)	9.052	9.052
F000	470.0	470.0
F000’	466.52	
h,k,lmax	11,12,13	11,12,13
Nref	3379	3351
Tmin,Tmax	0.083,0.257	0.127,0.344
Tmin’	0.053	

Correction method= MULTI-SCAN

Data completeness= 0.992 Theta(max)= 26.460

R(reflections)= 0.0196(3311) wR2(reflections)= 0.0506(3351)

S = 1.108 Npar= 199

The following ALERTS were generated. Each ALERT has the format
test-name_ALERT_alert-type_alert-level.
Click on the hyperlinks for more details of the test.

Alert level G

PLAT154_ALERT_1_G The su’s on the Cell Angles are Equal (x 10000) 200 Deg.

---

0 **ALERT level A** = Most likely a serious problem - resolve or explain

```
  0 ALERT level B = A potentially serious problem, consider carefully
  0 ALERT level C = Check. Ensure it is not caused by an omission or oversight
  1 ALERT level G = General information/check it is not something unexpected

  1 ALERT type 1 CIF construction/syntax error, inconsistent or missing data
  0 ALERT type 2 Indicator that the structure model may be wrong or deficient
  0 ALERT type 3 Indicator that the structure quality may be low
  0 ALERT type 4 Improvement, methodology, query or suggestion
  0 ALERT type 5 Informative message, check
```

It is advisable to attempt to resolve as many as possible of the alerts in all categories. Often the minor alerts point to easily fixed oversights, errors and omissions in your CIF or refinement strategy, so attention to these fine details can be worthwhile. In order to resolve some of the more serious problems it may be necessary to carry out additional measurements or structure refinements. However, the purpose of your study may justify the reported deviations and the more serious of these should normally be commented upon in the discussion or experimental section of a paper or in the "special_details" fields of the CIF. checkCIF was carefully designed to identify outliers and unusual parameters, but every test has its limitations and alerts that are not important in a particular case may appear. Conversely, the absence of alerts does not guarantee there are no aspects of the results needing attention. It is up to the individual to critically assess their own results and, if necessary, seek expert advice.

Publication of your CIF in IUCr journals

A basic structural check has been run on your CIF. These basic checks will be run on all CIFs submitted for publication in IUCr journals (*Acta Crystallographica*, *Journal of Applied Crystallography*, *Journal of Synchrotron Radiation*); however, if you intend to submit to *Acta Crystallographica Section C* or *E*, you should make sure that full publication checks are run on the final version of your CIF prior to submission.

Publication of your CIF in other journals

Please refer to the *Notes for Authors* of the relevant journal for any special instructions relating to CIF submission.

PLATON version of 24/03/2011; check.def file version of 16/03/2011

Datablock Compound18 - ellipsoid plot

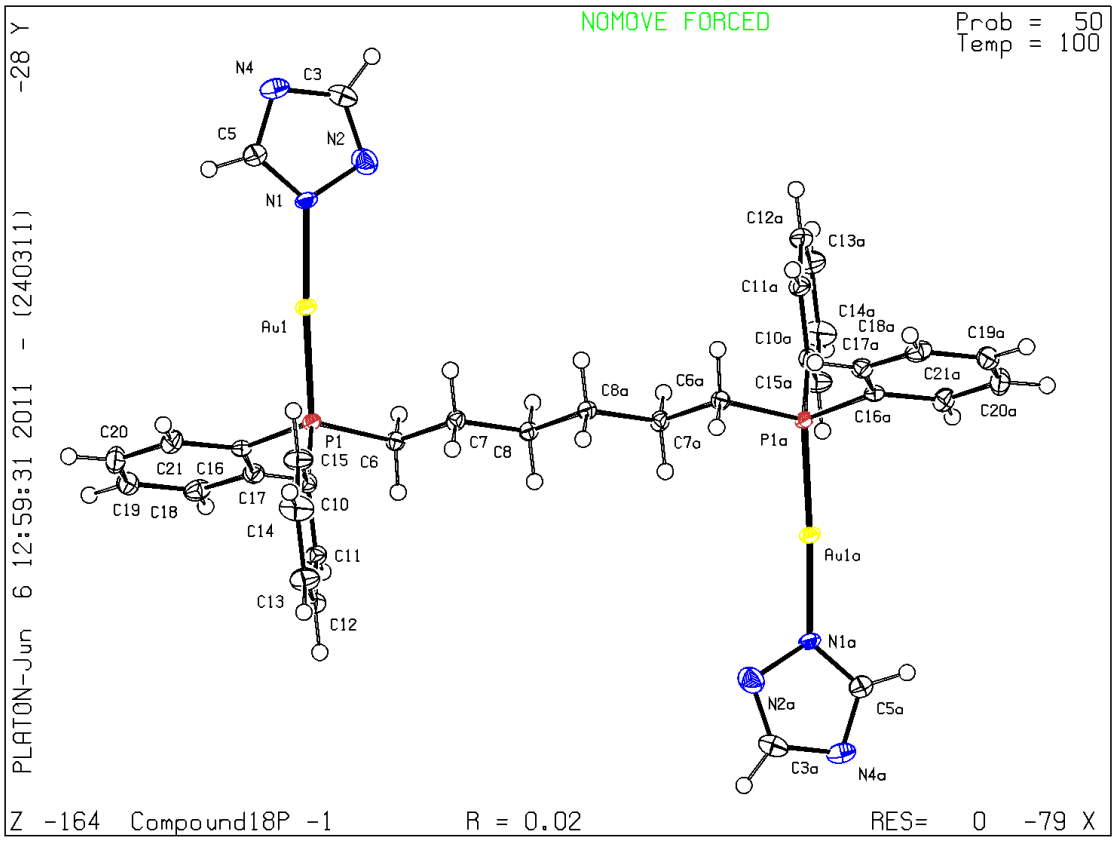

checkCIF/PLATON report

You have not supplied any structure factors. As a result the full set of tests cannot be run.

No syntax errors found. CIF dictionary Interpreting this report

Datablock: I

Bond precision: C-C = 0.0249 A Wavelength=0.71073

Cell: a=18.156(5) b=21.701(6) c=12.304(4)
alpha=90 beta=123.616(4) gamma=90
Temperature: 150 K

	Calculated	Reported
Volume	4037(2)	4037(2)
Space group	C 2/m	C2/m
Hall group	-C 2y	-C 2y
Moiety formula	C58 H54 Au4 N4 P4	C58 H54 Au4 N4 P4, 2Cl
Sum formula	C58 H54 Au4 N4 P4	C58 H54 Au4 Cl2 N4 P4
Mr	1718.81	1789.70
Dx,g cm-3	1.414	1.484
Z	2	2
Mu (mm-1)	7.353	7.478
F000	1612.0	1680.0
F000'	1598.25	
h,k,lmax	21,25,14	21,25,14
Nref	3556	3348
Tmin,Tmax	0.105,0.280	0.202,0.368
Tmin'	0.079	

Correction method= MULTI-SCAN

Data completeness= 0.942 Theta(max)= 24.710

R(reflections)= 0.0697(2256) wR2(reflections)= 0.1756(3348)

S = 1.068 Npar= 160

The following ALERTS were generated. Each ALERT has the format
test-name_ALERT_alert-type_alert-level.
Click on the hyperlinks for more details of the test.

Alert level B

PLAT029_ALERT_3_B _diffrn_measured_fraction_theta_full Low 0.94
PLAT342_ALERT_3_B Low Bond Precision on C-C Bonds (x 1000) Ang .. 25

Alert level C

```
CHEMW03_ALERT_2_C The ratio of given/expected molecular weight as
            calculated from the _atom_site* data lies outside
            the range 0.99 <> 1.01
           From the CIF: _cell_formula_units_Z                    2
           From the CIF: _chemical_formula_weight          1789.70
           TEST: Calculate formula weight from _atom_site_*
           atom     mass    num     sum
           C        12.01   58.00  696.64
           H         1.01   54.00   54.43
           N        14.01    4.00   56.03
           P        30.97    4.00  123.90
           Au      196.97    4.00  787.86
           Calculated formula weight             1718.86
DIFMX01_ALERT_2_C  The maximum difference density is > 0.1*ZMAX*0.75
            _refine_diff_density_max given =      7.410
            Test value =      5.925
DIFMX02_ALERT_1_C  The maximum difference density is > 0.1*ZMAX*0.75
            The relevant atom site should be identified.
REFLT03_ALERT_3_C  Reflection count < 95% complete
           From the CIF: _diffrn_reflns_theta_max           24.71
           From the CIF: _diffrn_reflns_theta_full          24.71
           From the CIF: _reflns_number_total               3348
           TEST2: Reflns within _diffrn_reflns_theta_max
           Count of symmetry unique reflns         3556
           Completeness (_total/calc)             94.15%
THETM01_ALERT_3_C  The value of sine(theta_max)/wavelength is less than 0.590
            Calculated sin(theta_max)/wavelength =    0.5882
PLAT022_ALERT_3_C Ratio Unique / Expected Reflections (too) Low ..       0.94
PLAT041_ALERT_1_C Calc. and Reported SumFormula    Strings  Differ          ?
PLAT043_ALERT_1_C Check Reported Molecular Weight ................    1789.70
PLAT051_ALERT_1_C Mu(calc) and Mu(CIF) Ratio Differs from 1.0 by .       1.67 Perc.
PLAT068_ALERT_1_C Reported F000 Differs from Calcd (or Missing)...          ?
PLAT094_ALERT_2_C Ratio of Maximum / Minimum Residual Density ....       2.68
PLAT097_ALERT_2_C Large Reported Max.  (Positive) Residual Density       7.41 eA-3
PLAT213_ALERT_2_C Atom P1              has ADP max/min Ratio .....       3.20 prola
PLAT241_ALERT_2_C Check High      Ueq as Compared to Neighbors for         C9
PLAT250_ALERT_2_C Large U3/U1 Ratio for Average U(i,j) Tensor ....       3.49
```

Alert level G

```
FORMU01_ALERT_2_G  There is a discrepancy between the atom counts in the
            _chemical_formula_sum and the formula from the _atom_site* data.
            Atom count from _chemical_formula_sum:C58 H54 Au4 Cl2 N4 P4
            Atom count from the _atom_site data:  C58 H54 Au4 N4 P4
CELLZ01_ALERT_1_G Difference between formula and atom_site contents detected.
CELLZ01_ALERT_1_G ALERT: Large difference may be due to a
            symmetry error - see SYMMG tests
           From the CIF: _cell_formula_units_Z    2
           From the CIF: _chemical_formula_sum  C58 H54 Au4 Cl2 N4 P4
           TEST: Compare cell contents of formula and atom_site data

           atom    Z*formula  cif sites diff
           C         116.00    116.00    0.00
           H         108.00    108.00    0.00
           Au          8.00      8.00    0.00
           Cl          4.00      0.00    4.00
           N           8.00      8.00    0.00
           P           8.00      8.00    0.00
PLAT002_ALERT_2_G Number of Distance or Angle Restraints on AtSite          6
PLAT003_ALERT_2_G Number of Uiso or Uij Restrained Atom Sites ....          8
```

```
PLAT606_ALERT_4_G VERY LARGE Solvent Accessible VOID(S) in Structure       !
PLAT860_ALERT_3_G Note: Number of Least-Squares Restraints .......       37
```

```
   0 ALERT level A = Most likely a serious problem - resolve or explain
   2 ALERT level B = A potentially serious problem, consider carefully
  15 ALERT level C = Check. Ensure it is not caused by an omission or oversight
   7 ALERT level G = General information/check it is not something unexpected

   7 ALERT type 1 CIF construction/syntax error, inconsistent or missing data
  10 ALERT type 2 Indicator that the structure model may be wrong or deficient
   6 ALERT type 3 Indicator that the structure quality may be low
   1 ALERT type 4 Improvement, methodology, query or suggestion
   0 ALERT type 5 Informative message, check
```

It is advisable to attempt to resolve as many as possible of the alerts in all categories. Often the minor alerts point to easily fixed oversights, errors and omissions in your CIF or refinement strategy, so attention to these fine details can be worthwhile. In order to resolve some of the more serious problems it may be necessary to carry out additional measurements or structure refinements. However, the purpose of your study may justify the reported deviations and the more serious of these should normally be commented upon in the discussion or experimental section of a paper or in the "special_details" fields of the CIF. checkCIF was carefully designed to identify outliers and unusual parameters, but every test has its limitations and alerts that are not important in a particular case may appear. Conversely, the absence of alerts does not guarantee there are no aspects of the results needing attention. It is up to the individual to critically assess their own results and, if necessary, seek expert advice.

Publication of your CIF in IUCr journals

A basic structural check has been run on your CIF. These basic checks will be run on all CIFs submitted for publication in IUCr journals (*Acta Crystallographica*, *Journal of Applied Crystallography*, *Journal of Synchrotron Radiation*); however, if you intend to submit to *Acta Crystallographica Section C* or *E*, you should make sure that full publication checks are run on the final version of your CIF prior to submission.

Publication of your CIF in other journals

Please refer to the *Notes for Authors* of the relevant journal for any special instructions relating to CIF submission.

PLATON version of 24/03/2011; check.def file version of 16/03/2011

Datablock I - ellipsoid plot